

NG3-19201

Space Programs Summary No. 37-21, Volume III

for the period March 1, 1963 to April 30, 1963

The Deep Space Instrumentation Facility

OTS PRICE

XEROX	\$	<u>8.60</u>
MICROFILM	\$	<u>2.63</u>

jpl

JET PROPULSION LABORATORY
CALIFORNIA INSTITUTE OF TECHNOLOGY
PASADENA, CALIFORNIA

May 31, 1963

Space Programs Summary No. 37-21, Volume III

for the period March 1, 1963 to April 30, 1963

The Deep Space Instrumentation Facility

**JET PROPULSION LABORATORY
CALIFORNIA INSTITUTE OF TECHNOLOGY
PASADENA, CALIFORNIA**

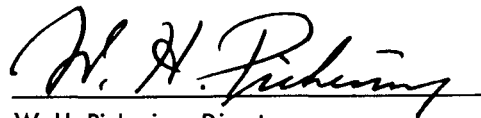
May 31, 1963

Preface

The *Space Programs Summary* is a six volume, bimonthly publication designed to report on JPL space exploration programs, and related supporting research and advanced development projects. The subtitles of all volumes of the *Space Programs Summary* are:

- Vol. I. The Lunar Program (Confidential)
- Vol. II. The Planetary-Interplanetary Program (Confidential)
- Vol. III. The Deep Space Instrumentation Facility (Unclassified)
- Vol. IV. Supporting Research and Advanced Development (Unclassified)
- Vol. V. Supporting Research and Advanced Development (Confidential)
- Vol. VI. Space Exploration Programs and Space Sciences (Unclassified)

The *Space Programs Summary*, Volume VI is an unclassified digest of appropriate material from Volumes I through V, plus the space science instrumentation studies of the JPL Space Sciences Division.



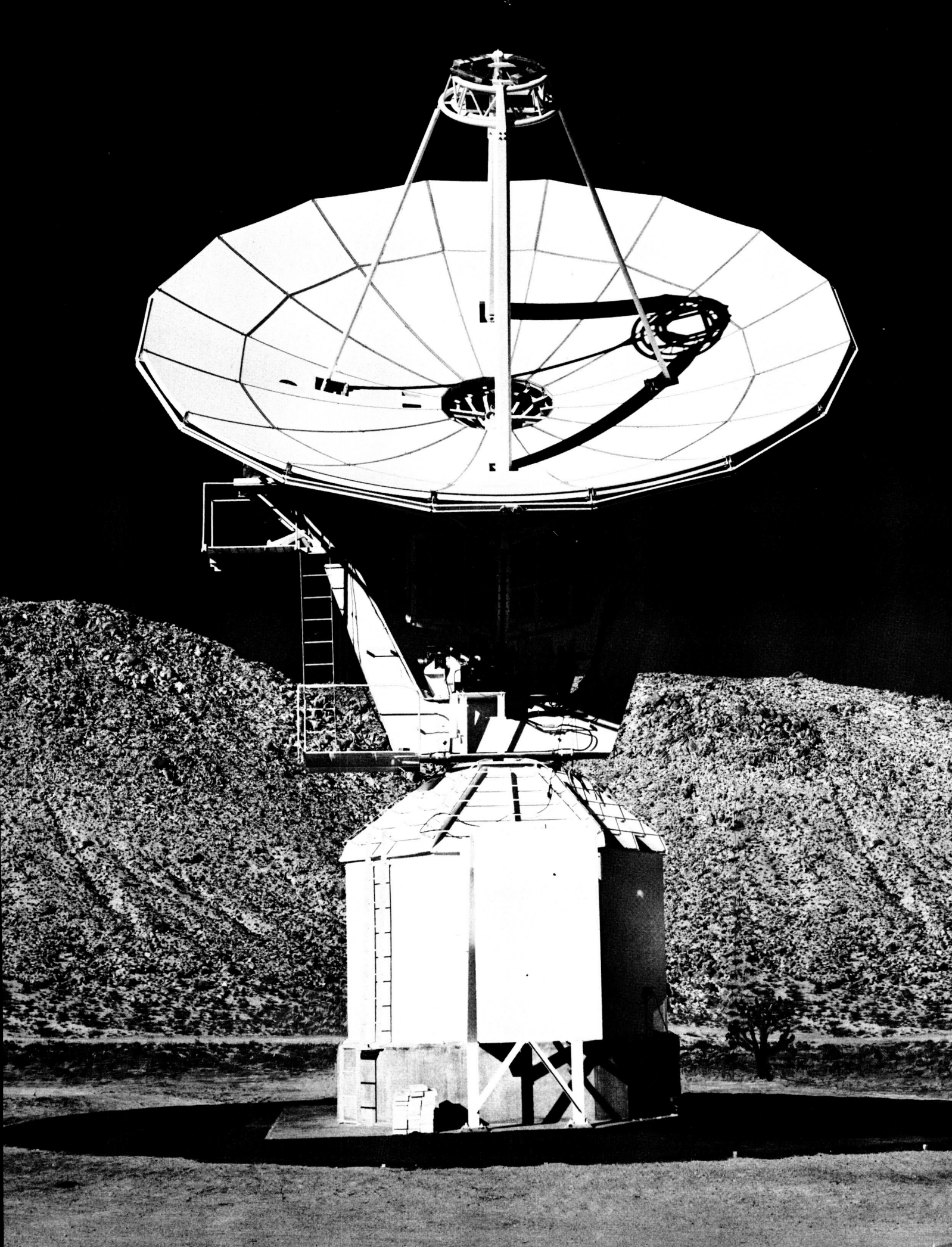
W. H. Pickering, Director
Jet Propulsion Laboratory

Space Programs Summary No. 37-21, Volume III

Copyright © 1963, Jet Propulsion Laboratory, California Institute of Technology
Prepared under Contract No. NAS 7-100, National Aeronautics & Space Administration

Contents

I. Résumé	1
II. Engineering Development	4
A. Laboratory Testing of Flow Corporation Drag Spheres	4
B. Digital Instrumentation System	7
C. Installation of Safety Equipment at Woomera	14
D. Mark I Ranging Subsystem	16
Reference	18
III. Research and Development	19
A. Experimental Low-Noise Systems	19
B. Ground Antennas	24
C. Planetary Radar	40
D. Ranging System Development	62
E. Tiefort Mountain Antenna Range	83
References	84
IV. Advanced Antenna System	85
A. Synopsis	85
B. Supporting Studies	86



I. Résumé

The DSIF is a precision tracking and data acquisition network which is designed to track, command, and receive data from deep space probes. It utilizes large antennas, low-noise phase-lock receiving systems, and high-power transmitters at stations positioned approximately 120 deg around the Earth. Its policy is to continuously conduct research and development of new components and systems and to engineer them into the DSIF so as to continually maintain a state-of-the-art capability.

Engineering developments. A wind measurement system set up on the site of the future 210-ft antenna makes use of 12-in. diameter spheres to measure wind velocity in three directions. Linearity, response, and hysteresis tests have been made on one of the spheres in order to determine the accuracy of the wind measurements.

The digital instrumentation system, which has been initially installed at Goldstone, makes use of two general purpose computers. Each computer uses a parallel, random access, coincident current, magnetic core memory and serial arithmetic operation. Both computers have the same word size, instruction format, machine cycle time and input-output capability; however, one unit has more

instructions and faster execution times. Each computer has an automatic power failsafe system.

Staircases, platforms, and instrument cages have been installed at the Woomera Station to increase the safety of personnel working on the antenna and collimation tower.

The Mark I ranging subsystem is designed to furnish unambiguous range measurements to a range of 8×10^5 km. In order to do this, the pseudo-random binary digital codes are generated in the receiver and transmitter coders and are made up of several components which are combined in different forms to create various code lengths; they are also acquired or synchronized separately to decrease acquisition times. A 1-Mc, 31-stage, open-ended shift register is used as the timer and a Chinese number generator provides the numbers which must be added (or subtracted) to the cumulative range tally to obtain the doppler count.

Low-noise systems. Normal noise temperature calculations of a traveling wave maser assume a high gain per unit length. This is reasonable at bath temperatures of 1.5 to 2.5°K, but is not necessarily valid at a temperature

of 4.2°K which is typical of cryogenic refrigerators. Measured data at 2300 Mc gives minimum and maximum noise temperatures of 4 and 9.3°K, respectively.

A mobile Dicke radiometer with a horn antenna was used to measure the average noise temperature of automotive ignition and fluorescent lamps. They were found to produce a flux density as much as -183 and -187 dbm/cps/m², respectively, at 50 ft.

Ground antennas. The 30-ft antenna at the Goldstone Venus site has been fitted with a Cassegrain feed system which is a $\frac{1}{4}$ -scale model of the feed that will be used on the 210-ft antenna. Using the Tiefert Mountain antenna range and a calibrated 6-ft antenna near the focal point of the 30-ft antenna, gain, beam width, and radiation patterns will be measured at about 16.5 Gc, which is 7 times normal frequency for the 210-ft antenna. A servo test program is continuing in an effort to determine the cause of discrepancies between the results of dynamic and transfer function tests.

As part of a program to determine the relationship between deformations of the surface of a paraboloidal antenna and RF performance, it is planned to physically distort the surface of the 30-ft antenna and to measure its change in performance. A computer program has been developed to calculate the change and a comparison has been plotted with actual measurements. Close agreement was noted.

An instrumentation van for testing antennas is nearly complete.

A metallic cylinder, or tunnel, was placed over the rim of a 6-ft antenna to provide isolation between it and the 85-ft antenna on which it was mounted. Using various "tunnel" lengths, antenna patterns and gain measurements were made. Calculations show that the antenna noise temperature can be reduced from 16.7 to 3.7°K and that the tunnel can be a useful and practical device for reducing antenna temperatures of small paraboloidal antennas.

Planetary radar. Measurements made on the double cavity 2388-Mc maser at the Venus site shows that there is an insignificant increase in noise temperature due to waveguide mismatch, and that there is an increase in gain and a decrease in noise temperature with an increase in ambient temperature. Reasons for this characteristic are unknown and are being investigated.

After investigating six proposals by different manufacturers, one was found which appears capable of building a satisfactory water rotary joint for use on large antennas. It will use a hard carbon face. Testing of the completed product will be done at JPL.

The Mod IV ranging equipment is essentially a digital phase tracking loop which provides a continuous real-time measurement of target range. In addition, it provides ephemeris programmed signals for use in spectrum, radiometer, and multiple range gate analysis of the radar echoes and an ephemeris-controlled keying signal to control the alternate connection of transmitter and receiver to a single antenna.

Actual operations of the 100-kw transmitter revealed several deficiencies which have been corrected and reduced since the last radar experiment. The klystron amplifier, RF water load, and transmitter control cabinets were returned to the manufacturer for repair. The "crow-bar" or high-voltage protective device was modified to provide a large gap when the generator field was activated; better rectifier tubes were obtained and an unwanted resonance in the input to the power supply filter was essentially eliminated by adding a 0.0625 μ fd capacitor in parallel with the high-voltage cable.

The Mod IV planetary radar receiver is presently undergoing extensive evaluation tests prior to being installed at the Venus site for use in planetary radar experiments. The receiver has five separate channels; synchronous, AM spectrum, CW spectrum, ranging, and noise and operates with reference frequencies obtained from a synthesizer which receives coherent 1-Mc and 10-kc signals from an atomic frequency standard oscillator. Cooling is accomplished with liquid cooled heat sinks. Noise figure, bandwidths, mixer conversion efficiency and RF carrier tracking loop threshold, limiter suppression factor, closed-loop frequency response, bandwidth variation with signal strength, loop phase error with frequency offset, and internal coherent interference measurements have all been made.

An automatic acquisition device has been developed for use with phase-locked clean-up loops. It makes use of a relay operated short on one of the resistors in the loop filter which widens its bandwidth until acquisition occurs, at which time an AND gate operates to remove the short and narrow the bandwidth when the reference frequency, VCO frequency and a "no beat" condition all are present.

Ranging system development. The Mod III ranging equipment is a development from the Mod II equipment which has been described previously. It is somewhat different in physical construction, has additional peripheral devices and a greater input-output capacity. Although primarily developed for real-time automatic range acquisition and tracking at interplanetary distances, small additional features have been added so that it is essentially a general purpose stored program computer capable of on-line data handling and processing, automatic station check-out and sequential and simultaneous control of other equipment. Input capacity is 128 word channels (25-bit, 1-Mc binary code-sequence words) and output capacity is 32 channels with 128 channels of on-off signals (64 internal and 64 external). Normal input is from a paper tape reader and normal outputs are a paper tape punch and digital strip printer.

Because of the general nature and complexity of the Mod III ranging equipment a set of programming, operating and maintenance manuals, check and diagnostic routines, and subroutines are being prepared. Some have already been published.

Whenever the sidebands of a modulated carrier have as much or more power than the carrier it is possible to lock a phase-locked receiver on to one of the sidebands rather than the carrier. Several methods have been proposed for automatically preventing this. One which looks very promising theoretically is now being tried experimentally. It makes use of the principle that, with 50%

duty cycles on a monostatic radar, only odd numbered sidebands are present and these will be symmetrical with respect to the carrier. By measuring this symmetry and automatically cancelling all symmetrical voltages, a receiver phase-lock loop can be made to lock on the only voltage left which is the carrier. Lock indicators are provided.

The above principle is also being tried with telemetry modulation of a continuous carrier when strong signals are available. Another proposal being investigated utilizes a synchronous sideband detector where the local reference is available to measure a component of the dynamic phase error whose frequency is equal to the product of the fundamental modulation frequency and the order of the sideband to which the receiver is locked. It is hoped that this system will be useful for weak signals and fast acquisition on a monostatic radar.

Tiefort Mountain antenna range. This range is now complete with heliport, towers, buildings, power generators and X-band equipment. S-band test equipment for use with the Echo site will be installed later.

Advanced Antenna System. Contract negotiations with the Rohr Corporation for the construction of a 210-ft antenna at Goldstone have been completed and the contract is in the process of being approved. Supporting studies are being conducted at JPL particularly through the use of the STAIR Computer Program which has been modified to calculate the weight moment of inertia.

II. Engineering Development

A. Laboratory Testing of Flow Corporation Drag Spheres

A series of laboratory tests has been conducted on a drag sphere manufactured by the Flow Corporation, Cambridge, Mass. The sphere used for the tests is considered representative of the drag spheres mounted on the wind towers at the Mars site (Fig. 1). The spheres are mounted on the 300-ft tower at the following elevations:

One drag sphere at 5 m.

One drag sphere at 10 m.

Three drag spheres at 20 m.

One drag sphere at 40 m.

One drag sphere at 80 m.

The two 30-ft towers have one drag sphere each, located 10 m above ground.

The drag sphere determines wind velocity by measuring the wind force exerted on a 12-in. diameter sphere. In principle, the sphere behaves like the familiar pitot-static pressure probe in that its reading is directly proportional to the square of the wind velocity. The drag sphere is omnidirectional and provides separate electrical outputs for each of the mutually perpendicular axes (North-South, East-West, up-down). The drag sphere is mounted on and surrounds a three-axis flexure force balance, which in turn is mounted on a quadripod pipe stand (Fig. 2).

Wind forces acting on the sphere are transmitted via the welded frame (Fig. 3) to the flexure rods to produce parallel motions of a few thousandths of an inch. Differential transformer coils fixed to the quadripod pipe stand

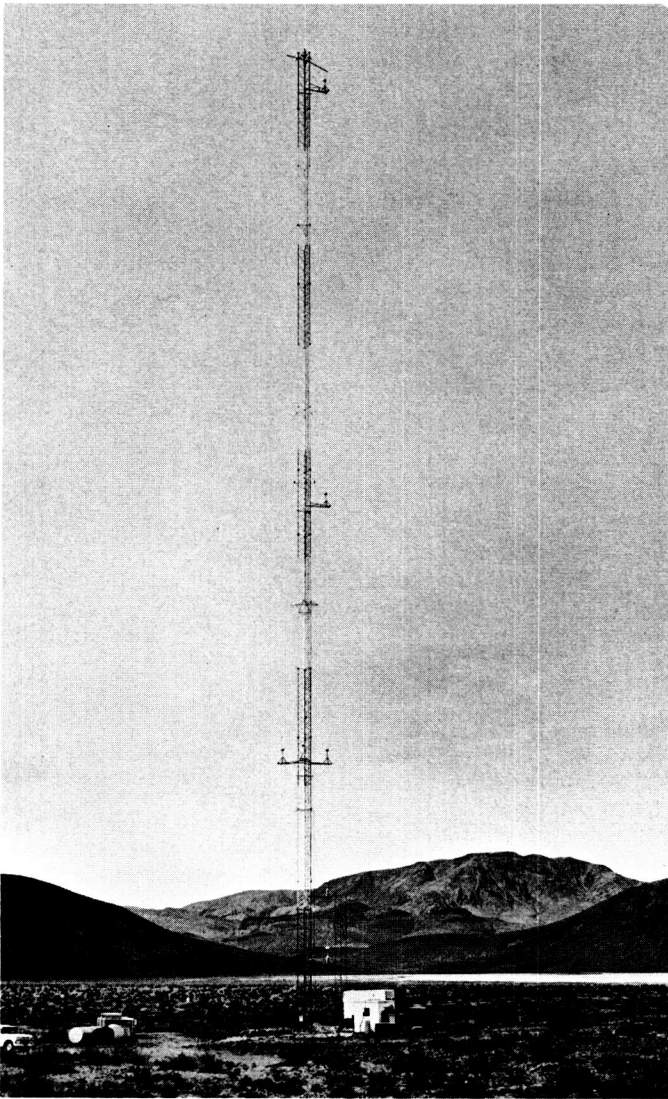


Fig. 1. Wind towers at Mars site

produce electrical measurements proportional to the flexure rod displacements which are, therefore, proportional to the wind force on each axis.

The laboratory tests consisted of (1) voltage output versus force measurements to determine linearity, (2) response tests, and (3) hysteresis tests. A calibration fixture was fabricated so that it could be mounted on the quadripod pipe stand (Fig. 4) and rotated through 360° in order to apply a force on each axis. It was designed so that it could be used to calibrate the remaining drag spheres without removing them from the wind tower.

In order to measure output voltage as a function of force, a series of weights was suspended via pulleys on

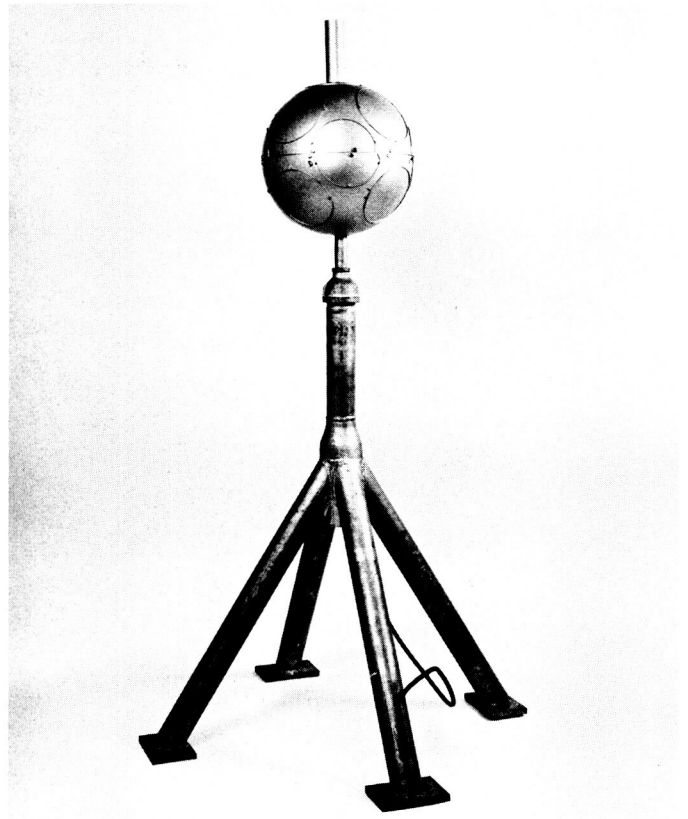


Fig. 2. Quadripod pipestand

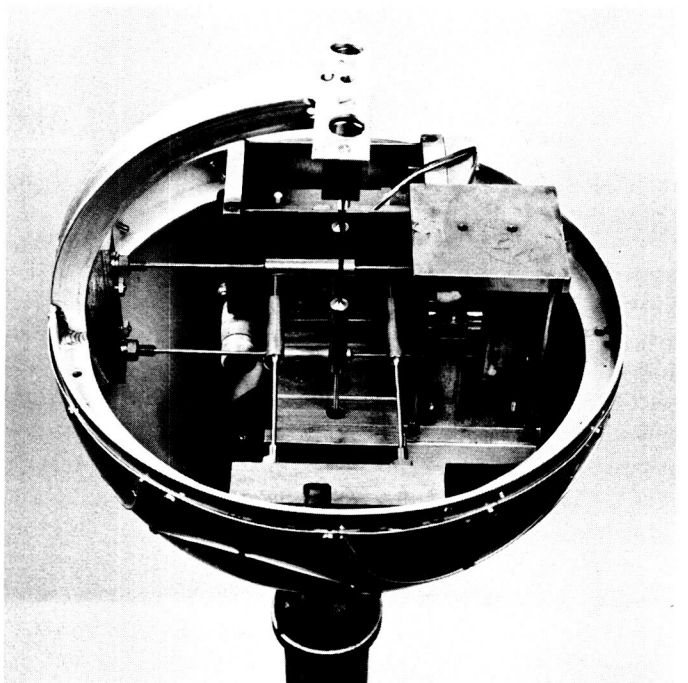


Fig. 3. Welded frame

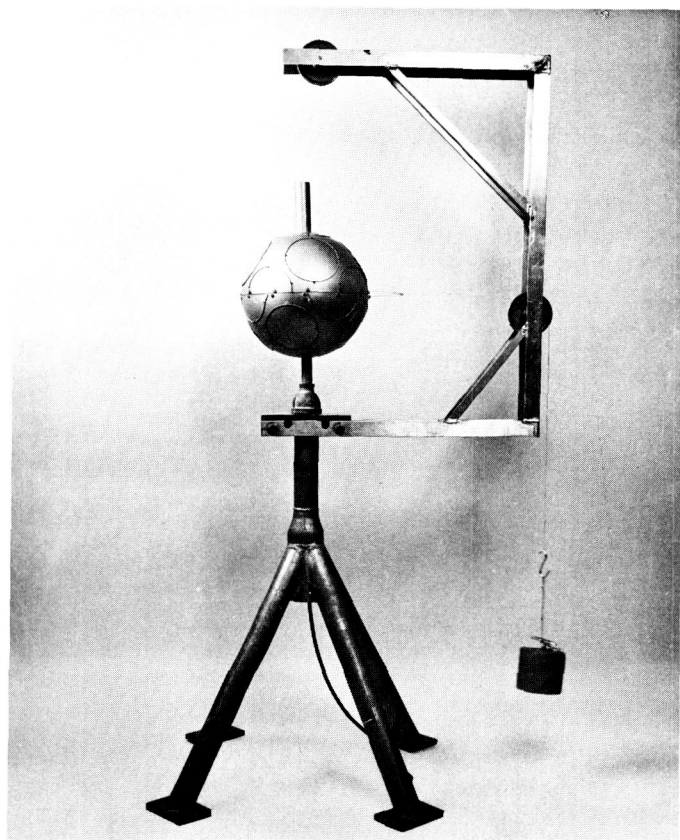


Fig. 4. Calibration fixture mounted on quadripod pipestand

each axis and several voltage readings taken for each weight. The results of these tests indicated (Figs. 5, 6, and 7) that the output voltage of each axis was linear with respect to the force applied.

Tests were also conducted to determine the natural resonant frequency of the drag sphere. The first test consisted of suspending a weight from the North-South axis and then cutting the weight loose while measuring the output voltage on a Sanborn recorder. Because the output voltage would drive the recorder off scale, little could be determined from this test. A second test was made by tapping on the pipe stand and recording the output voltage. This test indicated a resonance of approximately 8 cps. Tapping on the side of the drag sphere yielded the same results. Preliminary records of data from the drag spheres on the wind tower also show an 8-cps frequency. According to the Flow Corporation, the natural resonance frequency is 40 cps. Additional investigation of the 8-cps resonant frequency is required to isolate the source of this discrepancy.

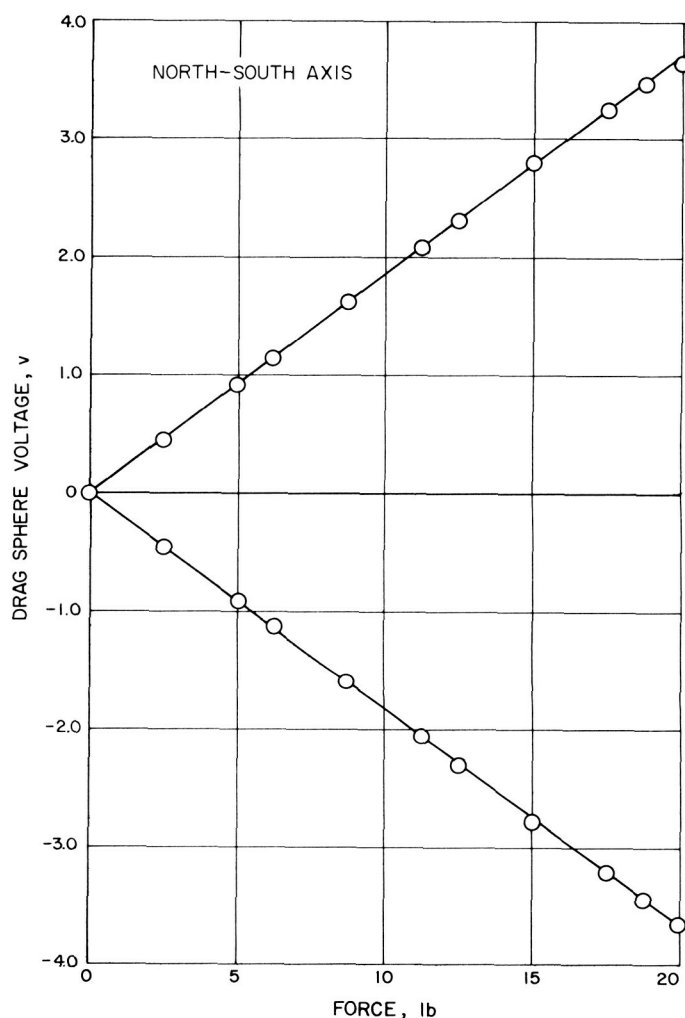


Fig. 5. Drag sphere voltage versus force, North-South axis

Tests were also conducted to determine the error due to hysteresis in the flexure members. The test consisted of applying a force from each direction and recording the voltage after the force was removed. Approximately 20 readings were made for each axis. Flow Corporation's specification stated that the errors due to hysteresis were:

North-South axis, 0.17% of full-scale load.

East-West axis, 0.38% of full-scale load.

Up-down axis, 0.05% of full-scale load.

Information and techniques developed in calibrating the drag sphere in the laboratory will be used to calibrate the drag spheres on the wind towers, using the entire wind measurement system, including the ground recording equipment.

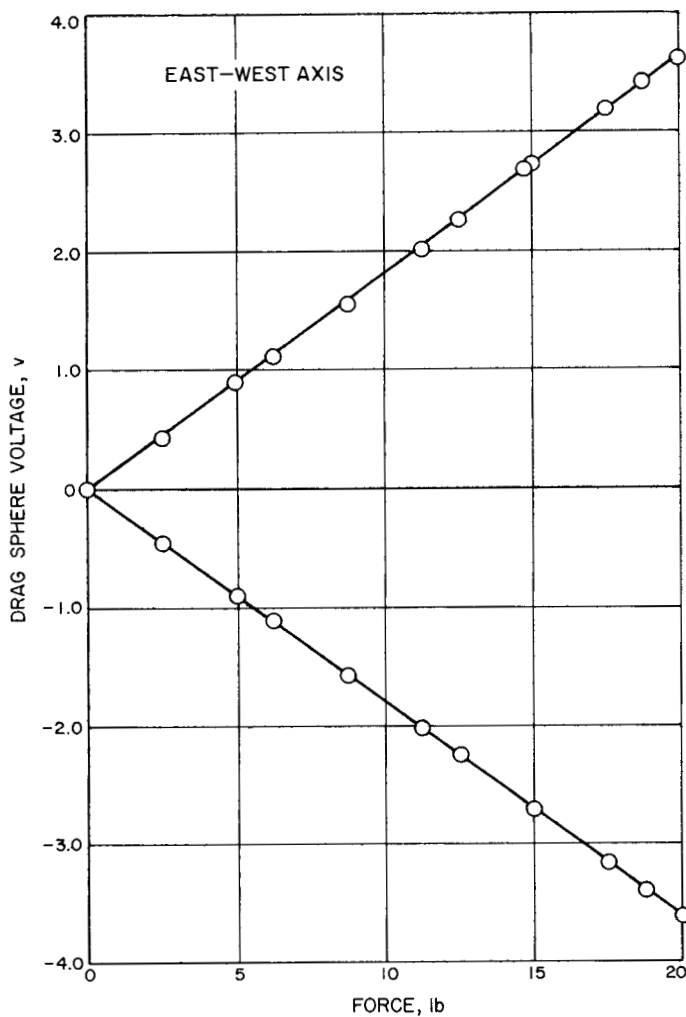


Fig. 6. Drag sphere voltage versus force, East-West axis

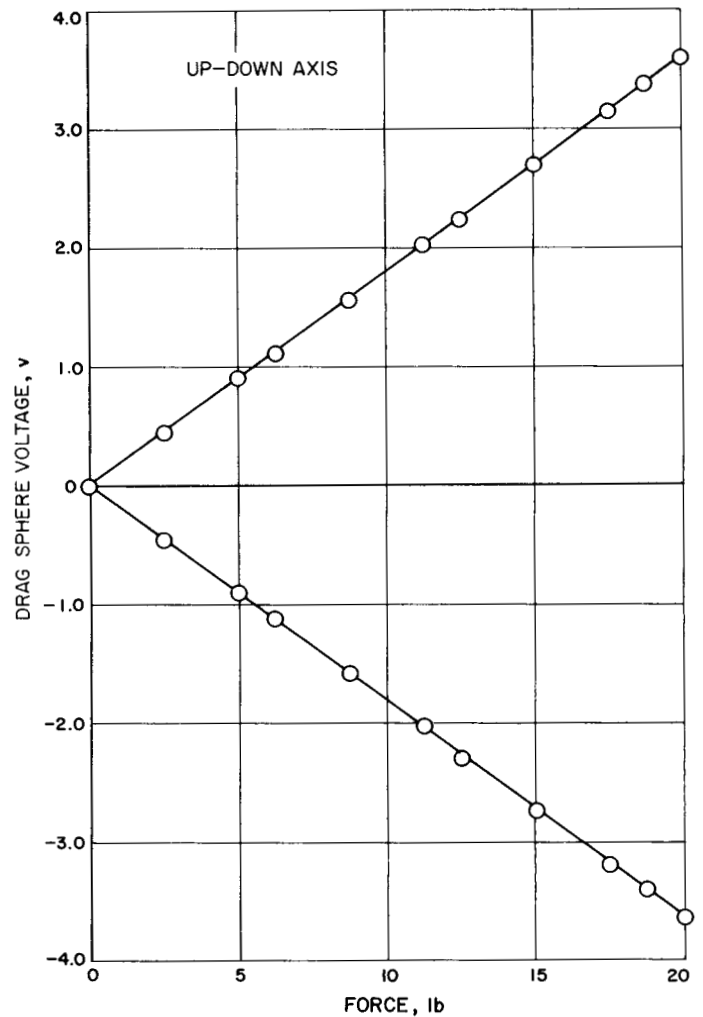


Fig. 7. Drag sphere voltage versus force, up-down axis

B. Digital Instrumentation System

The previous two articles on the digital instrumentation system (SPS 37-16, -20) gave a general description of the complete system. Details of the two general purpose digital computers used in the system will now be given.

There are two computers, a Scientific Data Systems (SDS) Model 910, and a SDS Model 920. They are solid state, general purpose, digital machines which use a

parallel, random access, coincident current, magnetic core memory and have serial arithmetic operations. Both are completely modular and contain all silicon semiconductors. Internal operations are binary with two's complement arithmetic being used. General characteristics of the two computers are presented in Table 1.

a. Basic computer structure and operation. The basic computer structure (Fig. 8) is used in both Models 910 and 920. Table 2 shows the instruction list for the two machines. This table, along with Table 1, points out the main difference in the capabilities of the computers. It will be noted that the 920 has more instructions with faster execution times for several of the common instructions, but that the word size, instruction format, machine cycle time and input-output capabilities of the computers are the same.

Table 1. General characteristics of 910 and 920 computers

Word size: 24 information bits plus one parity bit		
Memory size:		
910	2048 words (expandable to 16,384 words)	
920	4096 words (expandable to 16,384 words)	
Operating speeds:		
Typical execution times (including memory access and indexing)		
Add:	910	16 μ sec
	920	16 μ sec
Multiply:	910	248 μ sec
	920	32 μ sec
Floating point operations (24-bit Mantissa + 9-bit exponent):		
Add:	910	640 μ sec
	920	192 μ sec
Multiply:	910	656 μ sec
	920	184 μ sec
(39-bit Mantissa + 9-bit exponent)		
Add:	910	1984 μ sec
	920	368 μ sec
Multiply:	910	2040 μ sec
	920	272 μ sec

The computers use a 24-bit single address instruction. Table 3 shows the instruction format and provides a breakdown of the programming functions of the fields.

The computer has nine registers (Fig. 8) which are implemented in three different methods. The S-, M-, and O-registers use the usual RS-type flip-flops. The P- and C-registers use flip-flops designated as "repeaters" which will automatically reset when they receive an "enable" signal input.

The A-, B-, X-, and W-registers are one-word recirculating registers using dynamic, serial, shift circuits with repeater flip-flops at the "read" and "write" ends. To hold information, they must constantly shift and recirculate in a fashion similar to delay lines. When writing into these recirculating registers a "not recirculate" term is enabled for the registers involved.

Briefly, the function of each register is:

- (1) The A-register is the accumulator for the computer and is employed in all arithmetic, logical, and shifting operations. It has a write flip-flop (Aw) (repeater) followed by 23 stages of dynamic delay, a read flip-flop (Ar), and a flip-flop designated the "now" flip-flop (An). To maintain recirculation the Aw and Ar flip-flops are always enabled. The A-register is exactly 26 bits in length and must recirculate to maintain internally stored information, as in a delay line.

- (2) The B-register is implemented in the same manner as the A-register. It acts as an extension of the least significant end of the A-register for double precision operations and for shift operations.
- (3) The C-register is an arithmetic and control register used in multiplying, dividing, and other operations. All instructions brought from memory first appear in the C-register before decoding. Address modification and parity generation and detection take place in the C-register.
- (4) The M-register is the read-write register for the core memory, receiving information from memory during a read process and holding information for storage in memory during a write process. It is cleared just prior to receiving information to be stored or just prior to receiving information from memory. Contents of the C-register are transferred to M for storage when writing new data.
- (5) The O-register (7 bits) contains the instruction code of the instruction being executed. This register does not shift and only receives information.
- (6) The P-register is the program counter, containing the location from which the instruction was taken. It is increased by one, just preceding the time when the memory must be addressed for the next instruction. The P-register transfers its contents to the S-(address) register in parallel, and is composed of 14 repeater flip-flops.
- (7) The S-register holds the address of the memory location to be accessed. It remains in a static state when the memory is actively reading or writing. The S-register receives its address information in parallel from the P-register and from the C-register. (The address field of the instruction is the C-register.)
- (8) The W-register is implemented in the same manner as the X-register and is part of the W-buffer. Its basic function is to hold information on input and output.
- (9) The X-register is the index register. The least significant 14 bits are added to the address of the instruction before execution, if there is an index tag in bit 1 of the instruction. Implementation is with an Aw flip-flop (repeater) followed by 24 stages of dynamic delay and the Xn (now) repeater flip-flop.

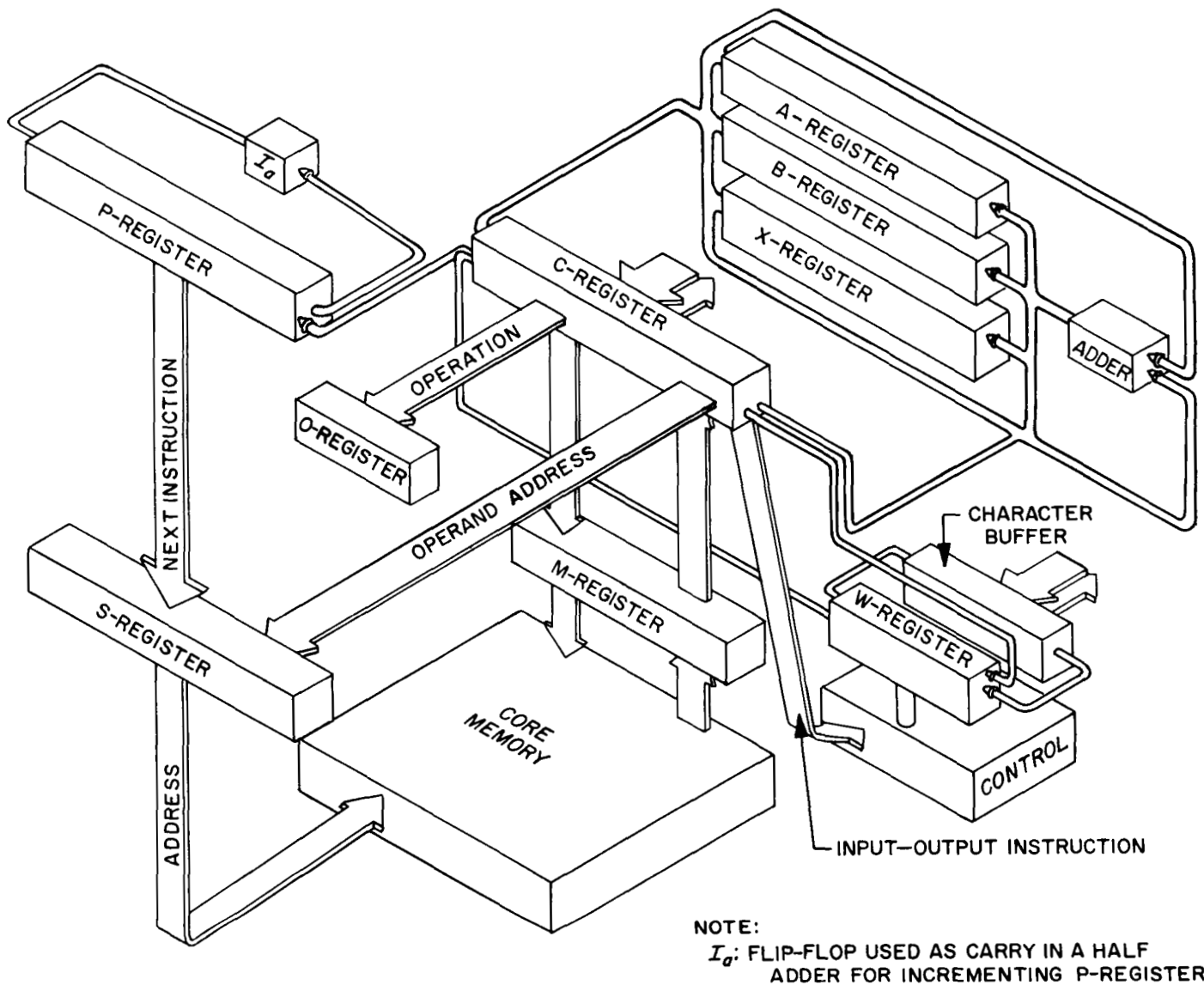


Fig. 8. Basic computer structure

b. Data flow. Generally, data flow through the computer is as follows:

The P-register holds the 14-bit address of the next instruction to be executed. The address held in the P-register is transferred in parallel to the 14-bit S flip-flop register setting up the address lines in the core memory for access to the word position addressed. The contents of the desired word are then transferred in parallel to the 24-bit M-register from memory. (During memory accessing or storing, the S-register always holds the desired address, and the M-register contains the operand or accepts it from memory.) In the M-register, the instruc-

tion just received from memory is transferred in parallel to the 24-bit C-register where its fields are distributed in parallel as follows:

The 6-bit-instruction-code-field is transferred in parallel to the 6-bit O-register where it is used to control execution of the instruction. Depending upon the instruction to be executed, the address field containing the memory address of the desired operand is transferred in parallel to the S-register. During the execution of the instruction the operand is serially shifted out of the C-register and into the W-register, adder, A-register, B-register, or X-register.

Table 2. SDS Model 910 and 920 instruction list

Instructions		Time ^a				Instructions		Time ^a	
Designation	Name	910	920			Designation	Name	910	920
Load-store	LDA Load A	2	2			Register change	CLA Clear A	—	1
	STA Store A	3	3				CLB Clear B	—	1
	LDB Load B	2	2				CLR Clear AB	1	1
	STB Store B	3	3				CAB Copy A into B	—	1
	LDX Load index	2	2				CBA Copy B into A	—	1
	STX Store index	3	3				XAB Exchange A and B	1	1
Arithmetic	XMA Exchange M and A	—	3			Shift	BAC Copy B into A, clear B	1	1
	ADD Add M to A	2	2				ABC Copy A into B, clear A	1	1
	ADC Add with carry	—	2				CXA Copy index into A	—	1
	ADM Add A to M	—	3				CAX Copy A into index	—	1
	MIN Memory increment	3	3				XXA Exchange index and A	—	1
	SUB Subtract M from A	2	2				CBX Copy B into index	—	1
	SUC Subtract with carry	—	2				CXB Copy index into B	—	1
	MUL Multiply	—	4				XXB Exchange index and B	—	1
	MUS Multiply step	2	—				STE Store exponent	—	1
	DIV Divide	—	28				LDE Load exponent	—	1
	DIS Divide step	2	—				XEE Exchange exponents	—	1
	BRU Branch unconditionally	1	1				CNA Copy negative into A	—	1
	BRX Increment index and branch	1, 2	1, 2			Control	RSH Right shift AB	N + 2	2 + (N + 1)/2
	BRM Mark place and branch	2	2				RCY Right cycle AB		
Branch-skip	BRR Return branch	2	2				LSH Left shift AB	N + 2	2 + (N + 1)/2
	SKS Skip if signal not set	1, 2	1, 2				LCY Left cycle AB		
	SKE Skip if A equals M	—	2, 3			Input-output	NOD Normalize and decrement X	1	1
	SKG Skip if A greater than M	2, 3	2, 3				HLT Halt	1	1
	SKR Reduce M, skip if negative	—	3				NOP No operation	1	1
	SKM Skip if A = M on B mask	2, 3	2, 3				EXU Execute	1	1
	SKN Skip if M negative	2, 3	2, 3				EAX Copy effective address into index	2	2
	SKA Skip if M and A do not compare ones	2, 3	2, 3				MIW M into W-buffer when ready	2 +	2 +
	SKB Skip if M and B do not compare ones	—	2, 3				WIM W-buffer into M when ready	3 +	3 +
							MIY M into Y-buffer when ready	2 +	2 +
Logical	ETR Extract	2	2				YIM Y-buffer into M when ready	3 +	3 +
	MKG Merge	2	2				POT Parallel output	3 +	3 +
	EOR Exclusive OR	2	2				PIN Parallel input	3 +	3 +
							EOM Energize output M	1	1

^aTime is given in computer cycle times. Each cycle time is 8 μ sec. Instructions that have conditional execution times are given with both times. Where instructions are not applicable to both computers, the computer not having the built-in instruction has a dash located under it in the Time column.

During the execution of "store" instructions, the operation and address of the instruction is transferred to the S-register to set up the store address. The data to be stored is then shifted into the C-register from its present location, and the information transferred in parallel to the M-register which stores it in memory.

To communicate with external devices such as photo tape, magnetic tape, punch, and typewriter, the computer uses the W-buffer with its associated character buffer as shown in Fig. 8. During an input process, 6-bit characters from the external device are transferred into the character buffer in parallel. When the W-buffer "control" detects that a character has been received, it shifts the character into the W-register; and when the W-register contains the desired number of characters, a

signal is sent to the computer to store the information held in the W-register into memory. For output the inverse operation is used; the information is shifted from the C-register to the W-register, and the computer returns to its previous program. The W-register now shifts one character at a time into the character buffer where it is sent out in parallel to the external device. When the W-buffer control detects that the W-register is empty, it signals the computer to load the W-register with another word for output.

c. Timing.

Pulse counter. Computer timing is derived from a 3.25-Mc clock by a 26-bit, modified, gray-code counter. Outputs from the counter are decoded for use in the computer logic. The data word is represented by the

Table 3. Instruction word format of the SDS 910 and 920 computers

	R	X	INSTRUCTION CODE								ADDRESS FIELD															
TP	0	1	2	3	4	5	6	7	8	9	10	11	12	13	14	15	16	17	18	19	20	21	22	23	24	
Bit number			Function																							
0			Relative address bit. A "1" in this position causes the location of the instruction to be added to the address at loading. This bit is not used in the logic of the computer.																							
1			Index register bit. A "1" in this position causes the contents of bits 10 through 23 of the index register (X register) to be added to the address portion of the instruction prior to execution.																							
2 through 8			Instruction code. The contents of bit 2 (programmed operator bit) determines the method of interpretation of the remaining 6 bits. If bit 2 contains a "0," the contents of bits 3 through 8 are decoded as a normal instruction. If bit 2 contains a "1," the instruction code is used to determine a subroutine entrance address.																							
9			Indirect address bit. A "1" causes the computer to interpret bits 10 through 23 of the instruction (possibly modified by indexing as the memory location where the effective address of the instruction may be found. A "0" causes bits 10 through 23 (possibly modified by indexing) to be interpreted as the effective address of the instruction.																							
10 through 23			Address. These bits normally determine the memory address referenced by the instruction code.																							
Positions 24 and TP are not available to the programmer; these are used as buffer or guard positions in the logic.																										

entire 26 bits with a resulting machine cycle time of 8 μ sec. The computer word is 24 bits, an extra 2 bits from the pulse counter serving as guard bits. The first bit of the word and guard bit is T24 and the last bit of the word and guard bit is Tp (Table 3).

Phase control. Various internal operations, such as transfers of information, clearing registers, read from memory, etc., which must take place during the reading and execution of instructions, are controlled by eight phases, designed ϕ 0 through ϕ 7. The phase counter (or register) is clocked by the Tp term from the pulse counter. The phases that are set into the register are a function of the phase the register is in and the instruction being operated upon. A general description of these eight phases follows:

- (1) Phase 0 (ϕ 0) is the beginning of all instructions. Instructions start at ϕ 0 T24 with the new instruction in the C-register and the instruction cleared to "NOP" (Table 3). If instruction requires only one cycle time for execution this phase steps directly to ϕ 5. Indexing and indirect addressing are processed in ϕ 0. Also, the memory regenerates the instruction (writes it back into memory because of destructive read-out) and fetches the operand. At ϕ 0 T24 the instruction code is transferred to the O-register.
- (2) Phase 1 (ϕ 1) is the set-up or preparation phase for the shift instructions. This phase inhibits pulsing the memory for an operand.
- (3) Phase 2 (ϕ 2) is the wait-phase for the input-output instructions. The computer idles in this phase until the data are ready. If the data are ready before the instruction is given, then ϕ 2 is bypassed except for the parallel input-output instruction, where ϕ 2 will last only one cycle time for data to be transferred.
- (4) Phase 3 (ϕ 3) is the execution phase for shifting and usually requires several word times. The duration of this phase is dependent upon the number of shifts required.
- (5) Phase 4 (ϕ 4) is the second cycle time of three cycle instructions which write data into memory. During ϕ 4, the P-register is incremented for accessing the next instruction, and the word to be stored is shifted serially into the C-register.
- (6) Phase 5 (ϕ 5) is the execution phase for some single cycle instructions. The C-register does not shift and parity is not checked.
- (7) Phase 6 (ϕ 6) is the main execution phase of instructions requiring an operand, but no memory modifications. These are the two cycle instructions, and include conditional skips which may require three cycles.
- (8) During Phase 7 (ϕ 7) cycle memory regeneration (or new storage) and next instruction access are performed.

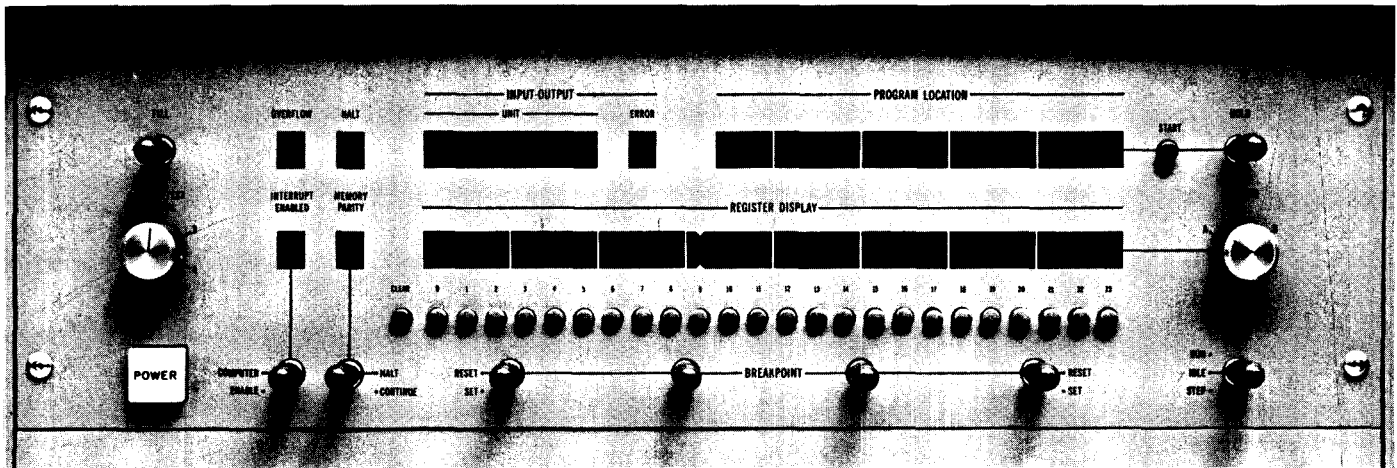


Fig. 9. Computer control panel

d. Methods of input-output.

Single bit input-output. The 910 and 920 are provided with instructions which transmit a pulse to set external signals and test the status of these signals. The address portion of each instruction is used to identify the external signal and over 16,000 distinct signals can be connected.

Input-output buffer system. The input-output buffer, or W-register, contains a full word register plus the associated control circuitry to transmit full data words to and from the computer's memory and 7-bit characters to and from external devices. Parity detection-generation is automatically performed in the buffer; the parity bit is not part of the computer word.

When the W-register has been filled on input (or emptied on output), an interrupt occurs to cause the computer to unload (or fill) the buffer. The programmer has the option, however, of disabling the interrupt prior to starting if the computer is not to perform simultaneous computation and input-output. In this case, when the input-output instruction is executed, the computer will "lock up" this instruction until the W-register has been emptied or filled.

A character counter, as set by the program, determines the number of characters required to fill the buffer. The number of characters can be set from 1 to 4. While the W-register is being emptied (or filled from the external device) other computations can be performed.

Parallel input-output. Data can be transferred between the computers and other devices, one word at a time (24

bits in parallel). When the parallel input instruction is executed, a "ready" signal plus the 14 address bits are transmitted to the peripheral unit. The address bits uniquely identify the unit to be connected. The ready signal causes the external unit to transmit up to 24 information bits directly into the C-register. After the information has been transmitted, the external unit sends a "complete" pulse to the computer. When received by the computer, memory parity is generated and the word is stored in the memory location determined by the address.

Parallel output functions in a similar manner.

External memory interlace. The computers are designed so that external devices may communicate directly with the computer's memory while internal computation is being performed.

Information is entered into (or taken from) the W-buffer and computation is automatically halted when the buffer is full (or empty). An externally held address controls the operation of the memory during this period, which is two machine cycles. The computer is then restarted. Since none of the internal registers are effectively affected, the computer can be halted during a long instruction. The maximum transfer rate is in excess of 60-kc characters per second.

e. Priority interrupt system. Each computer has two priority interrupt channels for handling asynchronous input-output devices in conjunction with the input-output buffer. Each channel causes the computer to interrupt to a unique memory location corresponding to

the interrupt channel number. When an interrupt signal is received, the present instruction is completed and control is transferred to the memory location corresponding to the channel number. The present contents of the P-register are stored and the program branches to the designated subroutine.

The interrupt system may be enabled or disabled by the program, as required, or may be manually enabled from the control panel, over-riding the interrupt status set by the program. Each computer also has 16 external interrupt channels, expandable to a total of 900.

f. Automatic power fail-safe system. Each computer has an automatic power fail-safe chassis to prevent information in the computer registers from being destroyed by loss of power. If the power should fail, this system provides for the contents of all registers and other volatile information to be automatically stored in core memory; also, further writing into core storage is inhibited during the decay period of the dc power supply outputs. Erroneous memory control is prevented during power-off and power-on operations. Power-off-on interrupt routines permit proper resumption of a program automatically after power is restored.

g. Control panel. The computer control panel (Fig. 9) permits operator intervention and displays the interval status of the computer. Displays and switches on the control panel are:

Displays.

- (1) *Program location.* The 14-bit P-register is continually displayed.
- (2) *Register display.* A 24-bit register display is provided in conjunction with a rotary selection switch. This display contains values of different interval registers depending on the locations of the rotary selection switch. The A-, B-, C-, X-registers can be displayed.
- (3) *Overflow.* The status of the overflow indicator is reflected by this display.
- (4) *Halt.* This display is turned on whenever "halt" is executed. It is turned off whenever an instruction other than "halt" is executed.
- (5) *Memory parity.* This indicator is turned on whenever a memory parity occurs.
- (6) *Interrupt enabled.* When this indicator is on the interrupt system is enabled.
- (7) *Input-output.* Six of these indicators reflect the address of the input-output unit presently connected to the W-register. The seventh indicator reflects the status of the input-output error indicator.

Switches.

- (1) *Clear.* When the computer is in "idle," depressing this switch clears the contents of the register being displayed.
- (2) *Register switches.* These 24 switches, located directly below the register display, permit insertion of information directly into the register being displayed.
- (3) *Run-idle-step.* This is a three-position toggle with two stationary positions and a spring-loaded momentary position in "step." In the "run" position, computation occurs at machine speed. In the "idle" position, the computer idles immediately after an instruction has been read from memory. In the "step" position, the instruction is executed and the computer returns to the "idle" state. The switch must be released to the "idle" position before another "step" may be performed.
- (4) *Register.* Function described under *register display*.
- (5) *Hold.* Prevents P-register from stepping.
- (6) *Memory parity.* Allows the computer to either "halt" or "continue" on memory parity errors.
- (7) *Interrupt enabled.* Allows for manual over-ride of computer interrupt disable instruction.
- (8) *Breakpoint.* Four switches that are used to control predetermined options within the program.
- (9) *Start.* Used to initiate the control section of the computer. The W-buffer is reset, the P-register is cleared, and "halt" is automatically executed.
- (10) *Fill.* Depressing this switch causes the computer to read one word (4 characters) automatically from Paper Tape Reader No. 1 into memory location 0002 and execute the instruction. A short "bootstrap" program can then be loaded and executed without further action by the operator. The "bootstrap" program is capable of loading a binary tape of any length into any portion of memory.

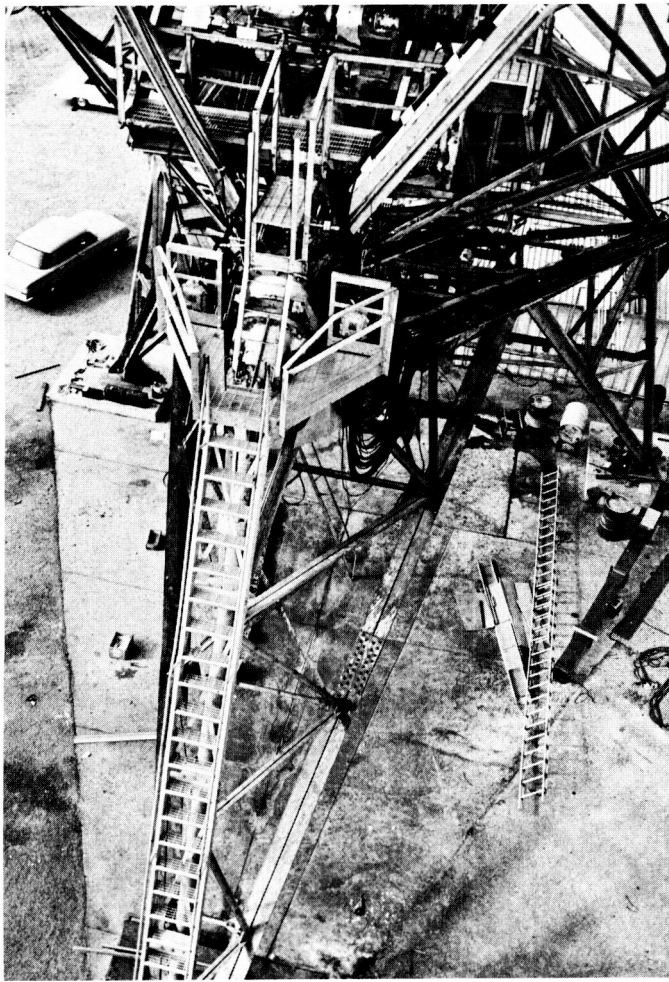


Fig. 10. North staircase and platform installed

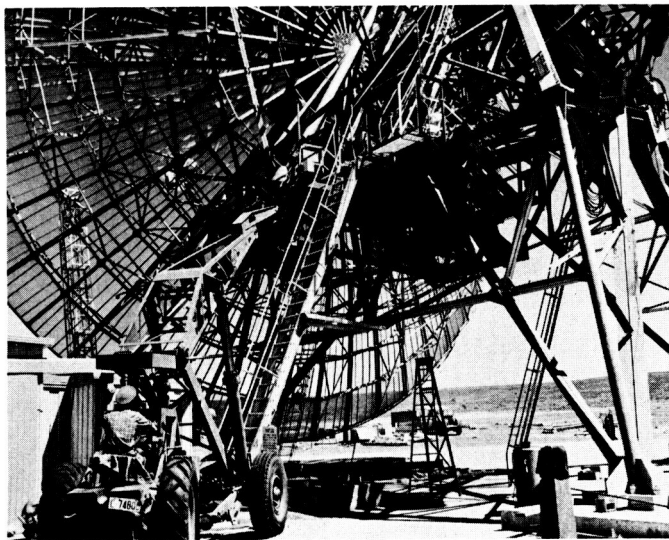


Fig. 11. South staircase installed

C. Installation of Safety Equipment at Woomera

The installation of equipment to improve the safety of maintenance personnel working aloft on the antenna began February 4, 1963 and was completed March 20, 1963.

Experience with some of the original rung-type ladders proved that they were difficult to negotiate while carrying tools or equipment. Where practical, the ladders were replaced with staircases designed by Blaw-Knox. In addition, cages and work rooms were installed to improve maintenance facilities.

- (1) Installation of a staircase and platform on the North side of the antenna (Fig. 10) and a staircase on the South side (Fig. 11).

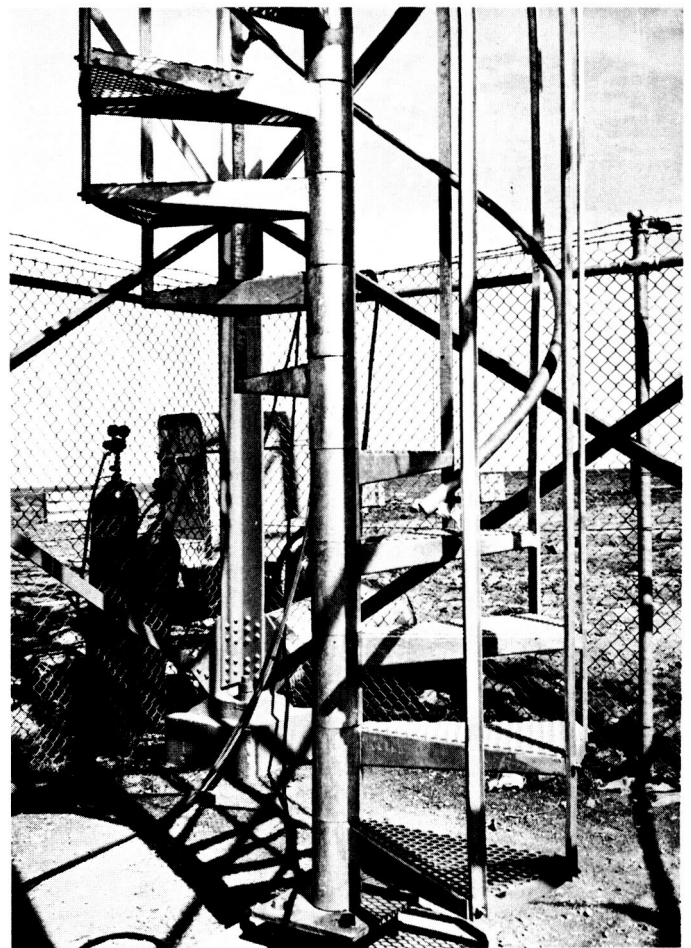


Fig. 12. Collimation tower spiral staircase

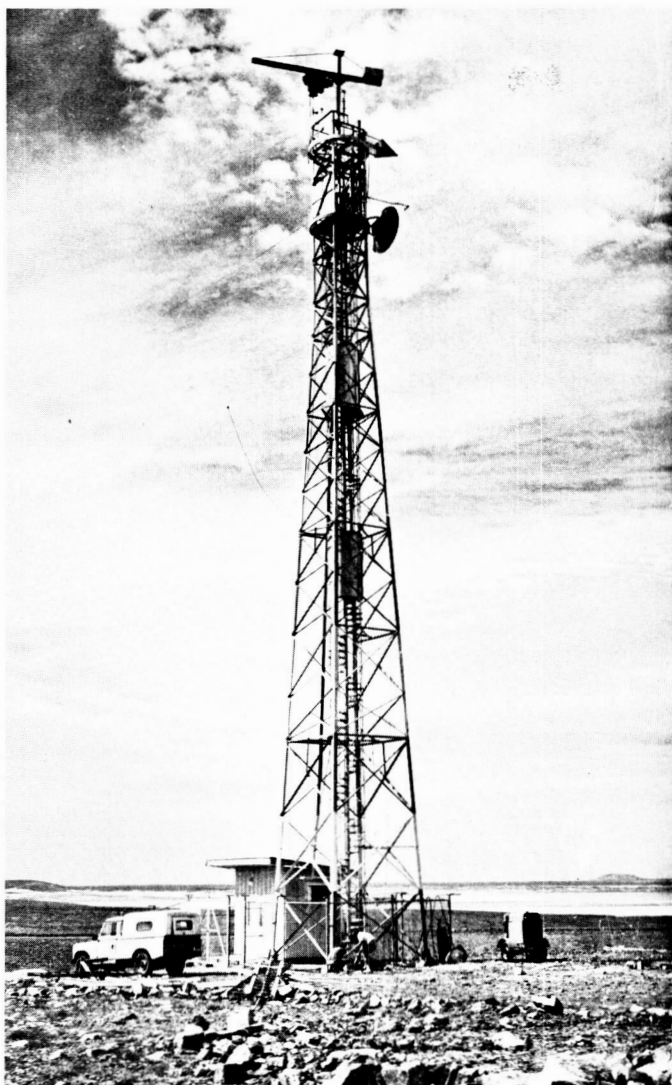


Fig. 13. Collimation tower showing jib crane at top



Fig. 14. Klystron cage and work rooms

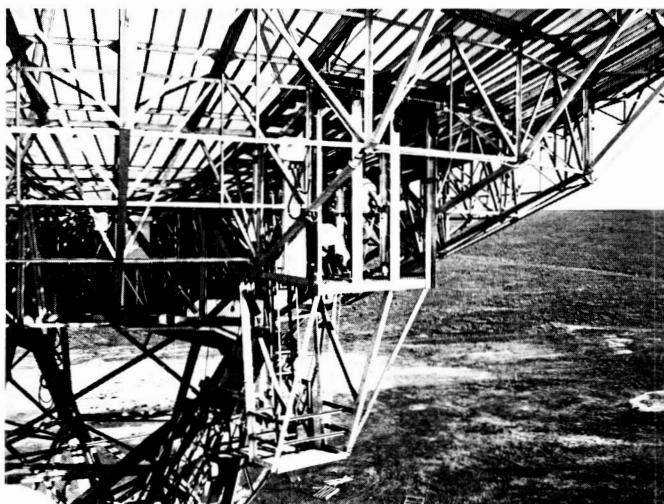


Fig. 15. Electronic cage

- (2) Installation of a spiral staircase up the center of the collimation tower (Fig. 12).
- (3) Installation of a jib crane at the top of the collimation tower (Fig. 13).
- (4) Installation of a klystron cage with work rooms in the back-up structure on the West side of the antenna (Fig. 14).
- (5) Installation of an electronic cage in the back-up structure of the antenna off the East declination bearing (Fig. 15).

The HA and Dec drives were also adjusted (Fig. 16) and the out-of-balance condition of the antenna tested. Out-of-balance readings were as follows:

- (1) Polar wheel measured 7,650 lb with the antenna dish pointed toward the East; 12,050 lb with the dish toward the West.
- (2) Declination wheel measured 2,100 lb with the dish toward the South; 5,100 lb with the dish toward the North.

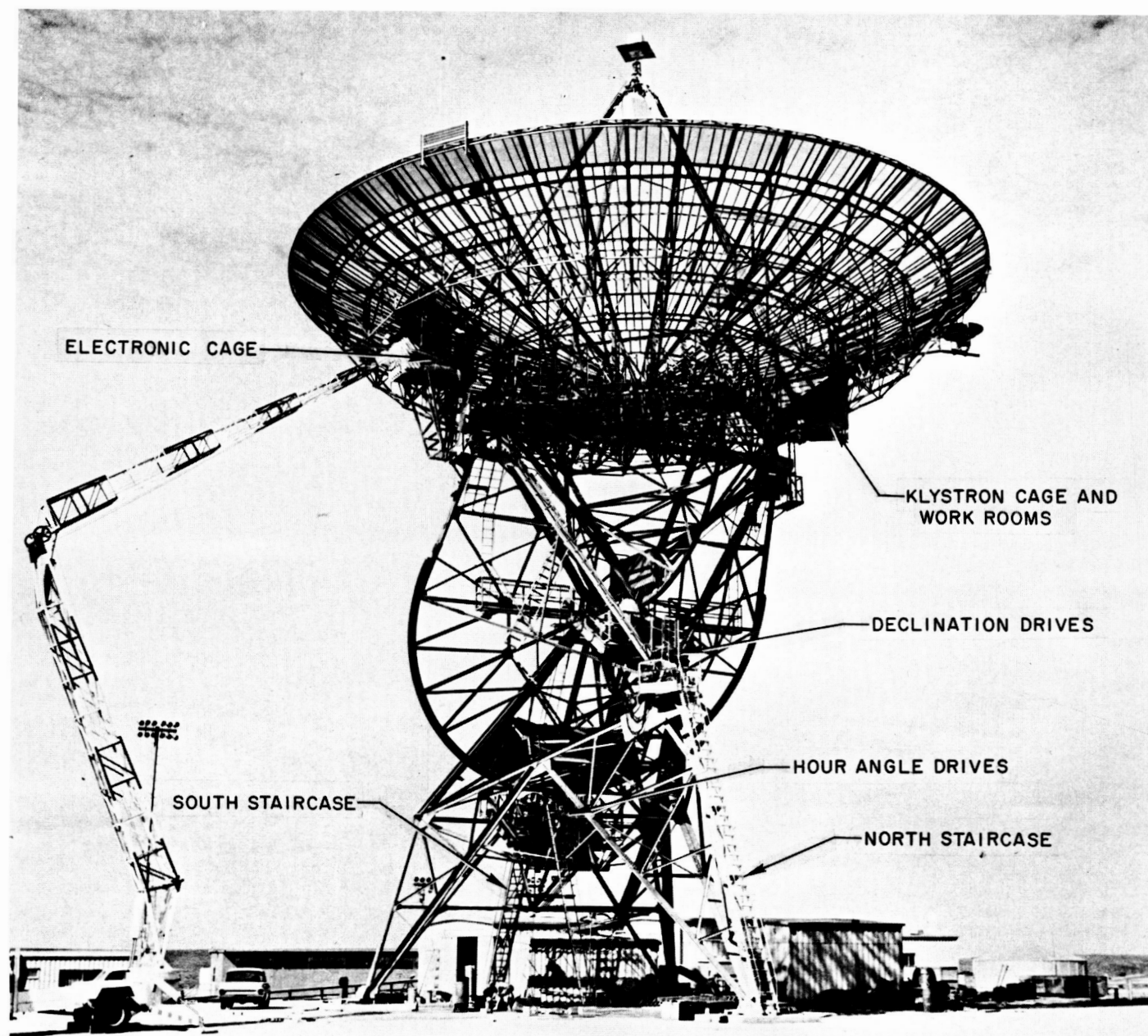


Fig. 16. Over-all view showing work performed

D. Mark I Ranging Subsystem

The Mark I ranging subsystem, the purpose and over-all description of which are to be found in the previous *Space Programs Summary* (SPS 37-20, Vol. III, pp 12-15), is being designed and built to equip the DSIF

with the capability of ranging on passive satellites and spacecraft *turnaround* transponders to distances of 800,000 km. This and subsequent *Space Programs Summaries* will detail the design and operation of the individual functional units of the subsystem.

1. Transmitter and Receiver Coders

The length of the pseudo-random binary digital code used for ranging determines the maximum unambiguous

Table 4. Code components used in ranging subsystem

Selected range	Bit length of code component	Component designation in XC	Component designation in RC
Moon or satellite	11	x	X
Moon or satellite	31	a	A
Moon	63	b_m	B_m
Satellite	7	b_s	B_s
Moon	127	c_m	C_m
Satellite	15	c_s	C_s

range that can be measured. The code is synthesized from several code components to minimize the steps, and hence the time, required for code acquisition. By choosing the components in accordance with certain mathematical criteria to feature two-level autocorrelation, the components are made individually acquirable. Complete code acquisition is the immediate result of having acquired all the components. The subsystem acquires an individual code component by phase shifting that component in the receiver coder, one bit at a time, while automatically monitoring the resultant degree of correlation between the code fed to the receiver and the code modulation returned from the spacecraft.

The pseudo-random binary digital codes, which modulate the ground-to-spacecraft carrier and detect the ranging modulation on the spacecraft-to-ground carrier, are generated in the transmitter coder (XC) and receiver coder (RC), respectively. The codes are made up of several components, suitably combined. The code components themselves are identical in the XC and RC. In Table 4, lower-case letters designate the components generated in the XC; upper-case letters designate those generated in the RC. The subscripts m and s are used to designate components used only in the long (Moon) or short (satellite) code, respectively.

All code components, except those of length 11, are generated in maximum-length shift registers. This is made possible by the fact that they contain $(2^n - 1)$ bits. The length-11 code components are direct-logic-generated Legendre sequences. Components of lengths 7 and 15 are generated in the same shift registers as components of lengths 63 and 127, respectively, suitably shortened by manual switch selection.

A word detector, provided for each code component in the XC and in the RC, generates a pulse each time that the component is repeated. A word coincidence detector, provided in the XC and in the RC, generates a pulse (w and W , respectively) each time the entire code

is repeated. During a ranging operation the time delay between w and W is determined by means of a counter-timer, which provides a visual read-out of the range for monitoring purposes.

a. Transmitter coder. A fifth code component, designated cl (clock), of 2-bit length, is generated in the XC only. The code components of the XC are combined in the Boolean logical form:

$$x \cdot cl + \bar{x} \cdot [(a \cdot b + b \cdot c + a \cdot c) \oplus cl]$$

The resultant code, in the form of a rectangular wave, is fed to the RF transmitter.

b. Receiver coder. The four code components of the RC are combined in accordance with the respective acquisition mode of the ranging subsystem as follows:

Acquisition Mode 1. Code $\bar{X} \cdot A$. This code serves to acquire components x and a of the modulation code on the returned signal.

Acquisition Mode 2. Code $\bar{X} \cdot B$. This mode serves to acquire component b .

Acquisition Mode 3. Code $\bar{X} \cdot C$. This mode serves to acquire component c .

Acquisition Mode 4. Code $\bar{X} \cdot (A \cdot B + B \cdot C + A \cdot C)$. This mode is used for ranging, acquisition having been completed.

The respective resultant code, in the form of a rectangular wave, is fed to the RF receiver.

Means are provided to synchronize the code components in the RC to those in the XC, preceding ranging acquisition. Means are also provided to shift the RC code components individually with respect to their counterparts in the XC, one bit at a time. A "shift-left" command causes one bit of the selected code component to be skipped once, shortening the component. Conversely, a "shift-right" command causes one bit of the selected code component to be repeated once, lengthening the component. The 1-bit offset with respect to the component's counterpart in the XC, resulting from such a shift, is then maintained.

2. Chinese Number Generator

When, in the course of code acquisition, a code component in the RC is shifted in phase by 1 bit, the corresponding phase shift of the combined code is not simply related to that 1-bit shift. The number of bits of phase

shift of the combined code engendered by a 1-bit shift on one of the components is referred to as the Chinese number of that component. This number is derived by an application of the Chinese Remainder Theorem of Number Theory (Ref. 1).

A definition of the Chinese numbers N_X , N_A , N_B , N_C of code components of lengths X , A , B , and C bits is given by:

$$N_X = 1 \text{ (Modulo } X) = 0 \text{ (Modulo } A) \\ = 0 \text{ (Modulo } B) = 0 \text{ (Modulo } C)$$

$$N_A = 0 \text{ (Modulo } X) = 1 \text{ (Modulo } A) \\ = 0 \text{ (Modulo } B) = 0 \text{ (Modulo } C)$$

$$N_B = 0 \text{ (Modulo } X) = 0 \text{ (Modulo } A) \\ = 0 \text{ (Modulo } B) = 0 \text{ (Modulo } C)$$

$$N_C = 0 \text{ (Modulo } X) = 0 \text{ (Modulo } A) \\ = 0 \text{ (Modulo } B) = 0 \text{ (Modulo } C)$$

The total length in bits of the code, which is the product of the lengths of its components, is referred to as the Modulo (or Mod) number; it is designated by the letter M . Thus,

$$M_m = X \cdot A \cdot B_m \cdot C_m$$

and

$$M_s = X \cdot A \cdot B_s \cdot C_s$$

Code component phase shifts totaling an integral number of Mod numbers thus result in zero combined-code shift.

Table 5 shows the actual numbers applicable to this subsystem.

The Chinese number generator provides the numbers, which must be added to (or subtracted from) the cumulative total in the range tally, for an RF doppler count, a clock doppler count, or a 1-bit shift of a code component during acquisition. The smallest range increment which can be tallied is that indicated by a $\frac{1}{2}$ -cycle RF doppler shift. This is arbitrarily tallied as 1 range unit (RU). Range increments can also be tallied as indicated by $\frac{1}{4}$ -cycle clock doppler shifts (on 500 kc, nominal). Such tallies are then equal to

$$\frac{1}{2} \left(\frac{\text{RF frequency}}{\text{clock frequency}} \right) \text{RU},$$

Table 5. Chinese numbers and Modulo numbers used in ranging subsystem

Moon code			
		Modulo number =	2,728,341 bits
X-component:	Length = 11 bits,	Chinese number =	992,124 bits
A-component:	Length = 31 bits,	Chinese number =	1,408,176 bits
B _m -component:	Length = 63 bits,	Chinese number =	736,219 bits
C _m -component:	Length = 127 bits,	Chinese number =	2,320,164 bits
Satellite code			
		Modulo number =	35,805 bits
X-component:	Length = 11 bits,	Chinese number =	32,550 bits
A-component:	Length = 31 bits,	Chinese number =	4,620 bits
B _s -component:	Length = 7 bits,	Chinese number =	15,345 bits
C _s -component:	Length = 15 bits,	Chinese number =	19,096 bits

corresponding to a shift of $\frac{1}{4}$ of 2 μsec , or 0.5 μsec . A shift of 1 bit ($=1 \mu\text{sec}$) in the course of code acquisition then corresponds to

$$\left(\frac{\text{RF frequency}}{\text{clock frequency}} \right) \text{RU}.$$

To convert the Chinese and Mod numbers in bits to Chinese and Mod numbers in range units, they must be multiplied by this ratio.

These ten products, as well as the numbers corresponding to the dopplers to be tallied, are generated in the Chinese number generator in series-binary form. They are obtained by adding (logical OR function) the appropriate timing pulses from the timer.

3. Timer

The timer is a 1-Mc, 31-stage, open-ended shift register. Each stage consists of a digital dynamic module, providing both direct and complemented outputs with sufficient power to drive 20 and 40 gate loads, respectively, throughout the subsystem.

An input pulse is provided to the timer every 31 μsec by the length-31 code component word detector of the transmitter coder. The "minor machine cycle" of the subsystem is defined as this 31- μsec period. A two-stage binary counter, also run by this pulse, defines the 124- μsec "major machine cycle" and its four minor phases.

Reference

1. Stewart, B. M., *Theory of Numbers*, pp. 130-131. The Macmillan Company, New York, 1952.

III. Research and Development

A. Experimental Low-Noise Systems

1. Traveling Wave Maser for DSIF

The development of a prototype 2295-Mc traveling wave maser (TWM) for the DSIF is nearly complete. Various aspects of the developmental problems have been discussed in recent *Space Programs Summaries* and, in this report, a critical review of the noise performance of traveling wave masers is given. It is shown in particular that when the gain per unit length of structure is low, the equivalent noise temperature of the TWM can become appreciable.

a. Noise temperature for TWM. The expression for noise temperature of a TWM has been derived by many investigators, and we shall here use the form given by Siegman (Ref. 1).

$$T_M = \frac{G-1}{G} \left[\frac{\alpha_s T_s}{\alpha_s - \alpha_0} + \frac{\alpha_0 T_0}{\alpha_s - \alpha_0} \right] \quad (1)$$

where

T_s = spin temperature

T_0 = structure temperature

α_s = gain coefficient per unit length of the TWM

α_0 = loss coefficient per unit length of the TWM

and

$G = e^{2(\alpha_s - \alpha_0)L}$ = net gain for a TWM of length L

The usual assumptions made in the discussion of TWM is that, generally, $G \gg 1$ and $\alpha_s \gg \alpha_0$.

Then it is seen that Eq. (1) becomes

$$T_M = T_s + \frac{\alpha_0}{\alpha_s} T_0 \quad (2)$$

Since T_s is generally a fraction of the bath temperature, i.e.,

$$T_s \simeq \frac{f_s}{f_p - f_s} T_0 \quad (3)$$

where f_s = signal frequency and f_p = pump frequency, it is seen that T_M can be very small. The system noise contribution originates in the input transmission line losses and in the follow-up receiver.

These results are a consequence of the assumption of high gain per unit length of structure. This assumption is a reasonable one for ruby masers operating at 1.5 to 2.5°K, but it is not necessarily valid for operation at 4.2°K or higher temperatures. At the latter temperatures

it is still possible to obtain high net gain, G ; however, the gain per unit length is small and a long structure is necessary. Eq. (1) now takes the approximate form

$$T_m \simeq \frac{\alpha_s T_s}{\alpha_s - \alpha_0} + \frac{\alpha_0 T_0}{\alpha_s - \alpha_0} \quad (4)$$

It is noted from Eq. (4) that if the coefficient for net gain per unit length, $\alpha_s - \alpha_0$, is small then T_m could become appreciable. A typical set of operating data with the prototype TWM at 2300 Mc is: $\alpha_s = 3.8$ db/in., $\alpha_0 = 1.4$ db/in., $T_0 = 4.3^\circ\text{K}$, T_s is ideally $T_0 (2.3/10.4) = 0.95^\circ\text{K}$ and, at worst, as high as T_0 or 4.3°K . Using these values, we have

$$T_m = 4^\circ\text{K} \text{ (minimum)}$$

and

$$T_m = 9.3^\circ\text{K} \text{ (maximum)}$$

These values are to be compared with $T_m = 0.95^\circ\text{K}$ for the very rough approximation $T_m = T_s$, which is usually made. The foregoing discussion indicates the need for careful design of a TWM when operating at elevated temperatures (42°K or higher) which the present state-of-art in closed-cycle refrigerators, unfortunately, requires. Particularly important is the need to reduce the forward loss of the structure (including ferrite).

2. Radio Frequency Interference—Automotive Ignition

During several UHF low-noise testing programs at the Goldstone Tracking Station, it has been found that motor vehicles caused microwave interference. A mobile Dicke radiometer has been constructed at the Laboratory to measure interference levels at 2.38 Gc. Of the vehicles tested to date the maximum flux density measured was approximately -183 dbm/cps/ m^2 at a distance of 50 ft. Interference produced by two 15-w fluorescent light bulbs was also measured and it was found to be approximately -187 dbm/cps/ m^2 at a distance of 50 ft.

a. Introduction. During several low-noise radiometric experiments at Goldstone, it was found that automotive microwave noise, was sufficiently intense to disrupt measurement operations. It was found, during attempts to measure the black body radiation of the planet Venus with a total power radiometer, that certain trucks completely jammed out the planetary thermal signal. The thermal emission of Venus produced approximately 0.2°K

temperature change (on September 20, 1962) which is equal to an input power change of $K\Delta TB = -205.6$ dbm/cps. To convert this to flux density, let us assume that the interfering signal entered the side lobes at isotropic level; then, $A = \lambda^2/4\pi = -29$ db(m^2), and the equivalent flux density is then -176.6 dbm/cps/ m^2 . This value represents the flux necessary to double the apparent change in temperature through the back lobes. However, it would have been desirable to measure 0.2°K to an accuracy of 10% so that the allowable flux density level should be set at -186.6 dbm/cps/ m^2 for back lobe interference. Drake and Ewen (Ref. 2) describe a radiometer which has a minimum resolvable sensitivity of 0.01°K which equals -218.6 dbm/cps and, if we assumed our antenna back lobe characteristics and 10% accuracy, we would have a minimum allowable flux density of -199.6 dbm/cps/ m^2 .

b. Measurements. To make the measurements, a Dicke radiometer was constructed. It operates as a double side-band receiver with a local oscillator frequency of 2.38 Gc. A 30-Mc IF is employed with a 9-Mc bandwidth. The noise figure was 5.5 db unswitched and 8.5 db when switching. Since the radiometer was to be used as a portable device, a Dicke system was chosen because of its relative insensitivity to line-voltage fluctuations and its short warm-up time requirements. The radiometer and horn antenna used are shown in Figs. 1 and 2. The devices around the mouth of the horn are sidelobe suppressors (which have not been tested yet). A rough measurement

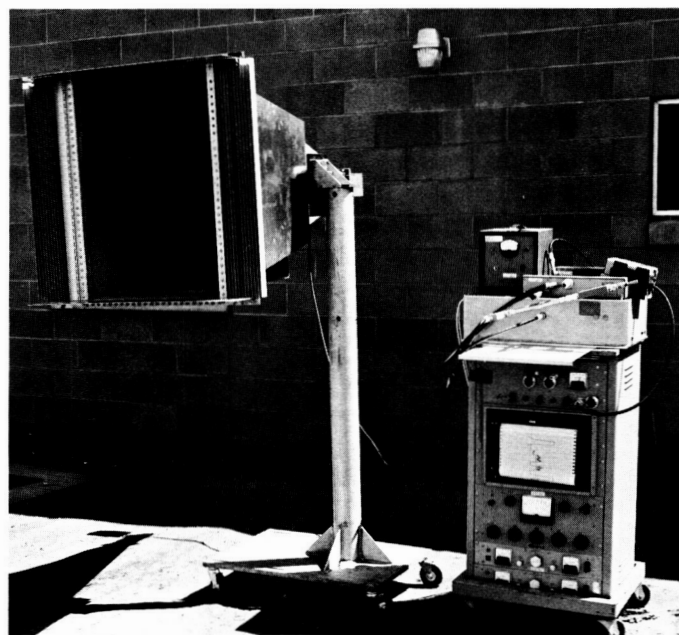


Fig. 1. Radiometer and horn

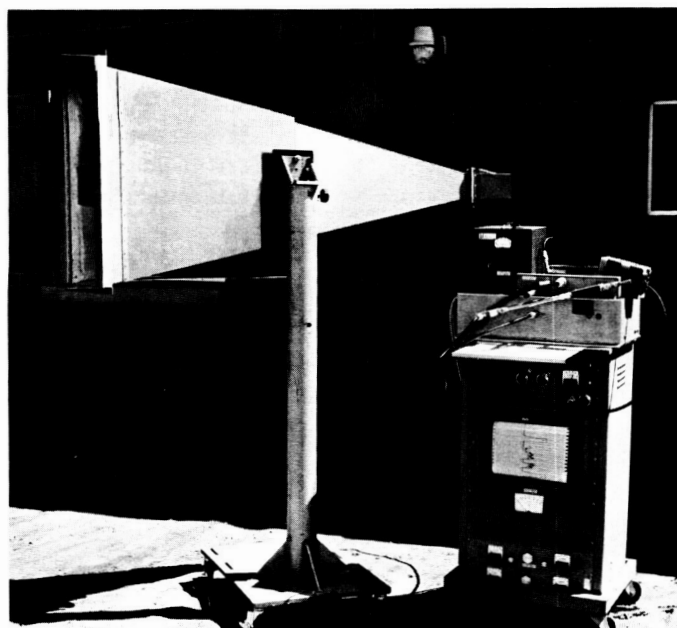


Fig. 2. Radiometer and horn, side view

of horn gain showed it to be 24.8 ± 1 db, which gives it an effective area of about 0.38 m^2 . In all the measurements made, the *E*-vector was horizontal.

The measurement procedure in all cases was to park the automobile 50 ft away from the horn in the main beam of the antenna, establish a signal level with the motor off, fire a gas tube pulse which increased the effective temperature by 100°K , let the radiometer settle to its original level, and then start the auto. It was not possible to simply drive the car through the main beam of the antenna since reflections from the metallic body changed the effective input temperature even with the motor off.

Fig. 3 shows the radio frequency noise produced by a 1954 Jaguar XK 120. The maximum noise level is approximately 38°K and occurs at the maximum rpm tried. After the motor was turned off, the radio was tried and found to contribute about 2°K , probably due to a noisy vibrator. Fig. 4 is the recording produced by a 1958 Volvo PV444. The maximum interference is about 7°K . Both pens are recording the same data.

Fig. 5 was produced by a 1962 International Pickup Truck. Turning the ignition on and off produced transients of as much as 19° with a 1-sec radiometer time constant (as were the time constants of the two preceding records). The maximum running temperature increase was about 6°K .

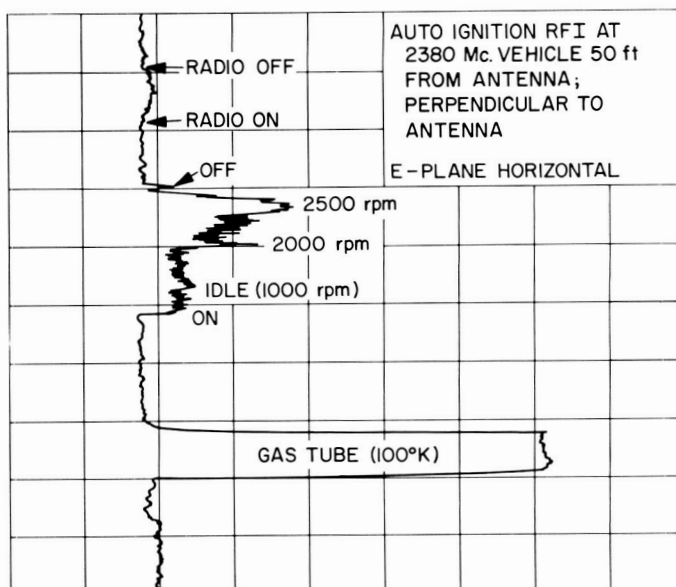


Fig. 3. 1954 Jaguar, 2.38-Gc interference

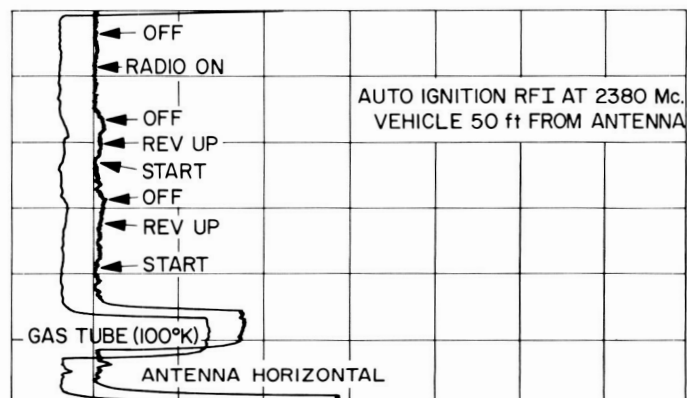


Fig. 4. 1958 Volvo PV444, 2.38-Gc interference

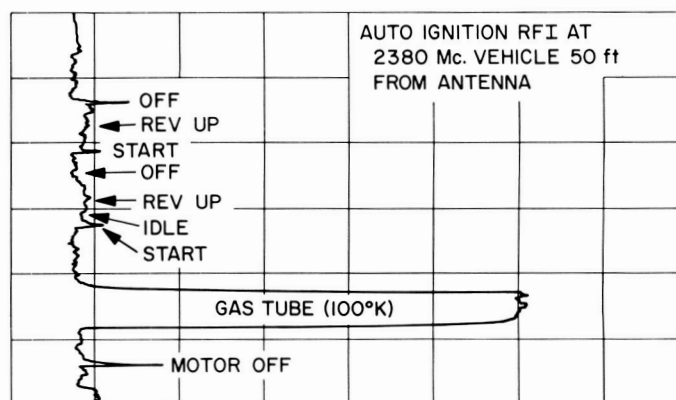


Fig. 5. 1962 International Pickup, 2.38-Gc interference

Fig. 6 shows the record of a 1962 Ford Falcon in which the temperature increase is approximately 6°K (the time constants of both pens were 1 sec). Fig. 7 shows the record produced by a 1959 Opel. Even though there was trouble starting, there is not sufficient signal to distinguish it from the system noise. Fig. 8 shows the record pro-

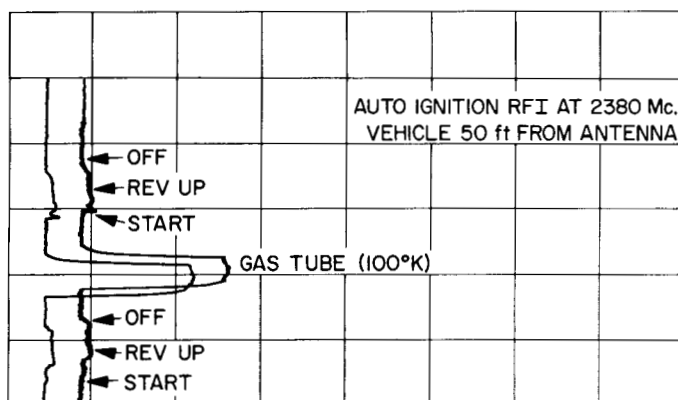


Fig. 6. 1962 Ford Falcon, 2.38-Gc interference

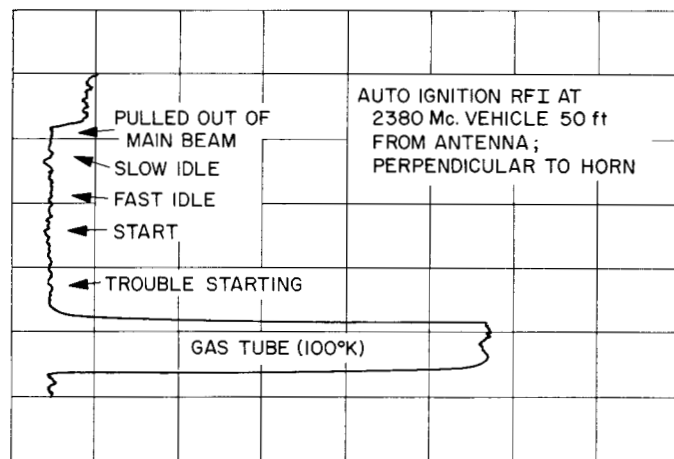


Fig. 7. 1959 Opel, 2.38-Gc interference

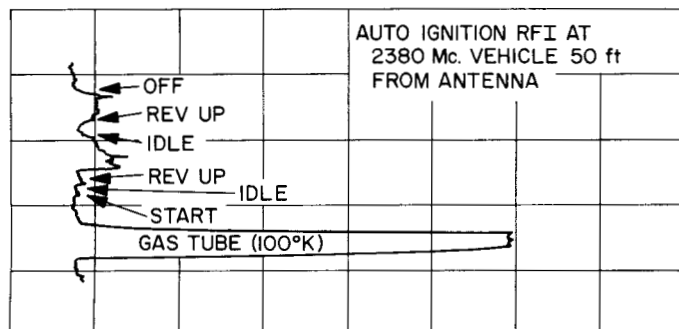


Fig. 8. 1956 Ford Station Wagon, 2.38-Gc interference

duced by a 1956 Ford Station Wagon; the maximum displacement was approximately 10°K . Fig. 9 is a record of the noise produced by a 1963 Porsche; the maximum signal appears to be less than 3°K .

Fig. 10 shows the record of a 1959 Renault Dauphine. One pen used a 5-sec time constant and the other used a 1-sec time constant. At the bottom of the record a 6° pulse can be seen from the driver getting into the car and a little later a 12° pulse from a truck driving through the beam. In this run the radiometer was attached to the horn antenna and a maximum signal of approximately 87°K was obtained. To prove that the signal was coming in at RF instead of IF, the antenna was replaced by a liquid nitrogen cooled load. It can be seen that there is no appreciable effect from the car with the nitrogen

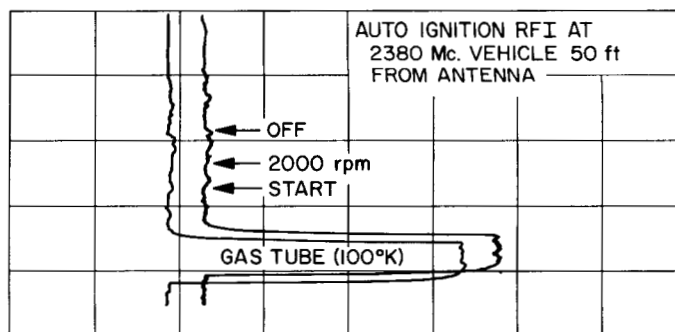


Fig. 9. 1963 Porsche, 2.38-Gc interference

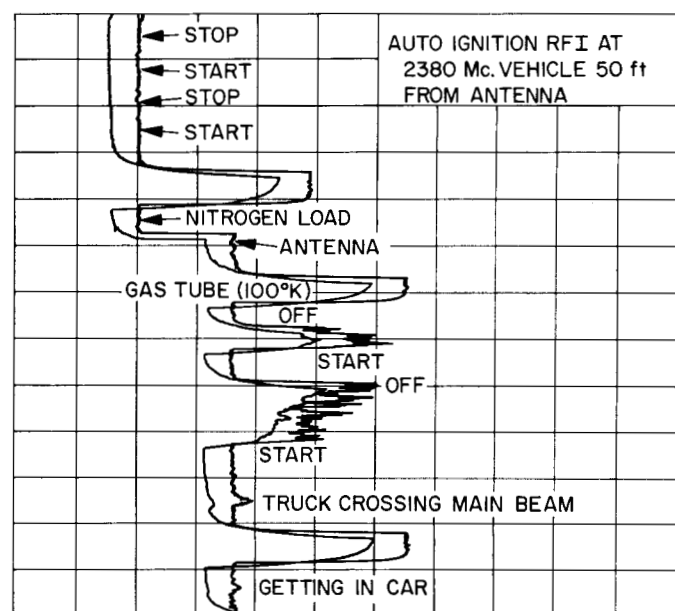


Fig. 10. 1959 Renault, 2.38-Gc interference

load on. Fig. 11 was produced by a six-cylinder 1960 Rambler Station Wagon which produces less than 4°K .

Fig. 12 shows the noise produced by a 1957 MGA. It can be seen that the interference level of this car is a very strong function of rpm. It appears that there is a resonance with a maximum of 100°K at 1500 rpm. When the speed is increased to 2500 rpm, the noise level is seen to decrease; upon deceleration, the level again rises.

A test was also run on a draftsman's-type fluorescent lamp containing two 15-w bulbs at 50 ft. Fig. 13 shows

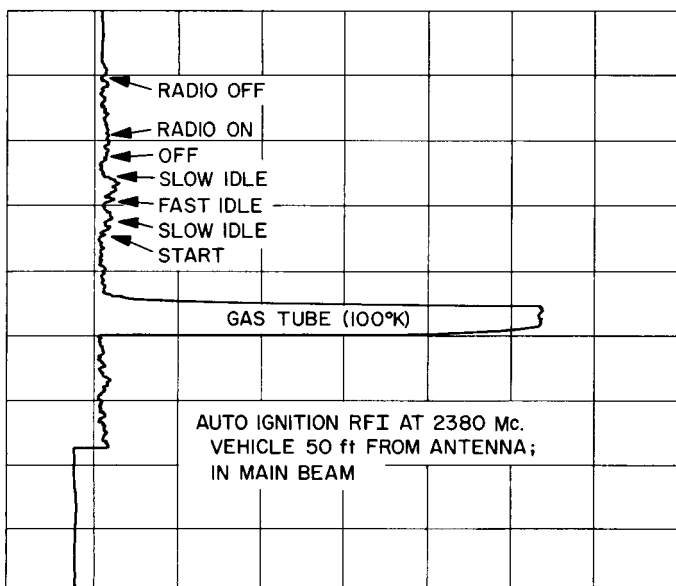


Fig. 11. 1960 Rambler (six cylinder), 2.38-Gc interference

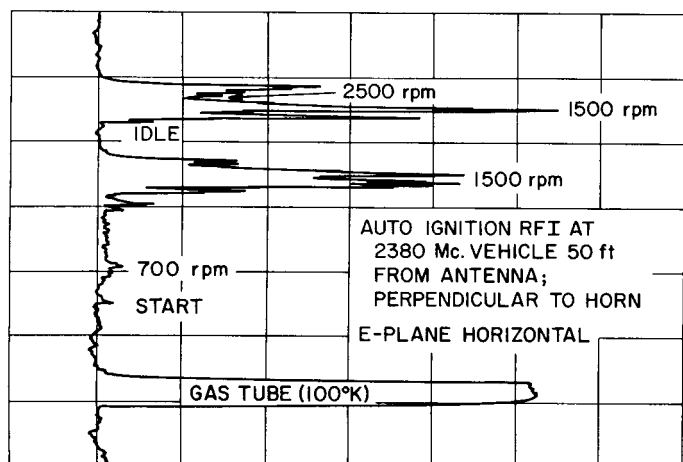


Fig. 12. 1957 MGA, 2.38-Gc interference

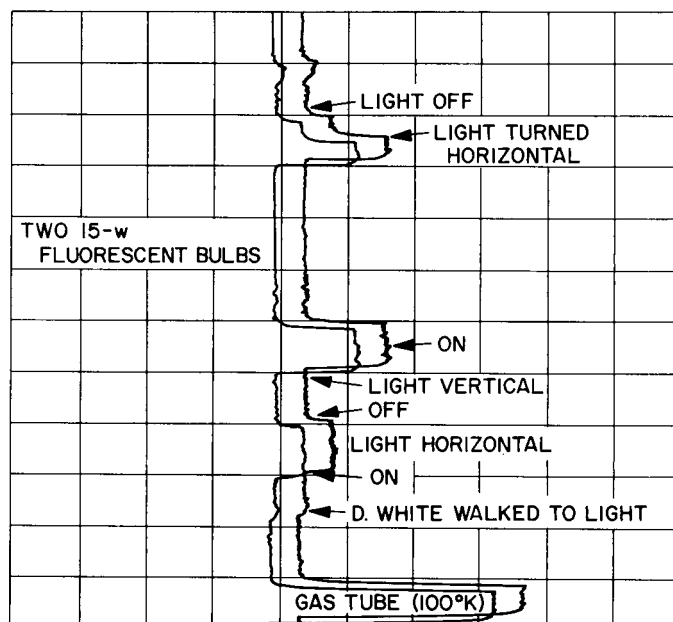


Fig. 13. Two 15-w fluorescent tubes, 2.38-Gc interference

the results. It can be seen that the level changed when someone approached the light to turn it on. With the horn horizontally polarized it was found that the fluorescent light bulbs produced 12°K when horizontal and 36°K when vertical.

Table 1 summarizes these results in terms of maximum temperature and flux density.

Table 1. Results of automotive noise on low-noise radiometric experiments

Source	Maximum temperature change, $^{\circ}\text{K}$	2.38-Gc flux increase at 50 ft, $-\text{dbm}/\text{cps}/\text{m}^2$
1954 Jaguar 120	38	-186.3
1958 Volvo PV444	7	-193.6
1962 International Pickup Truck	6	-194.2
1962 Ford Falcon (six cylinder)	6	-194.2
1959 Opel	Below threshold	
1956 Ford Station Wagon	10	-192.0
1963 Porsche	3	-197.2
1959 Renault Dauphine	87	-182.6
1960 Rambler Wagon (six cylinder)	4	-196
1957 MGA	100	-183
Fluorescent light (two 15-w tubes):		
Horizontal	12	-191.2
Vertical	36	-186.5

It should be pointed out that these measurements are made in terms of average temperature rather than peak values as usually reported in the literature. (See SPS 37-18, Vol. III and Refs. 2, 3, and 4.)

The data reported above includes a fairly limited sample. Schildknecht found that at 900 Mc trucks radiate 10 db more than autos. A larger sample is required to see if this is the case at 2.38 Gc.

Advanced Antenna System. Design, installation, and mechanical testing of the Cassegrain cone are described. The program for radio frequency tests on the antenna is discussed and some preliminary experimental and analytical results given. Analysis of the servo tests on the antenna is continuing.

a. Antenna structure. SPS 37-20, Vol. III contained the experimental data on the structural and mechanical characteristics of the completed antenna structure. Also presented were contour maps which describe the surface condition in all reflector attitudes while subjected to various environmental conditions.

B. Ground Antennas

1. 30-Ft Diameter Azimuth-Elevation Antenna

The 30-ft antenna has been fitted with a Cassegrain feed system which is a $\frac{1}{2}$ -scale model of the 210-ft

During the last 2-mo period, a Cassegrain feed system has been installed on the antenna. This report covers design, fabrication, and testing of the Cassegrain cone. Sections B-1-b and -c of this article outline the RF tests to be conducted on the Cassegrain system.

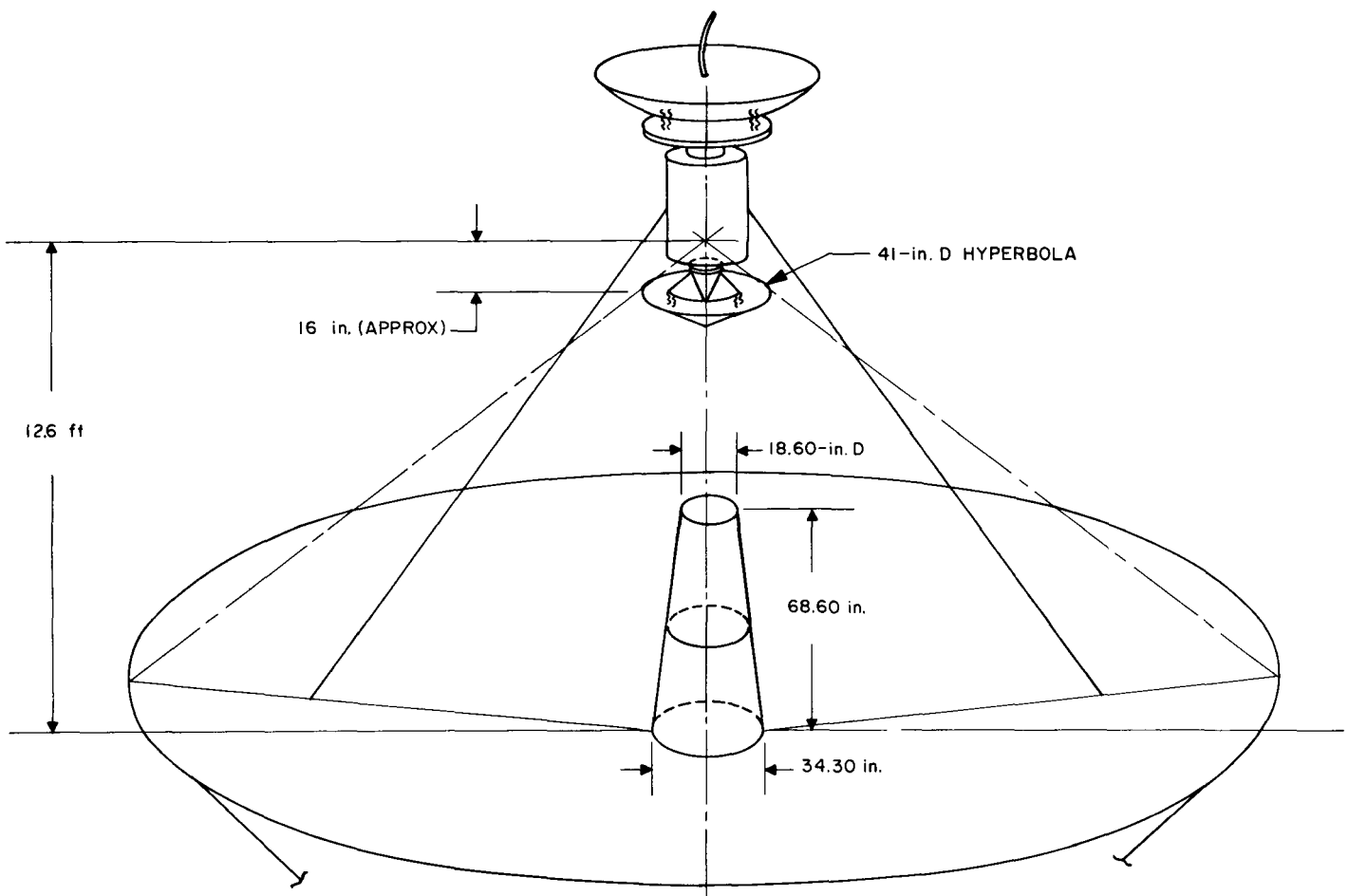


Fig. 14. Cassegrain cone assembly

Design parameters. The basic requirements in the design of the Cassegrain cone were to provide a high-rigidity, compact-size, and lightweight cone capable of supporting a feed system weighing 350 lb. Accessibility of optical instrumentation within the base of the cone and clear lines of sight to various antenna surface targets were other significant design criteria. See Fig. 14 for general description.

Testing of Cassegrain cone before installation. Tests were conducted at the manufacturer's (Rohr Corp.) plant to determine the maximum deflections of the Cassegrain cone without the influence of the antenna primary reflector deflections. Fig. 15 shows the two-section cone placed in a horizon look to measure its deadload deflections. The procedure for measuring its deflections was to first set the cone at the zenith look; by placement of a target on an arm at the end of the cone, an alignment telescope was located at the base plate and a zero reference was taken.

The deadload deflection of the cone was determined by rotating the cone assembly and measuring the displacement of the target:

- (1) Elevation angle of cone: 90° (zenith) antenna coordinates; telescope micrometer set to 0.0 in.

- (2) Elevation angle of cone: 180° (horizon look in a plunged attitude); displacement of target = 0.000 in.

The second set of measurements was conducted with a simulated feed load to determine the total deflection in the horizon look. To correctly load the feed cone about the center of gravity of the feed package, lead weights were attached (Fig. 16) at the separation point of the two cone sections and at the end of the top section:

- (1) Elevation angle of cone: 180° (horizon look in a plunged attitude).
 - (a) Total applied weight at the separation point = 142 lb.
 - (b) Total applied weight at the end of top section = 208 lb.
 - (c) The CG of the feed assembly = 54 in. from the cone base (parabola vertex).
- (2) The total deflection with the applied load = 0.005 in.

The total weight of the Cassegrain cone with covers but excluding the feed assembly was 320 lb.

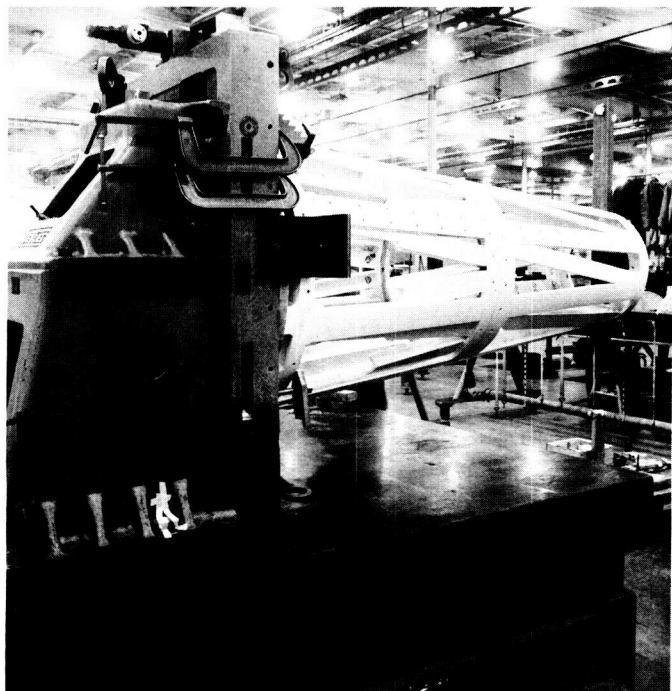


Fig. 15. Deadload deflection measurement
(cone only)

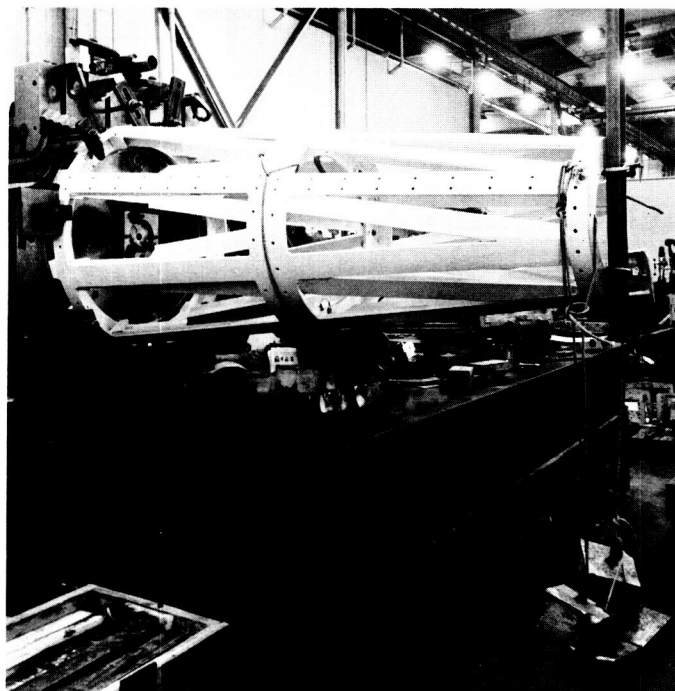


Fig. 16. Deadload deflection measurement
(with simulated feed)

Field installation. The basic design of the Cassegrain cone, its mount, and the modifications made to the antenna structure allow the antenna to be used as a Cassegrain or a prime focus system. Fig. 17 shows the mounting ring for the cone assembly. This ring is located below the surface plane of the parabola and is accessible by removal of the center surface panel. Fig. 18 shows the cone assembly attached to the base ring. Note the slotted windows at the separation point. These windows permit radial measurements by use of a gage bar to various reference targets on the face of the parabola without removal of the cone assembly. Fig. 19 shows the Cassegrain cone being installed. A special handling harness for installing the cone is fixed to the top of the cone; the harness also provides protection for the RF feed horn which protrudes above the Cassegrain cone.

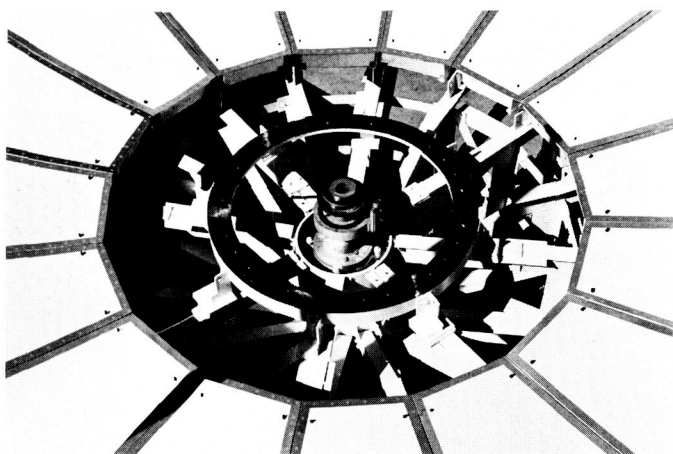


Fig. 17. Cassegrain cone mounting ring

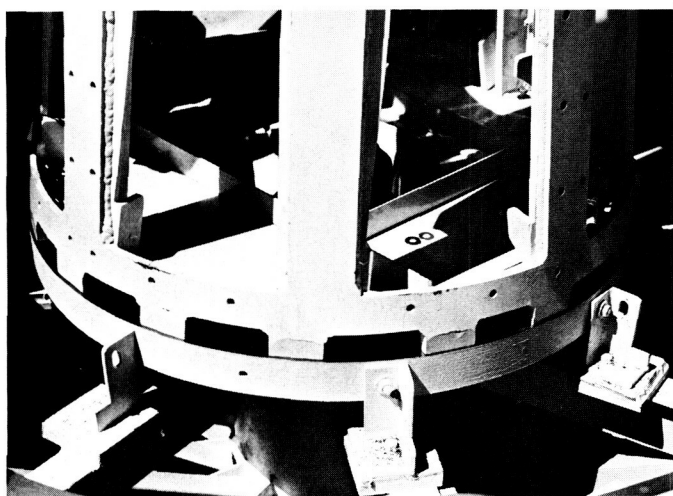


Fig. 18. Separation point, Cassegrain cone and mounting ring

The mounting ring and cone assembly were installed and aligned to a reference plane (datum targets) located within the antenna structure previously used for alignment of the paraboloidal surface. Upon completion of the installation, measurements were made to determine the combined deflections of the Cassegrain cone and the reflector structure. A Watts Microptic theodolite was used as the reference instrument to measure the axial alignment of the cone with respect to the prime surface (paraboloid) and the secondary reflector (hyperboloid) at the apex. The first measurement taken was to determine the displacement of the Cassegrain cone excluding the feed assembly at the horizon with respect to zenith:

- (1) Combined deflection of reflector and cone assembly.
 - (a) Reference: 90° elevation.
 - (b) Measurement: 180° elevation.
 - (c) Deflection: deadload = 0.038 in.
- (2) Combined deflection of reflector and cone assembly with simulated feed load.
 - (a) Reference: 90° elevation.
 - (b) Measurement: 180° elevation.

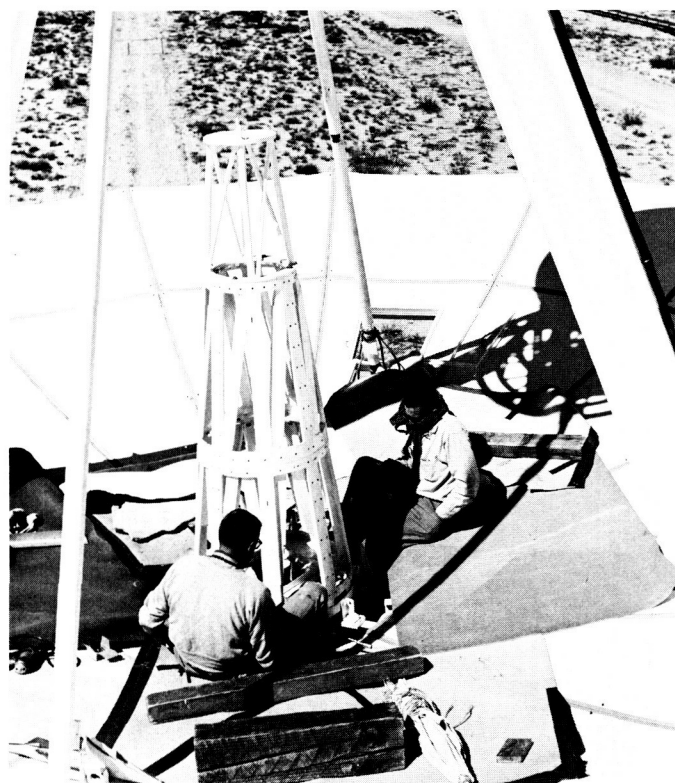


Fig. 19. Cassegrain cone assembly installation

- (c) Simulated load: 142 lb at central point of cone, 208 lb at the end of top section.
- (d) Deflection: deadload = 0.0535 in.

The results of the combined deflections indicate further measurements shall be undertaken to determine the areas contributing the excessive displacement of the Cassegrain cone under full load.

b. Servo tests. In SPS 37-20, Vol. III, the servo system test program on the 30-ft antenna was discussed. At the date of the writing, the data reduction for the dynamic testing portion of the program was not completed, and transfer function-network compensation had not been conducted. Subsequently, the network compensation portion has been conducted and the data reduction of the dynamic tests is continuing.

Preliminary interpretation of the data indicates inconsistencies when the servo transfer functions and the dynamic data are compared.

In the dynamic testing the driving source was a variable frequency generator and the motion data was recorded on 8-channel recorders. In the transfer function testing the driving source was a servo analyzer and the data reduction was performed by the analyzer. This data was then written on the data sheet in longhand.

The data from the two types of tests obtained can be reduced to the same dimensional form, that is, phase-amplitude versus frequency. A comparison of data indicates a wide discrepancy. Additional investigations will have to be conducted to resolve the questions.

c. RF tests on 30-ft antenna. The equipment necessary for the RF study program on the 30-ft antenna (SPS 37-19, Vol. III, pp. 32-35) has been installed and preliminary measurements necessary to evaluate the 30-ft antenna site, the X-band Cassegrain system, and Tiefort Mountain collimation station are in progress.

The measurements to be made include absolute gain, relative gain, beam width, beam position, beam shift, radiation patterns, focal point shift, and correlation of these effects with the measured 30-ft paraboloid distortions (SPS 37-20, Vol. III, pp. 28-31).

A 10-ft illuminator antenna at Tiefort (Fig. 20) has been gain calibrated (45 db) at 8450 Mc to accomplish the absolute gain measurements. The relative gain meas-

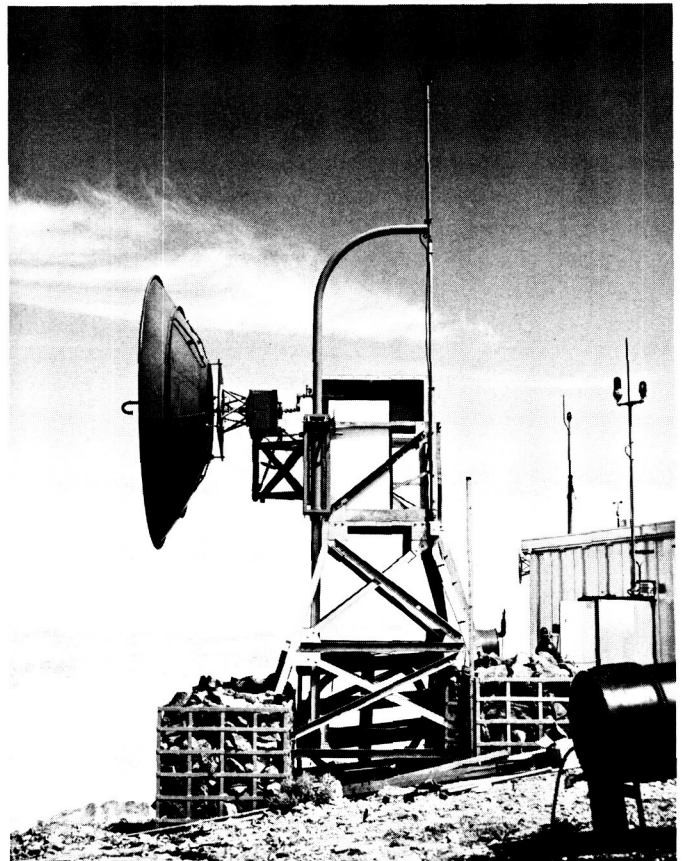


Fig. 20. Tiefort Mountain X-band illuminator

urements will be made by comparison with a 6-ft antenna mounted at the apex of the 30-ft antenna (Fig. 21). A waveguide sampling switch will be used to switch between the 6-ft antenna and the 30-ft antenna; the gain difference will be determined by a precision attenuator in the 30-ft antenna arm.

The first gain measurements will be made with the 30-ft antenna surface adjusted for the best paraboloid at the horizon. All future surface distortion gain measurements will be referenced to this first test. The gain changes due to surface distortions are expected to be from 0.1 db to ≈ 1 db. Certain tests may require scaling the surface distortions to make the measurements possible.

The beam width and beam shift measurements will be made using the datex angle position encoder and equal power level measurement technique. The antenna patterns will be made on a conventional pattern recorder; however, special synchros are being added to the antenna to allow a chart expansion of the main beam.

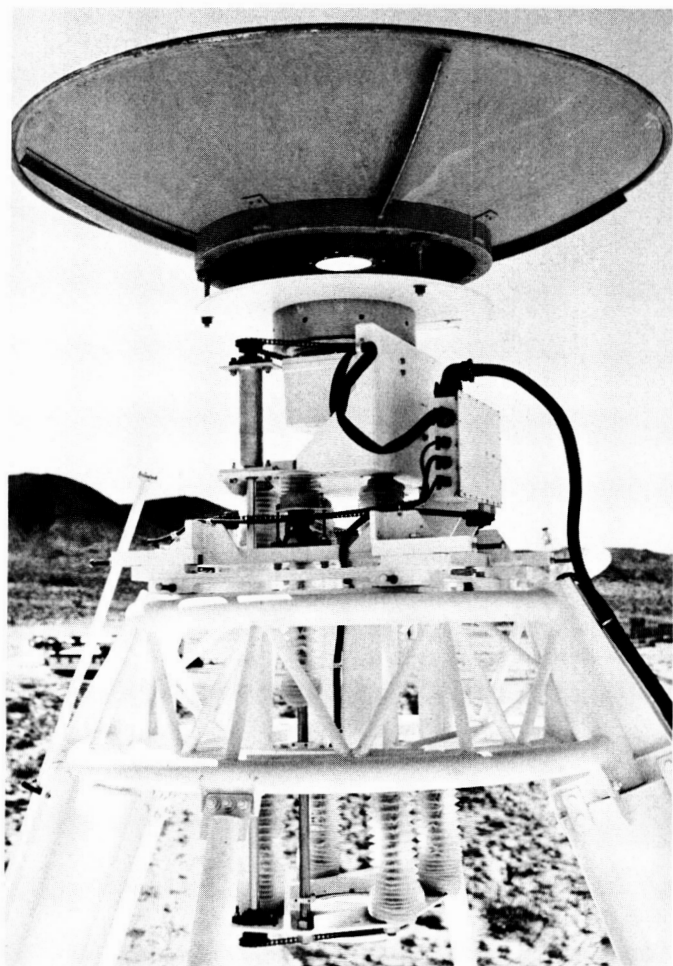


Fig. 21. Reference antenna and feed positioner

The focal point shift due to quadripod deflections or surface distortions will be investigated to determine loss of gain. An attempt will be made to experimentally measure the feed shift; but most of the compensation or corrections will come from predicted errors from either a best-fit paraboloid computation or predicted pattern computer program.

The Tiefert Mountain site will be used for illumination only with all receiving functions at the 30-ft antenna. A block diagram of the Tiefert equipment is shown in Fig. 22.

The 30-ft antenna has been equipped with a feed positioner to adjust a focal point feed in polarization and focus or a Cassegrain subreflector in focus. The 6-ft reference antenna is attached to the front of the feed positioner and rotates to change polarization.

A block diagram of the X-band receiver is shown in Fig. 23; the RF receiving equipment is located in the antenna electronics cage (Fig. 24). The pattern recorder, equipment for adjusting the feed positioner, and other miscellaneous control equipment is located in the Venus site control room (Fig. 25).

Fig. 26 shows the Cassegrain feed system on the 30-ft antenna. The Cassegrain rather than focal point feed system is used to provide direct support for AAS studies and continuity with existing work on the 85-ft antennas. The cone itself is a $\frac{1}{2}$ -scale model of the 210-ft unit. (The $\frac{1}{2}$ -scale frequency for the 210-ft antenna is approximately 16.5 Gc.) The feed system configuration is basically similar to the S-band configuration utilized in the 1962 Venus radar system. It utilizes a shaped beam subreflector and a dual mode conical horn for increased performance; Fig. 27 shows the configuration in detail. Complete amplitude and phase pattern measurements were performed on the feed horn-subreflector combination at JPL prior to installation in the 30-ft antenna. This data will be utilized in the performance prediction and analysis.

2. Radiation Pattern Computer Program

As described previously, a program exists to determine the relationship between paraboloidal antenna surface deformations and RF performance. This program consists of three simultaneous efforts:

- (1) The introduction and mechanical measurement of interesting surface contours in the 30-ft azimuth-elevation antenna.
- (2) Measurement of the RF effect of these distortions (initially at 8450 Mc).
- (3) The calculation of the RF effect of the distortions by computer program.

To implement the last of these, a program has been written for the IBM 7094 computer which numerically evaluates the scalar far-field radiation pattern integral (Ref. 5).

The radiation pattern calculation consists of an integration over the antenna aperture of the illumination function, taking into account the path length and surface phasing error parameters for each point on the aperture. Specifically, the power pattern, in spherical coordinates is given by:

$$G(\theta, \phi) = \left| \int_0^1 RW(R) dR \int_0^{360^\circ} e^{jh(\theta, \phi, R, \beta, k)} d\beta \right|^2 \quad (1)$$

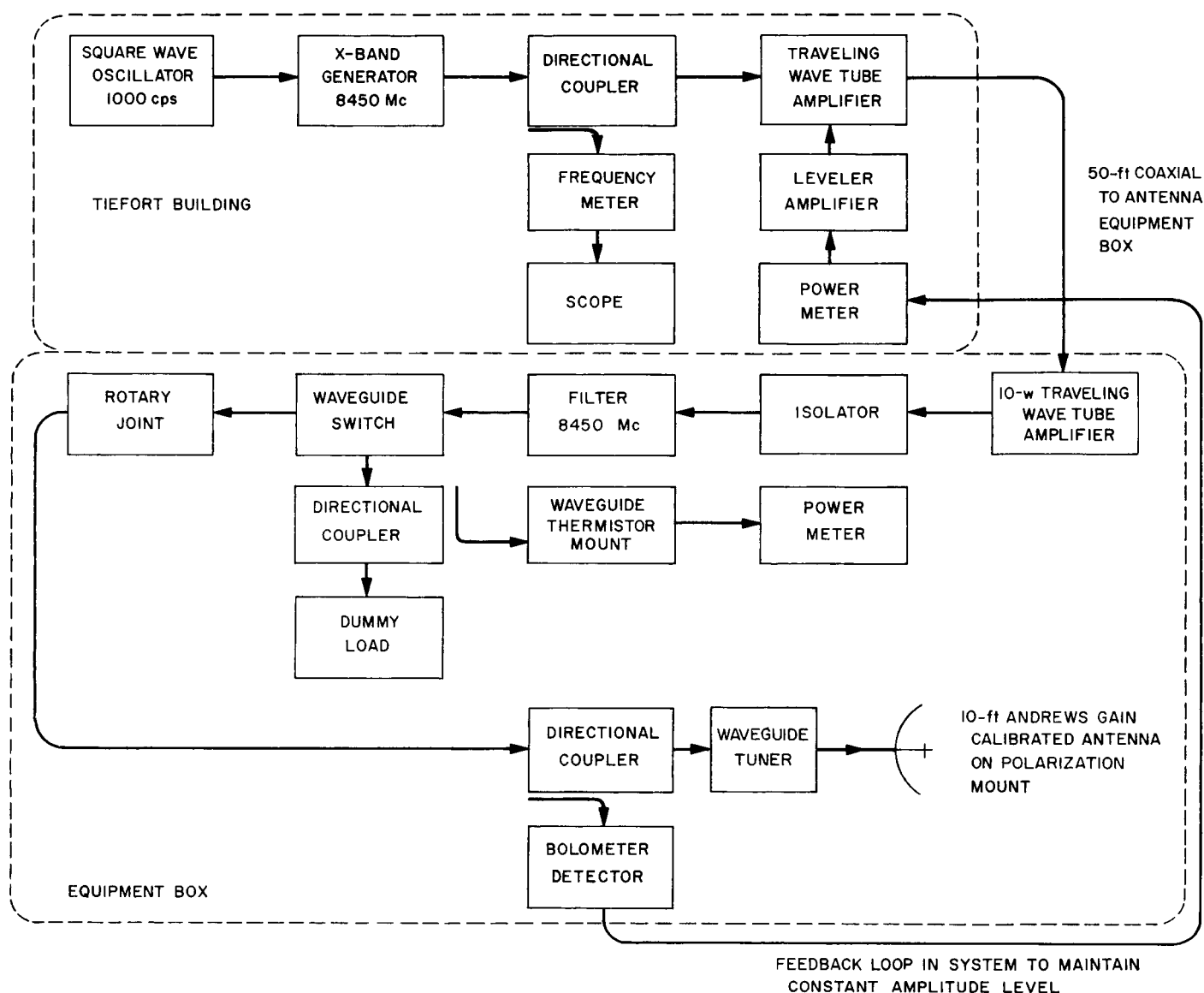


Fig. 22. Tiefert Mountain X-band transmitter

where

$$h(\theta, \phi, R, \beta) = h_1(R, \beta, k) + h_2(\theta, \phi, \beta, R, k) + h_3(R, \beta)$$

$$h_1(R, \beta, k) = k \left[1 + \frac{f - Z(R)}{\{[f - Z(R)]^2 + R^2\}^{1/2}} \right] dZ(R, \beta)$$

$$h_2(\theta, \phi, R, \beta, k) = kR \sin \theta \cos(\phi - \beta)$$

where

$$h_3(R, \beta) = \text{feed system phase error}$$

$$k = \text{free space propagation constant}$$

f = antenna focal length

$Z(R)$ = axial dimension of a point on the reflector surface

$dZ(R, \beta)$ = axial surface error of a point on the reflector

$W(R)$ = amplitude illumination function

R = normalized aperture radius

β = azimuthal angle of an aperture point

θ, ϕ = polar and azimuthal angles of point in space

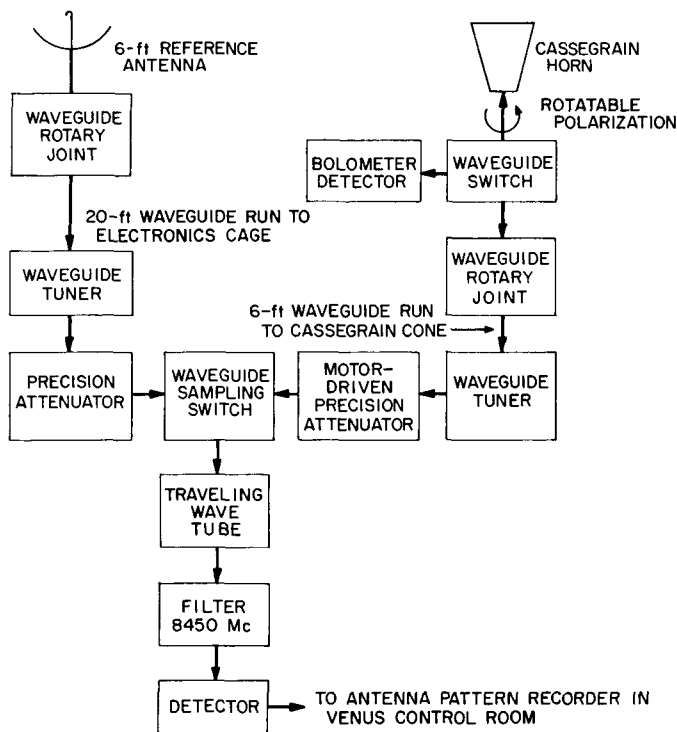


Fig. 23. 30-ft antenna receiving system

To operate the program, the following data is inputted:

- (1) Propagation constant, in.^{-1}
- (2) Focal length, in.
- (3) Number of aperture radii of integration.
- (4) Aperture radii, in.
- (5) Amplitude illumination function for each radius (relative voltage).
- (6) Number of azimuthal aperture angles of integration for each radius.
- (7) Azimuthal aperture angle (β) for each point, deg.
- (8) Phase illumination phase error for each point, deg.
- (9) Axial surface error for each point, in.
- (10) Azimuthal (ϕ) angles at which pattern is to be calculated, deg.
- (11) Number and limits of polar pattern angles for each azimuthal angle.

Output parameters of the program are the field strength radiation pattern, the radiation pattern in decibels, and the pattern phase angle. The output is normalized to the axial value with no surface error and no illumination phase error.

In order to prepare for the RF test program, three sample pattern calculations were performed for the 30-ft antenna operating at a frequency of 8450 Mc. All three cases utilize experimental amplitude and phase primary radiation patterns measured on the X-band Cassegrain feed system shown in Fig. 27 of Section III-B. In Case I (Fig. 28), the antenna surface is assumed perfect [$h_1(R, \beta, k) = 0$] and the feed system phase error is set to zero [$h_3(R, \beta) = 0$]. Case II is the same as Case I except that the feed system phase error is included, causing a loss of 0.12 db in peak gain, null filling, and a higher sidelobe level. Case III is the same as Case II except the 5° elevation angle gravity deadload surface distortions are included. For this case, the distortions depicted in Fig. 6, p. 30, of SPS 37-20, Vol. III, were used in the calculation. The pattern plotted in Fig. 28 is in the plane of antenna ribs 5 and 13 (approximately 11° from the vertical plane).

The results of Case III have been independently checked by the best-fit paraboloid computer program (SPS 37-20, Vol. III, pp. 55-56). Both the best-fit and the radiation pattern programs predicted a boresight shift of approximately 0.02° due to the deadload distortion. The statistical gain loss predicted by the best-fit program is 0.05 db, which compares favorably with the 0.07 db calculated by the radiation pattern program (the difference between Cases II and III).

An experimental radiation pattern, measured with a surface distortion similar to that assumed in Case III is plotted in Fig. 28. Further computer and experimental studies are being conducted, in an attempt to resolve the predicted and experimental pattern discrepancies. Computer studies are being performed to determine the quantitative effect of feed support blockage.

3. Antenna Instrumentation

The instrumentation system for use in research and development testing of the ground antennas at Goldstone is proceeding (SPS 37-20, Vol. III). The system will first be used at Goldstone during the resurfacing of the 85-ft azimuth-elevation antenna (June-July 1963). Fig. 29 shows the interior of the instrumentation trailer; it is now about 50% complete.

4. 6-Ft Paraboloid-Tunnel Experiments

A 6-ft diameter paraboloid using a "tunneling" fixture was used on the Goldstone Tracking Station (GTS) Venus

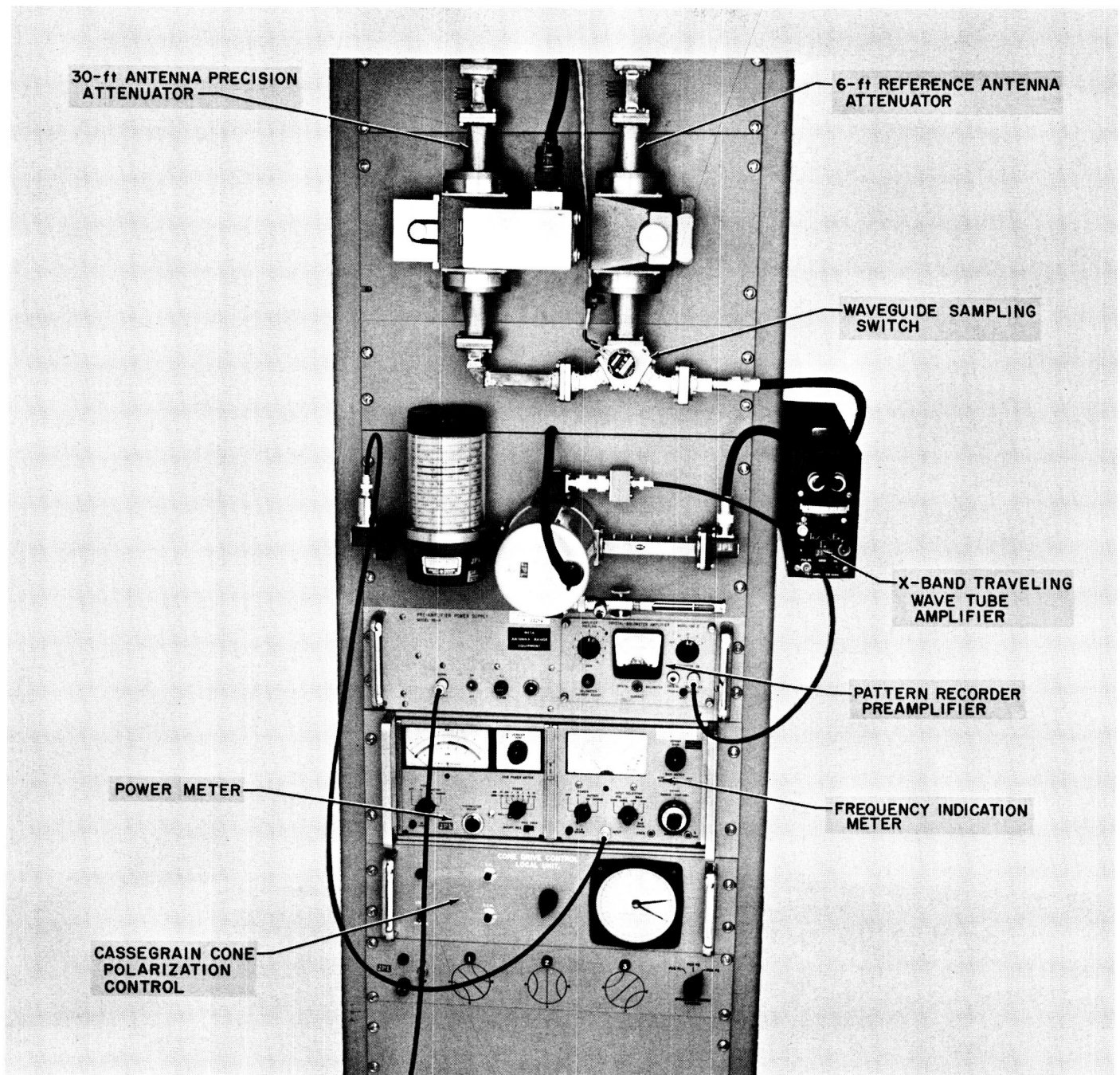


Fig. 24. 30-ft antenna RF receiving equipment

site 85-ft azimuth-elevation antenna apex. The special design was used to provide good isolation between the 6- and 85-ft antennas. An experimental investigation of the "tunneling" technique for antenna back lobe and noise temperature reduction is presented. Accurate antenna patterns and some relative gain data were obtained at 2388 Mc for a 6-ft diameter paraboloidal antenna with its tunnel set at various lengths. Assuming about 55%

aperture efficiency, calculations from pattern data showed that the effective zenith antenna temperature of about $16.7 \pm 5.0^\circ\text{K}$ for the no-tunnel antenna could be reduced to about $3.7 \pm 1.0^\circ\text{K}$ by using tunnels of lengths varying between 17 and 26 in. (Calculations for shorter tunnel lengths were not made.) It is concluded that the tunnel can be a practical and useful device for lowering antenna temperatures of small paraboloidal antennas.

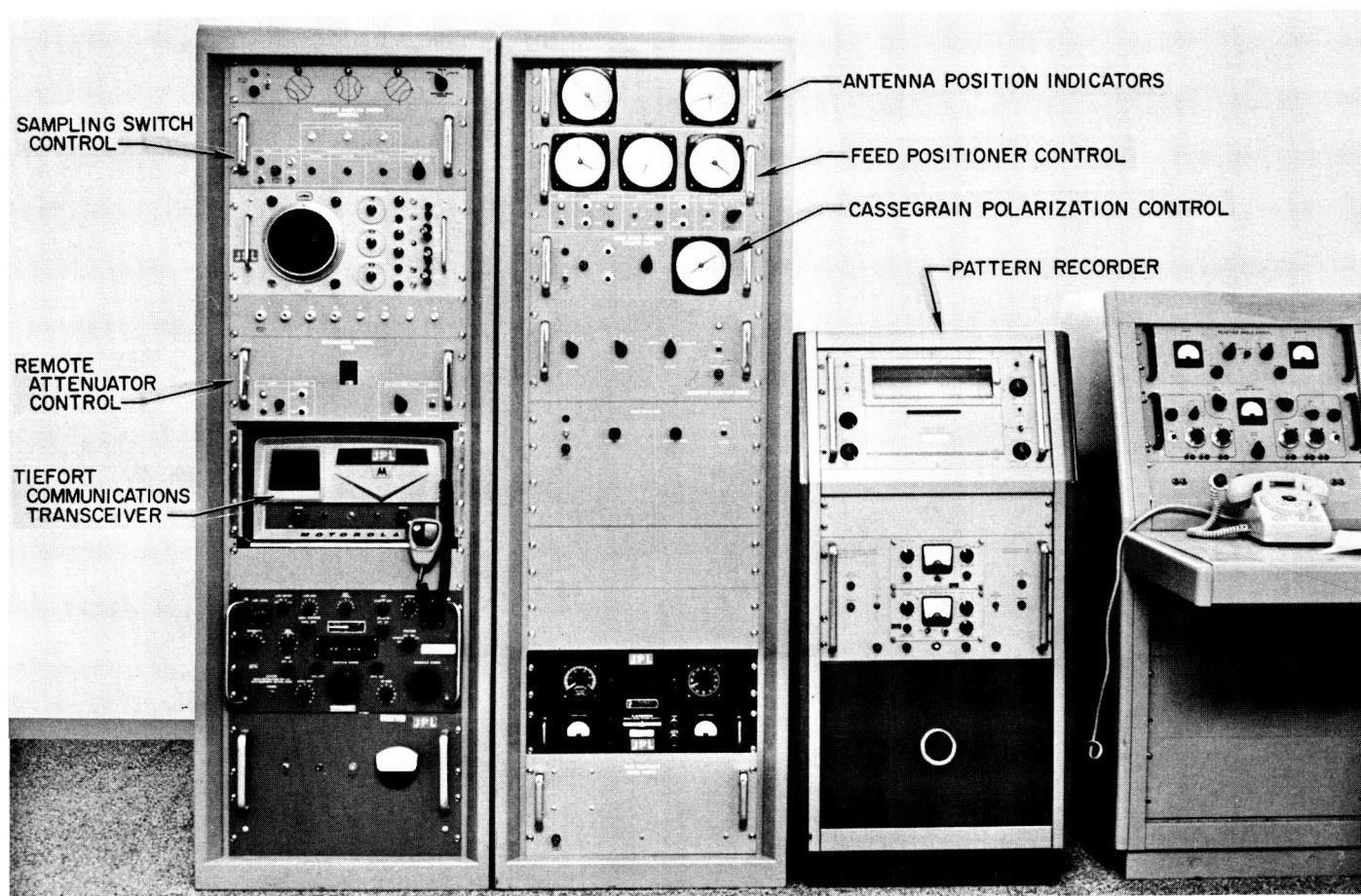


Fig. 25. Venus control room equipment

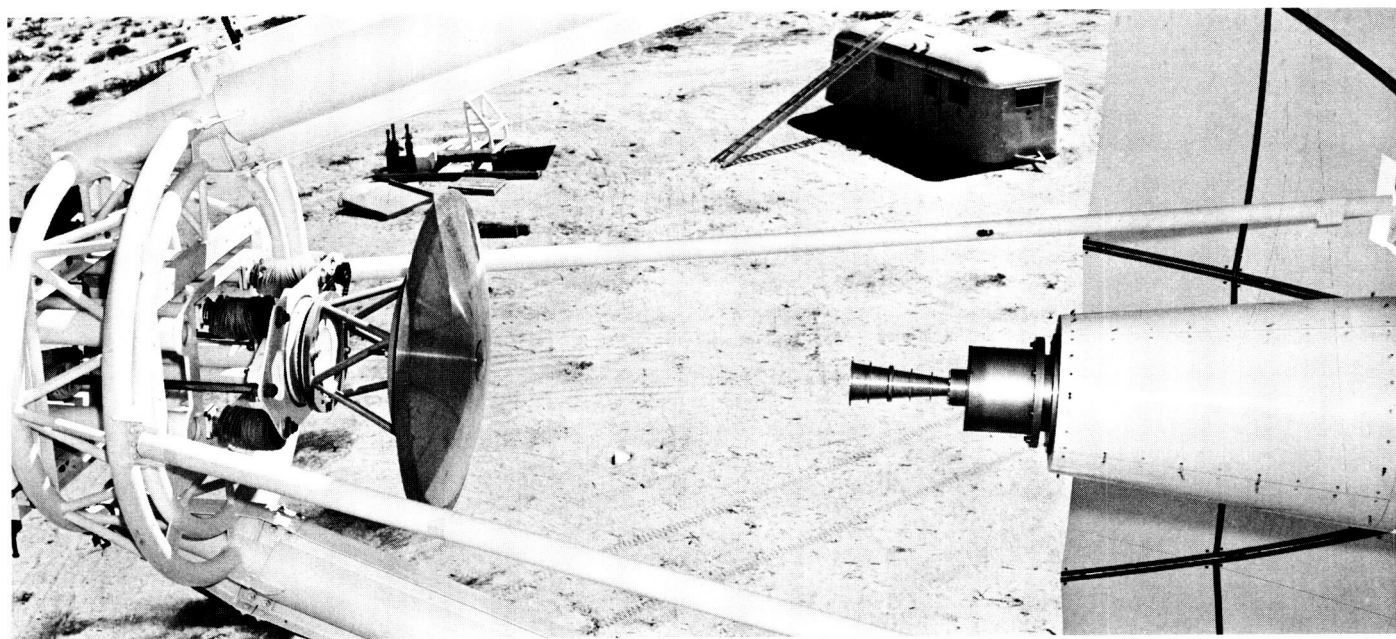


Fig. 26. 30-ft antenna Cassegrain system

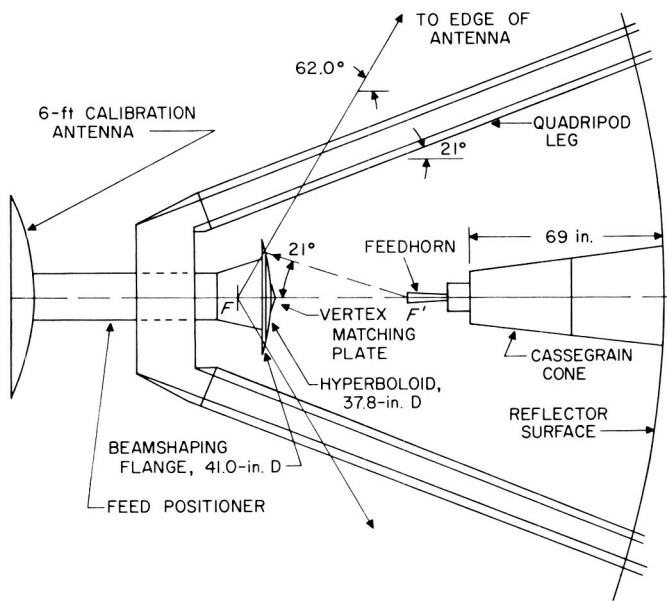


Fig. 27. 30-ft antenna feed system configuration



Fig. 29. Interior of instrumentation trailer

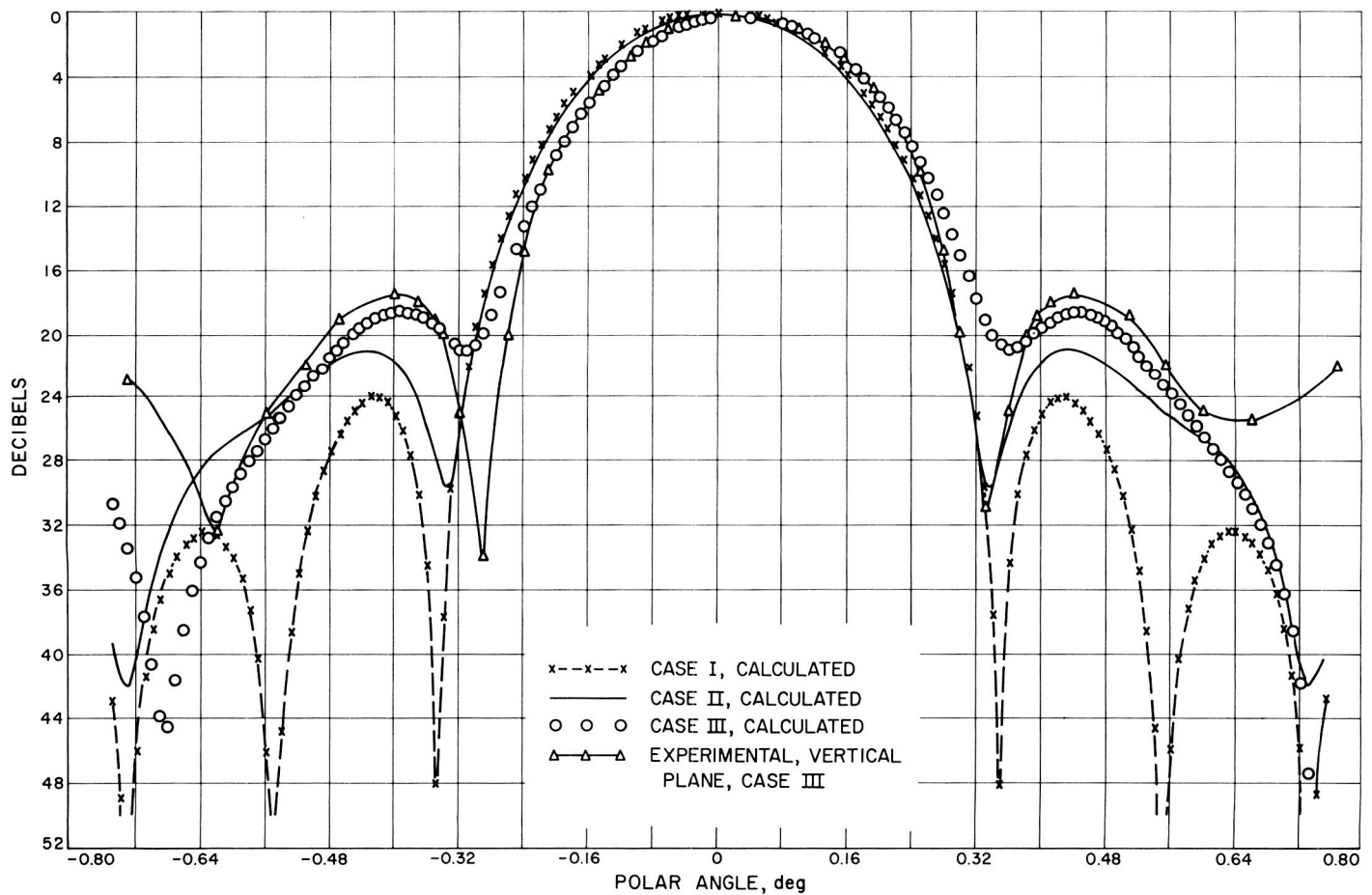


Fig. 28. 30-ft antenna patterns

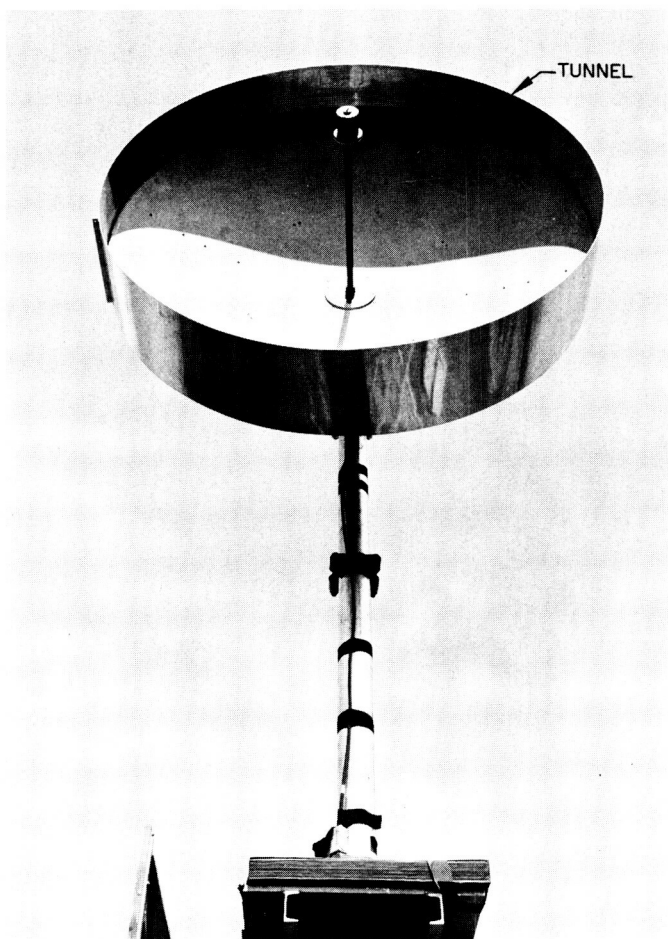


Fig. 30. 6-ft diameter paraboloidal antenna with an 8-in. tunnel

For recent lunar radar polarization experiments, a 6-ft paraboloid was mounted at the apex of the GTS Venus site 85-ft antenna. To provide good isolation between the 6- and 85-ft antennas, a tunneling fixture was mounted on the 6-ft dish. The tunneling fixture provides reduced level back and wide angle side lobes, and hence is useful in providing immunity from sources in the back or wide angle regions.

The experimental work was done during July–September 1961 in connection with low-noise antenna design studies. This recent application has stimulated collecting and discussing the data. The term “tunnel” is used to describe a metallic cylinder placed over the rim of the paraboloidal dish. Fig. 30 shows a photograph of the experimental 6-ft paraboloid with its tunnel, while Fig. 31 shows the operational version as used during the recent lunar radar experiment (*SPS 37-20*, Vol. IV).

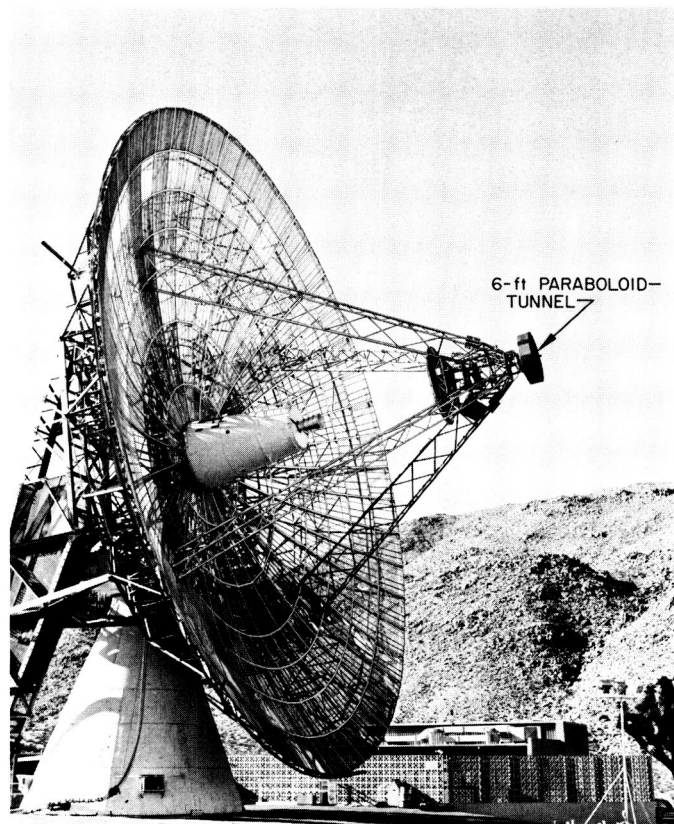


Fig. 31. 6-ft paraboloid–12-in. tunnel used on 85-ft diameter Venus site antenna during a lunar radar experiment

The 6-ft paraboloidal antenna used for 2388 Mc was the Andrew Corp. P6-24 model.

The method of investigation involved obtaining accurately calibrated radiation patterns and relative gain data as a function of tunnel position. From these data, approximate antenna temperature calculations were made. Investigations of the “tunneling” technique were made at 2388 and 960 Mc. Since only limited test data were obtained at 960 Mc, this report will present only the results obtained at 2388 Mc.

a. Radiation patterns. Data from radiation patterns for tunnels varying in lengths from 0 to 26 in. have been reduced, and side lobe and back lobe trends as a function of tunnel lengths may be seen in Fig. 32. Pattern trend studies were made for three principal radiation regions. The first principal region includes the first three side lobes between the first and fourth zeros; the second region starts from the fourth zero and includes all lobes up to 90° from the axis of the main beam; the third

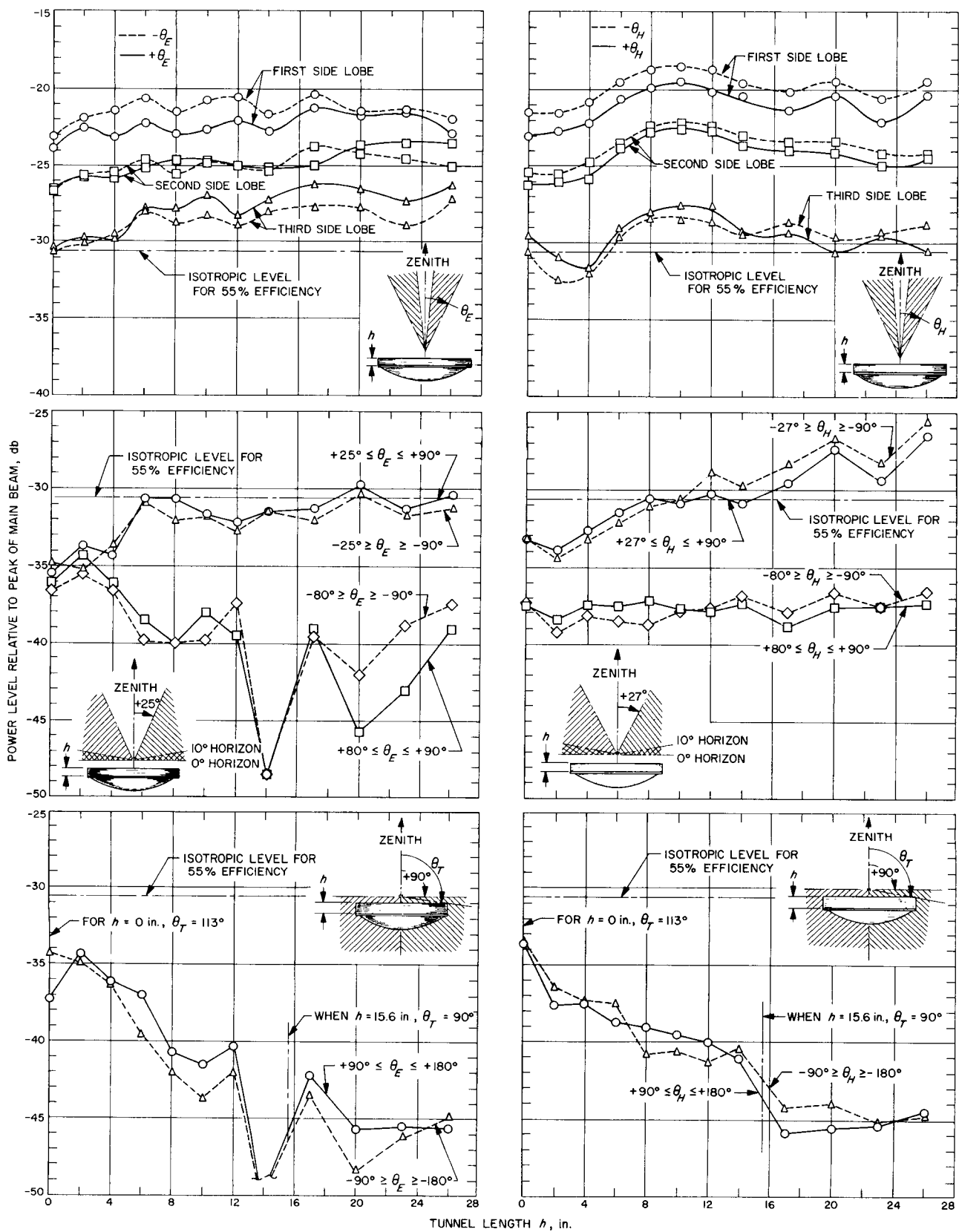


Fig. 32. Maximum radiation levels for E- and H-planes for 6-ft paraboloid-tunnel at 2388 Mc

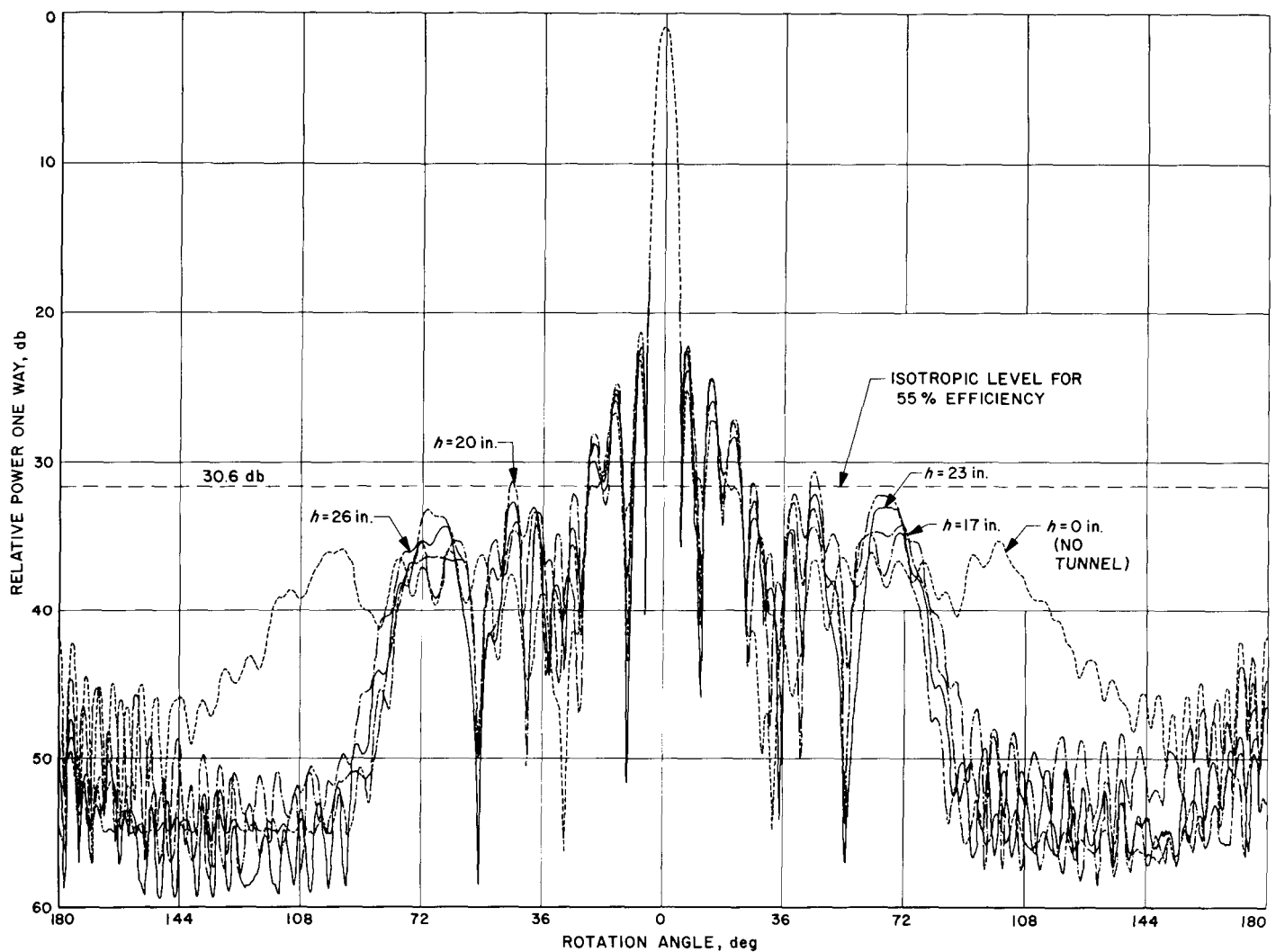


Fig. 33. E-plane patterns: $h = 0$ in.; $h = 17$ to 26 in., 2388 Mc

region lies between 90 and 180° . Only the highest side lobe level in each region was selected and plotted for a given tunnel position. The graphs are useful for showing a general trend of the maximum radiation levels in the three regions as the tunnel length is changed. The effects of tunnel length on the radiation patterns can be explained as follows:

If one were to view the paraboloidal dish surface from the feed position, then as the tunnel length is gradually increased, he would notice that more and more of the energy previously radiated into the spillover region would be cut off by the tunnel and then reradiated. A tunnel length of 15.7 in. completely cuts out the view of the secondary beam rear hemisphere when viewed from the feed. At this tunnel position, all energy should be radiat-

ing into the secondary beam forward hemisphere. In practice, this situation is not realized because of the effects of diffraction and edge currents. It can be seen from the experimental radiation patterns that the effects of reradiated spillover power into the forward hemisphere can be noticed on the raised levels of the first three side lobes.

b. Relative gain data. Relative gain measurements were made at three tunnel positions: 0 , 8 , and 12 in. The results are summarized in Table 2.

c. Antenna temperature calculations. Assuming (1) a circularly symmetric pattern, (2) a perfect horizon, and (3) uniform ground temperature (as a function of antenna angle) in the rear hemisphere, the effective zenith antenna temperature may be defined as follows:

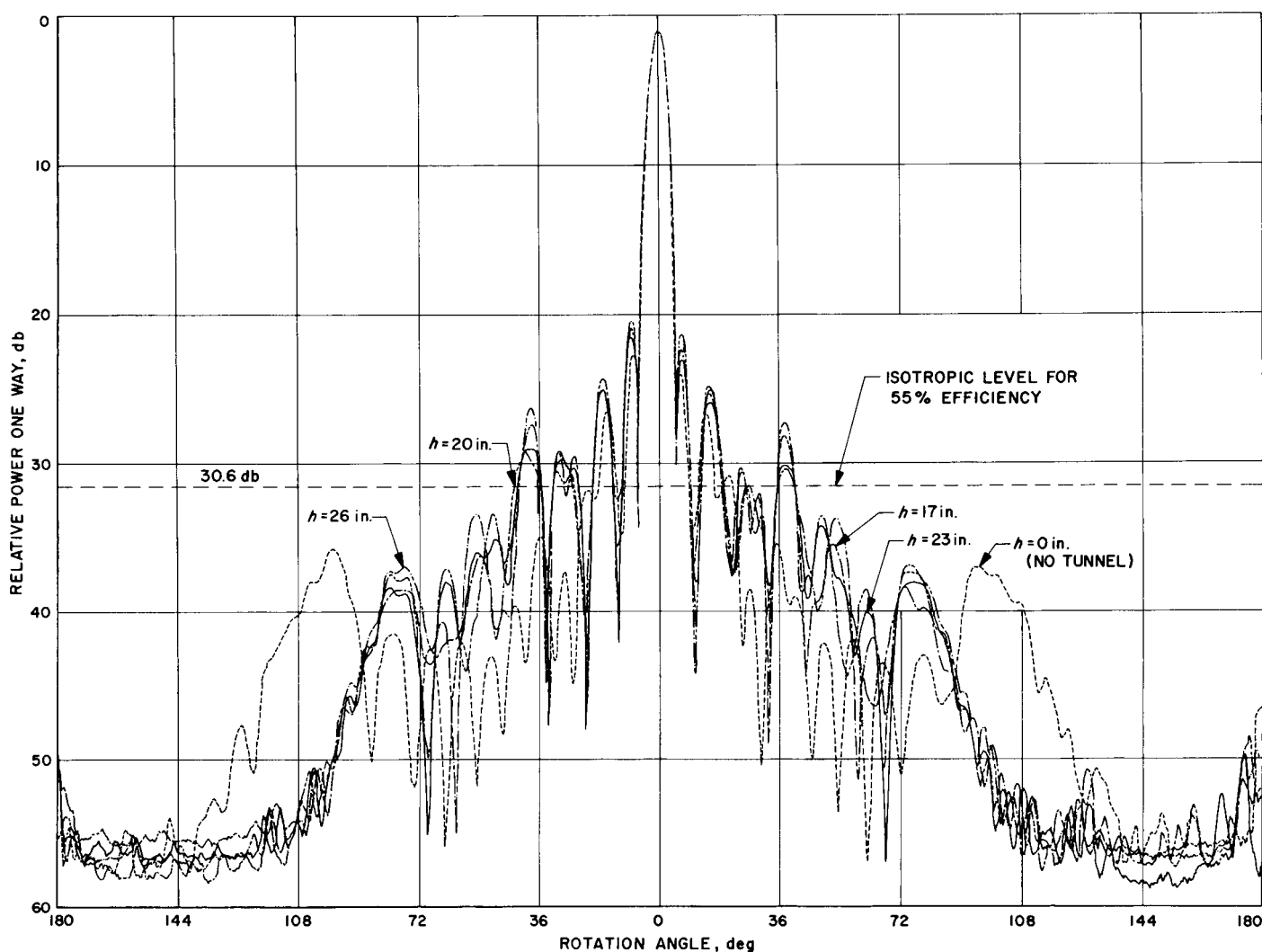


Fig. 34. H-plane patterns: $h = 0$ in.; $h = 17$ to 26 in., 2388 Mc

$$+ \frac{T_G}{2} \times \int_{90^\circ}^{180^\circ} G(\theta) \sin \theta d\theta \quad (1)$$

$$T_A = \frac{1}{2} \int_{0^\circ}^{90^\circ} G(\theta) T_{sky}(\theta) \sin \theta d\theta$$

where:

θ = polar antenna angle measured from zenith

$G(\theta)$ = antenna gain function

$T_{sky}(\theta)$ = sky temperature function

T_G = average ground temperature (240°K)

Table 2. Relative gain at 2388 Mc with and without tunnel

Tunnel length, in.	Relative gain, db
0	0.00
8	-0.22
12	-0.30

The sky temperature function is predicted by D. C. Hogg (Ref. 6). For antenna temperature calculations at 2388 Mc, the sky temperature at the horizon, $T_{sky}(90^\circ)$, was assumed to be approximately 16.6 db above the zenith sky temperature of 2.4°K. (The average ground temperature, T_G , was assumed to be 20.0 db above the zenith sky temperature.)

For a 6-ft diameter paraboloidal antenna having about 55% aperture efficiency, the maximum antenna gain at 2388 Mc will be 30.6 db above the isotropic level. For noise temperature calculations, it is desirable to have pattern information at radiation levels about 20 to 30 db below the isotropic level. To facilitate this purpose, 60-db dynamic range patterns were taken in the E- and H-planes for the 0-, 17-, 20-, 23-, and 26-in. tunnel cases. These 60-db patterns may be seen in Figs. 33 and 34. By graphical integration of Eq. (1) for the patterns shown in Figs. 33 and 34, the antenna temperature was calcu-

lated for the 0-, 17-, 20-, 23-, and 26-in. tunnel cases. Based on relative gain data information shown in Table 2, it was felt that the maximum gains for the 17- through 26-in. tunnel cases would not differ more than -1.0 db from the maximum gain for the 0-in. tunnel length case. The effects of a -1.0-db gain change on the antenna temperatures may be seen by comparing tabulated results given in Tables 3 and 4.

Other problem areas believed to be slightly less significant (for the 6-ft dish case) are:

Table 3. Results of zenith antenna temperature calculations for some 6-ft dish-tunnel cases at 2388 Mc. 30.6-db maximum antenna gain assumed for all tunnel cases

Define: $(T_A)_{sub-region} = \frac{1}{2} \int_{\theta_1}^{\theta_2} T(\theta) G(\theta) \sin \theta d\theta$									
Tunnel length, in.	Assumed maximum gain, db	Sub-region	0 to 6°	-90 to -6°	6° to 90°	-180 to -90°	90 to 180°	Total antenna temperature (T_A) , °K	Tolerances due to pattern inaccuracy $\Delta(T_A)$, °K
		Principal plane	Main beam contribution $(T_A)_{MB}$, °K	Side lobe contribution $(T_A)_{SL}$, °K		Back lobe contribution, $(T_A)_{BL}$, °K			
0	30.6	E-plane		1.0	1.1	17.1	18.0		
		H-plane		0.5	0.5	11.6	10.4		
		Average	1.6	0.8		14.3		16.7	±5.0
17	30.6	E-plane		0.8	1.0	1.2	1.6		
		H-plane		0.9	0.7	0.9	1.0		
		Average	1.6	0.9		1.2		3.7	+1.0 -0.5
20	30.6	E-plane		0.9	1.0	0.7	0.6		
		H-plane		1.1	1.0	1.1	0.9		
		Average	1.6	1.0		0.8		3.4	+1.0 -0.5
23	30.6	E-plane		0.9	0.9	0.7	1.0		
		H-plane		1.0	0.9	0.9	0.8		
		Average	1.6	0.9		0.9		3.4	+1.0 -0.5
26	30.6	E-plane		0.9	1.0	0.9	1.1		
		H-plane		1.2	1.1	1.1	1.0		
		Average	1.6	1.1		1.0		3.7	+1.0 -0.5

- (1) The relative accuracy of the pattern measuring system.
- (2) Distortion of the low-level portions of the patterns due to multipath.

It is felt that the average pattern values over the wide and back lobe regions were not greatly affected by multipath. (The effects of probable pattern inaccuracies may be seen in Tables 3 and 4.) These two problems might become very severe for pattern measurements of a larger antenna.

Ninety-deg cross-polarization patterns were also obtained, but their effects were not calculated into the tabulated results shown in Tables 3 and 4. Preliminary calculations made from the latter patterns showed that 90° cross-polarization components should not change the total antenna temperature significantly.

The experimental results indicate that the tunnel method is an effective and inexpensive technique for lowering the antenna back lobe level and reducing the antenna noise temperature. The usefulness of a tunnel for

**Table 4. Results of zenith antenna temperature calculations for some 6-ft dish-tunnel cases at 2388 Mc.
29.6-db maximum antenna gain assumed for all tunnel cases**

Define: $(T_A)_{\text{sub-region}} = \frac{1}{2} \int_{\theta_1}^{\theta_2} T(\theta) G(\theta) \sin \theta d\theta$									
Tunnel length, in.	Assumed maximum gain, db	Sub-region	0 to 6°	-90 to -6°	6 to 90°	-180 to -90°	90 to 180°	Total antenna temperature (T_A) , °K	Tolerances due to pattern inaccuracy $\Delta(T_A)$, °K
		Principal plane	Main beam contribution $(T_A)_{MB}$, °K	Side lobe contribution $(T_A)_{SL}$, °K		Back lobe contribution $(T_A)_{BL}$, °K			
0	29.6	E-plane		0.8	0.9	13.5	14.3		
		H-plane		0.4	0.4	9.2	8.3		
		Average	1.2	0.6		11.3		13.1	± 5.0
17	29.6	E-plane		0.7	0.8	1.0	1.3		
		H-plane		0.7	0.6	0.7	0.8		
		Average	1.2	0.7		1.0		2.9	+1.0 -0.5
20	29.6	E-plane		0.7	0.8	0.5	0.5		
		H-plane		0.9	0.8	0.8	0.7		
		Average	1.2	0.8		0.6		2.6	+1.0 -0.5
23	29.6	E-plane		0.7	0.7	0.6	0.8		
		H-plane		0.8	0.7	0.7	0.7		
		Average	1.2	0.7		0.7		2.6	+1.0 -0.5
26	29.6	E-plane		0.7	0.8	0.7	0.9		
		H-plane		1.0	0.8	0.8	0.8		
		Average	1.2	0.8		0.8		2.8	+1.0 -0.5

a given antenna would depend upon the original spill-over characteristics of the antenna without the tunnel.

C. Planetary Radar

1. Maser Instrumentation, System Temperature

Evaluation of the 2388-Mc maser receiving system has shown that the mismatch between the maser amplifier and antenna waveguide plumbing is not enough to contribute significantly to the system noise temperature. The principal effect of an increase in ambient temperature on the maser receiver appears to be an increase in maser gain (about 0.3 db/°F over the 69 to 80°F range) and a decrease in system equivalent noise temperature.

The 2388-Mc maser for the Venus radar experiment consists of two complete single-cavity amplifiers in one dewar with a common magnet and klystron power supply (SPS 37-17, Vol. III). In preparation for the Mars radar experiment, the maser was brought back to JPL for repairs and modification; after reinstallation, the equivalent noise temperature of the receiving system with the antenna at zenith (T_{SA}) obtained from averaging the measurement data was shown to be 36°K as compared to about 40°K prior to repair and modification (SPS 37-20, Vol. III, p. 38).

On March 25, 1963, measurements were performed to determine the noise temperature contribution caused from a mismatch between the maser receiver and the antenna system. If there is a mismatch between the maser receiver (Fig. 35) and the antenna, the noise radiated from the termination on the circulator between the two maser stages would reflect from the antenna into the receiver. The system temperature with the antenna at zenith was carefully measured by the Y-factor method using the Tucor noise source with an ambient termination and with a liquid nitrogen cooled termination on the isolation circulator, respectively. The measured difference in system noise temperature was about 0.1°K (actually less than the resolution of the measurement system). A 0.1°K noise temperature decrease with a 78°K liquid nitrogen cooled termination on the isolation circulator indicates only $0.1^{\circ}\text{K}/(290/290 - 78) = 0.13^{\circ}\text{K}$ contribution from the ambient termination due to mismatch between the antenna and receiver system.

A series of measurements was made on March 19, 1963, over a 9-hr period to determine the effect of ambient temperature changes on the maser amplifier low-noise receiving system. The air heater in the Cassegrain cone was turned on to give a slowly increasing ambient temperature. This was monitored inside the cone with a thermometer attached to the maser aluminum metal support. The outside temperature, total system noise temperature, maser gain, and parametric amplifier gain were also monitored as shown in the graph of Fig. 36. The principal effect of an increase in ambient temperature appears to be an increase in maser gain (about 0.3 db/°F over the

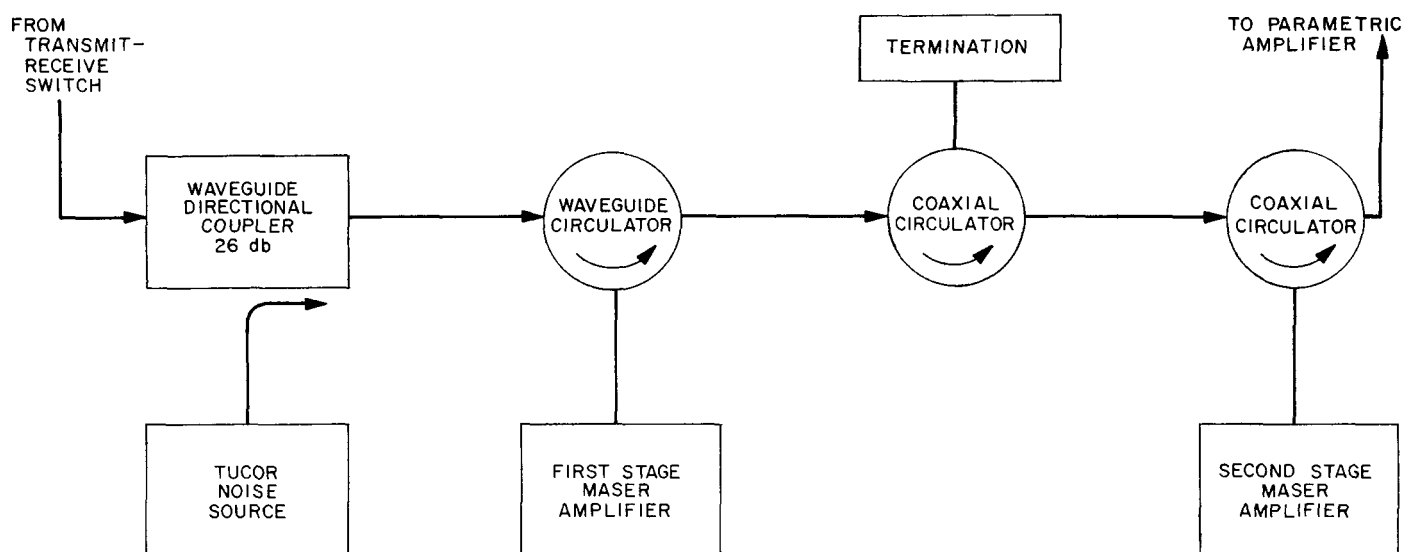


Fig. 35. 2388-Mc Venus radar two-stage cavity maser

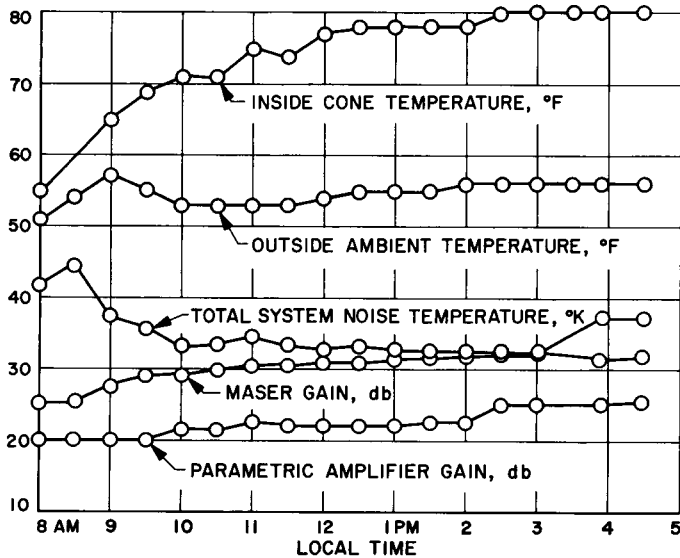


Fig. 36. Low-noise receiving system parameters and ambient temperatures

69 to 80°F range) and a decrease in system equivalent noise temperature. A portion of the decrease in system noise temperature ($\sim 1^\circ\text{K}$) is due to a decrease in the post-amplifier noise temperature contribution with an increase in maser gain. This leaves about 10°K change unaccounted—one possibility is an increase in loss of the circulator at low temperature. The characteristics of a circulator will be checked in the laboratory as a function of temperature.

It is expected that the operating center will be moved from the present trailers to the new permanent control building in June. The instrumentation racks for the maser receiving system will be rewired so that all cables will plug into connectors at the bottom of the racks. These connectors will be wired in parallel with the connectors presently installed at the top of the racks.

2. Water Rotary Joint for Azimuth-Elevation Antenna

The current design configuration in the water rotary joint development program is described. Seals of the face type are employed. Proposals from various seal sources were considered, and a selection was made.

The problems encountered thus far in the work to develop a high-capacity water rotary joint for the azimuth-elevation antenna are described in SPS 37-19, Vol. III and SPS 37-20, Vol. III. The decision was made to try to incorporate a face-type seal while still utilizing the orig-

inal inner shell assembly. Eight seal manufacturers were contacted to determine the feasibility of this approach.

Inasmuch as the medium we are trying to seal is deionized distilled water and there would not be any additional lubrication, a seal with self-lubricating qualities was considered to be the best approach. Of the eight manufacturers contacted, six replied with approaches that could possibly be incorporated. Below is a list of the various approaches suggested and JPL's comment.

- (1) A double lip utilizing Teflon and stainless steel. This is similar to the approach previously abandoned by JPL.
- (2) A face-type seal using Ni-resist and leaded bronze for the sealing surfaces. This is a proven combination that has been used in small face seals.
- (3) A face-type seal with bronze and stainless steel as the sealing surfaces. Life could be a problem with this combination.
- (4) Face-type with hard chrome and ceramic filled Teflon as the sealing surfaces. This is a material combination similar to the ones JPL has abandoned because of wear.
- (5) Face-type with hard chrome and carbon as the sealing surfaces. This is a proven combination used in smaller seals.
- (6) Face-type with stellite and carbon as the sealing surfaces. This is a proven combination used in seals of similar size.

After the evaluation, the vendors were asked to supply a list of proven application of their approach. These had to be of similar size operating under the same environmental conditions. Of all those contacted only one potential supplier (Borg-Warner) could reply favorably.

A visit to the Borg-Warner facilities affirmed our confidence in their approach. We were able to see actual hardware, both larger and slightly smaller than the seal they had presented. One of the seal sizes has been in use on many *Polaris* submarines for several years with more than satisfactory operation. While the actual operating conditions are considered secret, Borg-Warner was able to convince JPL that the conditions were more severe than would be experienced on the antenna.

From the seal proposal received, JPL developed a concept drawing shown in Fig. 37. Although the vendor makes all drawings, JPL will check all dimensional and

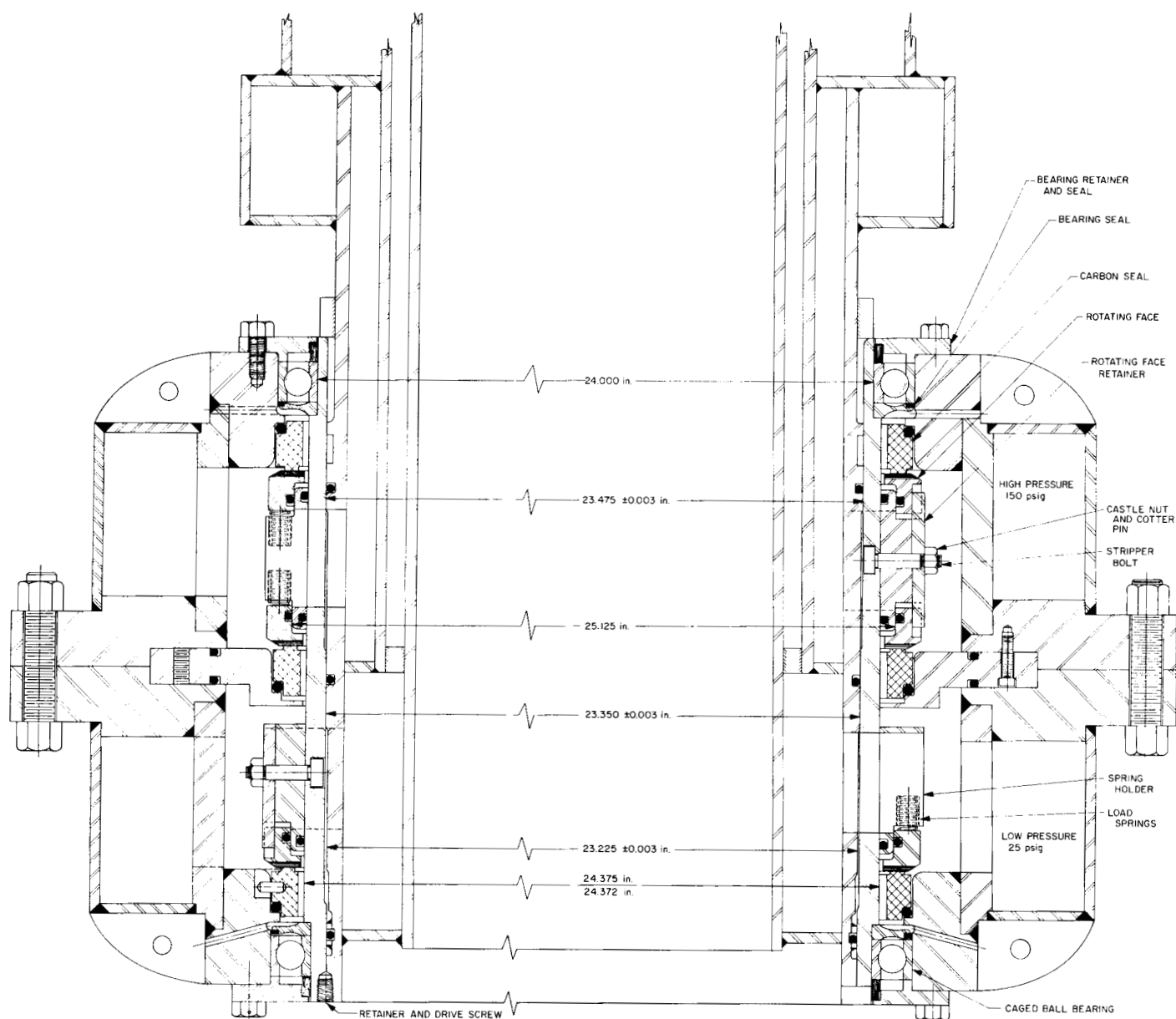


Fig. 37. Conceptual drawing for carbon face seal

stress computations. The maximum system operating pressure for the joint is 150 psig; however, the proof pressure for both supply and return will be 250 psig. JPL's stress calculation indicates that this proof pressure will afford adequate protection of the completed assembly.

Fig. 37, JPL's conceptual drawing, depicts all the major fabrication and assembly techniques felt necessary. Careful consideration was given to the assembly and disassembly procedures. Utmost care is required in the handling of the carbon faces. While the material has a high compressive strength and affords an adequate safety factor

when installed, it is extremely brittle and subject to nicking. Assembly and disassembly aids have been incorporated in the individual components.

All material used within the water cavities is stress relieved 316 SS to yield the highest long-term stability.

The contract with the vendor requires both proof pressure and leak testing. Leakage limitation allows for no visible fluid seepage. It is understood, however, fluid will be lost in the form of low-humidity water vapor. While absolute numbers are not available, it is felt that this loss

should not exceed 30 gal/yr, which is small in comparison to the normal expected losses from a reservoir pumping system.

JPL has assumed the responsibility for the dynamic testing prior to installation on the antenna. This test program will be the same as the one previously used in the plastic seal program.

3. Mod IV Ranging Equipment

One of the experiments associated with the Mod II planetary radar system (SPS 37-16, Vol. III, pp. 37-43) is a closed-loop range measuring experiment. This experiment yields time-of-flight data on planetary targets for possible use in refining the astronomical unit and/or planetary ephemerides and to improve planetary range measuring techniques.

Signal processing equipment necessary to implement the closed-loop range measuring experiment consists of an RF subsystem and a digital subsystem. The RF subsystem includes a low-noise amplifier preceding a microwave receiver (SPS 37-16, Vol. III, p. 40). The digital subsystem consists essentially of a phase tracking loop which tracks the phase of a binary coded signal reflected from the surface of a planet. This phase tracking loop provides a continuous real-time measurement of target range. The digital subsystem has been designated the Mod IV ranging equipment.

The Mod IV ranging equipment performs several functions in addition to the closed-loop range measuring experiment. One such function is to provide ephemeris programmed signals for use in spectrum analysis, radiometer analysis, and multiple range gate analysis of radar echoes from planets (SPS 37-18, Vol. III, pp. 42-46). These ephemeris programmed signals are derived from a digital tracking loop which tracks the range ephemeris. A second function is to provide transmit-receive keying signals to control the alternate connection of transmitter and receiver to the single antenna. The period of the on-off keying signals is determined from the range to the planet as given by the range ephemeris.

a. Ephemeris programmed signals. The phase of a radar echo from a planet at the input to the receiver (relative to the transmitted signal) is determined by the length of the round-trip path which the signal traverses. For correlation detection, a local model of the transmitted signal is required at the same phase as the received signal.

Since the length of the signal path is continually changing, the local signal must be continuously advanced or delayed in phase according to whether the Earth-planet distance is decreasing or increasing.

In the case of a carrier which is on-off amplitude-modulated by a square wave or a pseudo-noise (PN) sequence, the phase of the local signal can be advanced or delayed by deleting or repeating digit periods or fractions of digit periods in the modulating sequence. Commands to the local signal generator to change the phase of its modulation output are derived from a digital loop which tracks the range ephemeris. The loop consists of a binary subtractor, a number controlled oscillator (NCO), and a range tally register (Fig. 38). The input to the loop is a binary number, the ephemeris range number, which gives the Earth-planet round-trip distance in units of light microseconds as determined from the range ephemeris. The range tally register displays the loop value of range number. The difference between these two numbers (i.e., ephemeris range number-tally range number) is the error signal to the NCO. The error signal represents the number of light microseconds by which the loop must compensate so that the tally displays the ephemeris range number. The NCO operates on the error number to produce shift pulses which increment or decrement the tally according to whether the range to the target is increasing or decreasing. Since a change in target range implies a change in the phase of the local signal, the shift pulses from the NCO also serve to delay or advance the phase of the local signal by the same number of microseconds that the tally number has been changed.

Ephemeris range information is read into the loop from a punched paper tape at intervals of 8 sec. Each data sample on the tape yields a six-digit number which gives the tape time (as GMT) and a nine-digit number which gives the round-trip time to the planetary target in units of light microseconds. Time from the tape is displayed so that the tape may be synchronized with real time. The

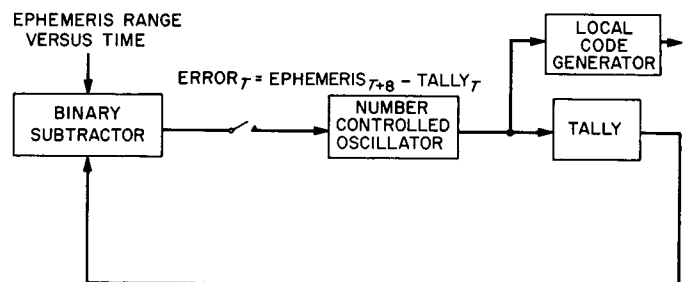


Fig. 38. Range ephemeris tracking loop

range number which is read from the tape at a particular value of tape time, say T , is the round-trip time to the target 8 sec later, that is, at time $T + 8$ sec. The loop compensates during the interval T to $T + 8$ sec, so that at time $T + 8$ sec, the loop displays the ephemeris value of range number corresponding to time $T + 8$ sec.

b. Range measuring system. A block diagram of the range measuring system is given in Fig. 39. The block labeled "bandpass filter" includes the maser, parametric amplifier, programmed local oscillator, and the various conversion and IF stages. All of the blocks to the right of the diode detector in Fig. 39 represent equipment which is located physically within the Mod IV ranging equipment.

The range measuring system operates as follows (Ref. 7): The transmitter code generator and the local code generator are initially synchronized and the tally set to zero. A transmit cycle is then started during which the transmitted carrier is on-off amplitude-modulated by the transmitter code times its clock at 0°. During the transmit cycle, the local code is shifted in phase relative to the transmitter code by the round-trip distance to the target in units of light microseconds as determined from the range ephemeris, and the tally incremented by the same number.

After the space to and from the target has been filled with energy, a receive cycle is started. The binary modulation on the received signal (the transmitted signal delayed by one round-trip time to the target) is recovered

in the receiver by means of a diode detector and limiter. The limiter is preceded by a capacitor which removes the zero frequency component in the post-detection spectrum. The recovered modulation is tracked by a phase-locked loop, and the tally operates to provide a continuous measurement of phase difference between the transmitter code and the local code, that is, a continuous measurement of target range. Range information is recorded at intervals of 8 sec both on a printed record and on punched paper tape.

The phase tracking loop causes the phase of the local code to track the phase of the received code. The phase error between the local code and the received code can be thought of as consisting of two components:

- (1) *Rate error.* The received code will be moving in phase relative to the local code because of the motion of the target. If the rate error between the two codes is removed, there remains (2).
- (2) *Displacement error.* The received code will be displaced in phase relative to the local code by some fraction of a code period. The magnitude of this displacement error is related directly to the difference between the actual round-trip time to the planetary target and the round-trip time as given by the range ephemeris.

The range rate is generated by taking first differences between successive range numbers on the ephemeris tape. Deriving the range rate from the tape is based upon the following observation. The ephemeris range numbers

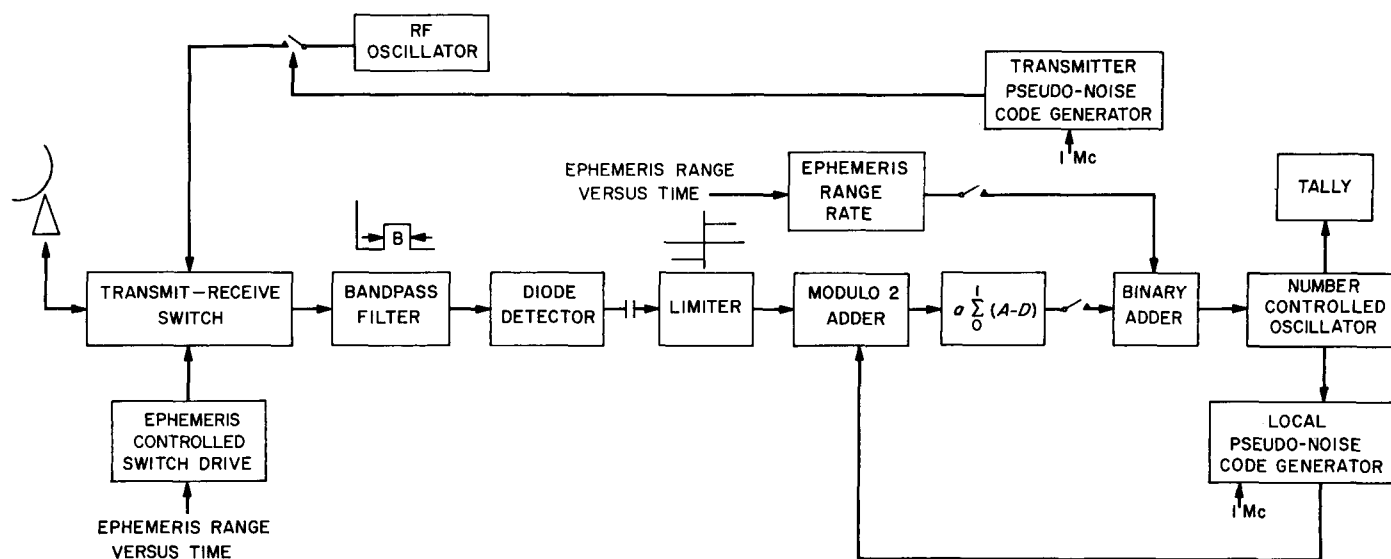


Fig. 39. Venus radar with amplitude modulated closed-loop range measuring system

are accurate to better than 1 part in 10^5 . Hence, assuming the velocity of Venus to be approximately 8 km/sec, the range error which accumulates over a 10-hr integration period (1 day's data run) is less than $(10^{-5})(8 \text{ km/sec})(3.6 \times 10^4 \text{ sec}) = 2.88 \text{ km}$. An error of this magnitude is negligible compared with the accuracy of the system. The rate error as formed is a binary number in units of light microseconds per 8 sec.

The displacement error between the received code and the local code is generated in the following manner. The received code times clock is added Modulo 2 on a microsecond-by-microsecond comparison basis to the local code times its clock shifted 90° in phase. Agreements between the two codes result in a unit increment to the integrator, whereas disagreements result in a unit decrement to the integrator. The integrator, then, accumulates sums of the form

$$\Delta = a \sum_0^1 (A - D)$$

where A = number of agreements, D = number of disagreements, a is a multiplicative constant determined from the dynamics of the loop, and the summation extends over an interval of 1 sec. These sums, which are binary numbers in units of light microseconds, are proportional to the displacement error between the received code and the local code. (Note that

$$\sum_0^1 (A - D) = 0$$

if the local code is in phase with the received code; that is, if the displacement is zero.)

The contents of the integrator are sampled once each second to obtain a value for the displacement error, and the rate error and displacement error are algebraically added to produce the error number input to the NCO. The NCO operates on this error number to produce shift pulses which shift the phase of the local code and simultaneously increment or decrement the tally by the same number of microseconds that the local code is shifted.

A displacement error between the received signal and the local code can be generated only during receive cycles. During transmit cycles, the integrator is not sampled, so that the only contribution to the error signal input to the NCO is the rate error as derived from the range ephemeris.

Both the cross-correlation between the received signal and local code and the displacement error between the two codes are continuously monitored during closed-loop operation to provide evidence that the loop is tracking. The displacement error is computed by addition Modulo 2 of the received code times clock and the local code times its clock shifted 90° in phase. In this case, however, the integrator computes sums of the form

$$\sum_0^T (A - D)$$

where T is variable. The contents of the integrator are sampled (destructively) at intervals of T sec, and the accumulated error converted to an analog voltage for display on a strip chart. The cross-correlation is computed by addition Modulo 2 of the received code times clock and the local code times its clock at 0° . The cross-correlation is also displayed as an analog voltage on a strip chart recorder. When the loop is tracking, the error voltage fluctuates about zero and the cross-correlation voltage about a maximum.

c. Number controlled oscillator (NCO). The NCO is an integral part of both the open-loop range ephemeris tracking system described in part *a*. and the closed-loop range measuring system described in part *b*. In each case, the NCO operates as a device which accepts as its input a binary number with sign, the error number, and produces as its output a corresponding number of shift pulses to change the phase of the local code and update the tally. During open-loop operation, a new error number is formed at the start of each 8-sec interval coincident with a read of the tape, but the error number for a particular interval remains constant throughout that interval. During closed-loop operation, a new error number is formed once each second.

The NCO consists of a storage register, called the shift control accumulator, and some associated logic (Fig. 40). Fundamental timing for the operation of the NCO is provided by an 8-sec time tick which occurs coincident with a read of the range ephemeris tape. Just prior to each 8-sec time tick, the shift control accumulator is zeroed. Following the occurrence of an 8-sec time tick, the absolute value of the error number is added into the shift control accumulator every 50 μsec . Following each addition, the content of the shift control accumulator is compared to a constant number. If the content of the shift control accumulator is less than the constant number, the addition process continues. If the content of the shift control accumulator is \geq the constant, a comparison-true

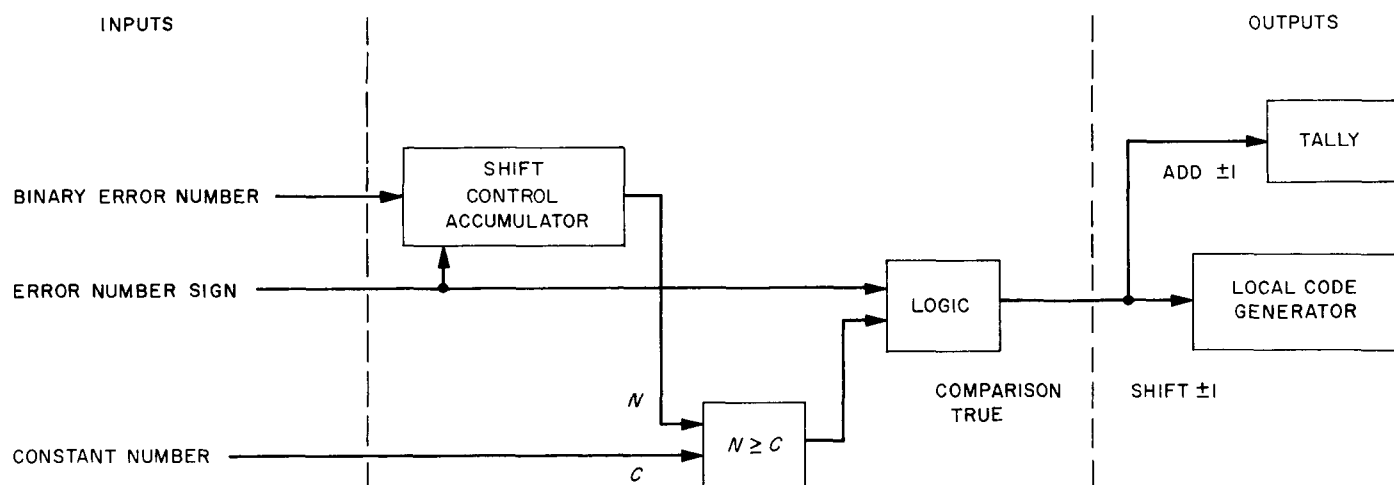


Fig. 40. Number controlled oscillator

pulse (shift pulse) is produced and the value of the constant number is subtracted from the content of the shift control accumulator. The addition process then repeats. The shift pulse performs two functions; viz., if the error number input is positive, the shift pulse increments the tally by one unit and delays the phase of the local code by $1 \mu\text{sec}$. If the error number is negative, the shift pulse decrements the tally by one unit and advances the phase of the local code by one microsecond.

The value of the constant number with which the content of the shift control accumulator is compared is determined as follows. The smallest nonzero error number possible is ± 1 . Assume that the error number at the start of an 8-sec interval is $+1$. Then the tally must be incremented by one unit and the local code delayed in phase by $1 \mu\text{sec}$ prior to the start of the next 8-sec interval. If the value $+1$ is added into the shift control accumulator every $50 \mu\text{sec}$ during the 8-sec interval, the content of the shift control accumulator will be 160,000 at the end of the interval. The constant for comparison is taken to be this value (actually somewhat less because of the time consumed in forming the error number following the 8-sec time tick); hence, the shift pulse occurs just at the end of the 8-sec interval. If the error were $+2$, one shift pulse would be produced at the end of 4 sec and a second shift pulse at the end of the 8-sec interval.

d. Transmit-receive keying signals. Signals to control the alternate connection of transmitter and receiver to the single antenna are provided from the keyer control, a subsystem of the Mod IV ranging equipment. Each transmit period lasts the correct length of time to fill the space to and from the target with energy. The receiver

then listens for an equal length of time before the next transmit period starts. The length of a particular transmit period starting, say, at time T , is the ephemeris range number on the punched paper tape corresponding to tape time $T - 8 \text{ sec}$.

The keyer control consists of a binary subtractor, a storage register, a negative number detector, and a pair of output flip-flops (Fig. 41). An ephemeris range number is loaded into the storage register at the start of each transmit period and each receive period. Every $50 \mu\text{sec}$ thereafter, the number 50 is subtracted from the content of the storage register until the remainder in the register becomes negative. When the sign of the remainder changes, the negative number detector produces an output which complements a pair of output flip-flops. The output flip-flops provide the control signals to the transmitter and receiver. Additional logic provides that the transmit and receive output flip-flops run out of phase with one another. The output of the negative number detector also resets the storage register and reloads a new value of the ephemeris range number so that the countdown process can start again.

e. Equipment. The Mod IV ranging equipment is housed in a two-bay assembly (Fig. 42). The right-hand bay contains two vertical slide-out frames which hold blocks of digital logic modules. The logic modules used are Computer Control Company Series-T digital modules. All logical operations are clocked by an internal 1-Mc clock which is derived from 1-Mc station reference signal. The left-hand bay contains the control panel and auxiliaries. Auxiliaries include a numerical indicator read-out which displays the range number, a second numerical

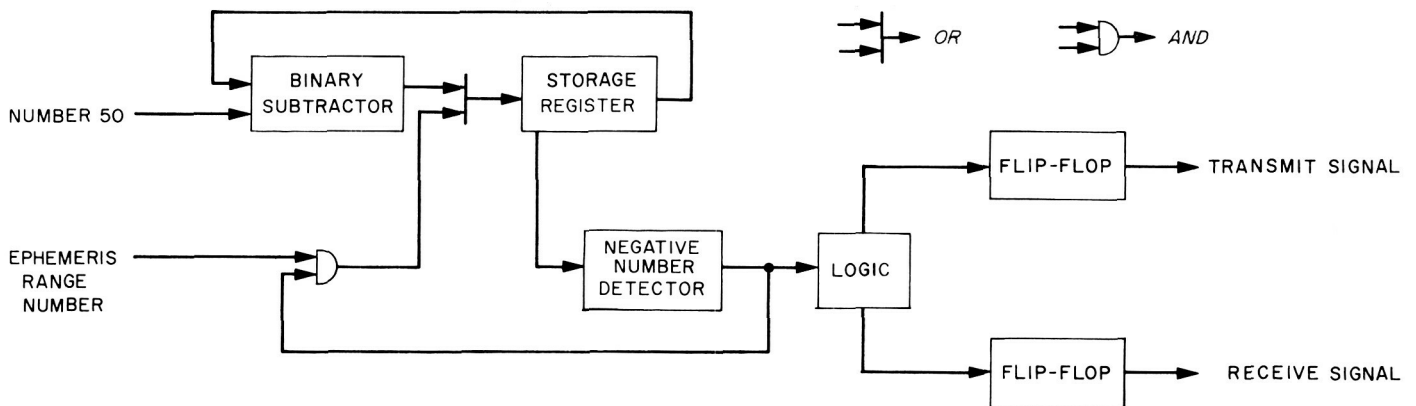


Fig. 41. Keyer control

4. Mod III Transmitting System, 2388 Mc, 100 kw

The Mod III transmitting system was described in SPS 37-19, Vol. III, pp. 23-27 and a status report was given in SPS 37-20, Vol. III, pp. 39-42. Since the last status report, one planetary radar experiment has been completed, and the time until the beginning of the next experiment is being used to correct known deficiencies.

a. 100-kw S-band klystron amplifier. The klystron amplifier, the RF water load, and the transmitter control cabinets were returned to the prime contractor for rework. A large number of small corrections was determined to be necessary as a result of the experience gained during the last radar experiment, and it was decided that these corrections could be best accomplished at the contractor's facility.

b. Beam power supply. As indicated in SPS 37-20, many problems have arisen in connection with the beam power supply. Two major problem areas were the crowbar and the rectifier. An intensive test and rework program was accomplished during this period of shutdown by engineers from the power supply subcontractor, General Electric Company. This work was expedited by use of a dc water load for testing the power supply. This load had not been available prior to this time. It will be permanently installed at the GTS Venus site.

Crowbar. The crowbar was modified and adjusted to provide a large gap at the time the generator field contactor closed. After closure of the generator field contactor, the gap automatically adjusts to the correct spacing for the dc voltage from the power supply. This large gap at the moment of contact closure prevents arc-over of the crowbar due to a switching transient. The crowbar

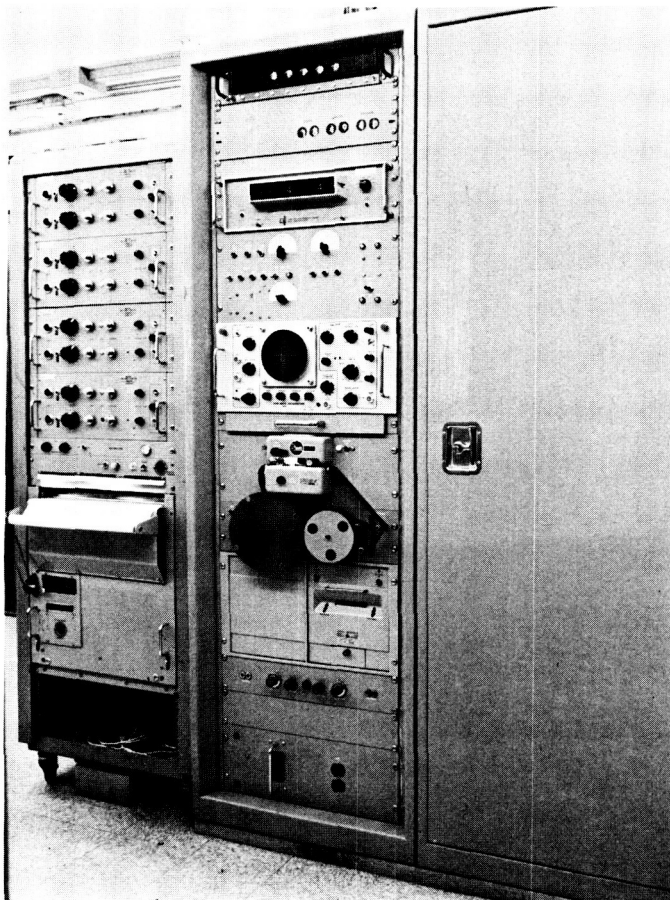


Fig. 42. Mod IV ranging equipment

indicator read-out which displays tape time, a digital clock which displays station time, an oscilloscope, a tape reader and tape spooler, and a printer. A strip chart recorder appears at the far left of Fig. 42.

travel may now be adjusted to be linear with dc voltage, thus increasing the reliability of action.

It was determined during the operational period that the crowbar reliability was impaired by damage to the trigger gap caused by sustained arc at the time the crowbar fired. While the generator field excitation is removed when the crowbar fires, the residual field produces sufficient voltage to maintain the arc once it is established. Complete removal of primary voltage to the transformer occurs only when the vacuum switches open. This problem has been reduced to a minimum by decreasing the time of operation of the vacuum switches in the line between the generator and the rectifier high-voltage transformer. As originally designed, the vacuum switches operated 4 sec after the generator field contactor opened from an arc. This vacuum switch operation has been reduced to 0.9 sec after field contactor opening. This will greatly increase the life of the trigger gap, and hence the reliability of the system.

Rectifier. Six new rectifier tubes were obtained from the tube manufacturer. These were an improved version of the original tubes furnished. The main improvement was a better technique for degassing the tubes during manufacture. These six tubes were carefully brought up to full voltage and current, and several tests were made to isolate possible causes for failure to obtain the specified power from the supply.

The ripple was measured at the input to the filter inductance in the power supply (Fig. 43). With 8.9-kv dc output, this ripple measured 5.7 kv peak-to-peak, or 64%. The theoretical ripple for the three-phase full wave rectifier is 12.7% peak-to-peak. It was determined that the capacity of the high-voltage cable following the rectifiers was resonating with the filter inductance at 2400 cps to produce this ripple. A $0.0625 \mu\text{fd}$ capacitor was connected in parallel with the cable capacitance, and the ripple was as shown in Fig. 44. The dc voltage at the time Fig. 44 was made was 10.2 kv, and the ripple was 1.2 kv peak-to-peak, or a reduction to 12%.

Measurements were also made to determine the transient effect of the crowbar on the rectifier tubes. The current impulse from a crowbar operation is as shown in Fig. 45. Prior to crowbar operation, the dc conditions were 38.5 kv and 4 amp. The crowbar peak current was 55 amp which was back to 4 amp in 100 msec. A series of readings was taken and from these it was determined that at 55 kv the peak dc current at crowbar operation would be approximately 88 amp or 14.7 per rectifier

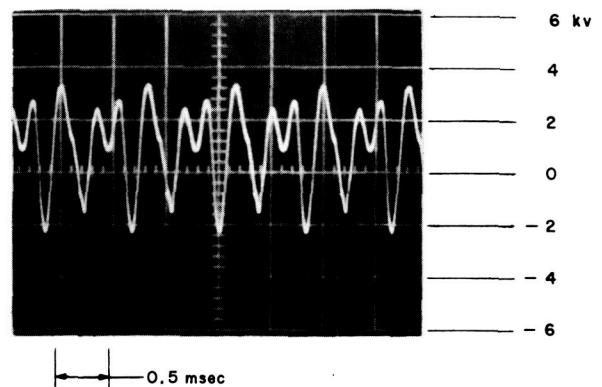


Fig. 43. Power supply ripple under conditions of resonance

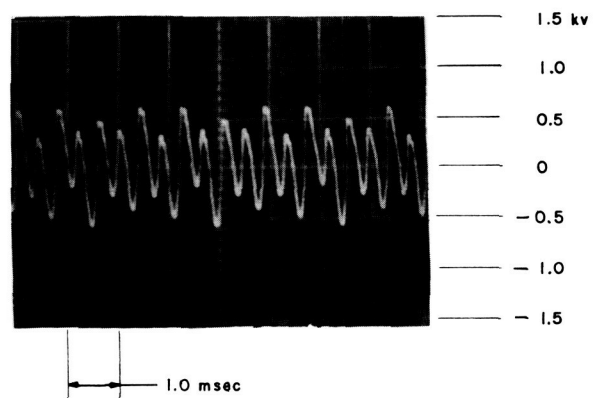


Fig. 44. Power supply ripple after resonance was suppressed

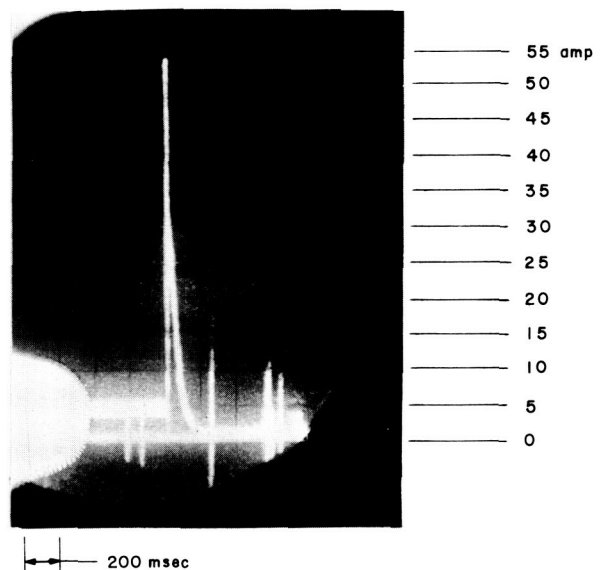


Fig. 45. Rectifier current impulse at time of crowbar

tube. This is well within the tube rating. The voltage transient was also measured during crowbar. As shown in Fig. 46, the voltage starts to decay immediately without an overshoot and is essentially zero in approximately 60 msec. From these measurements, it is concluded that the action of the crowbar is not detrimental to the rectifier tubes.

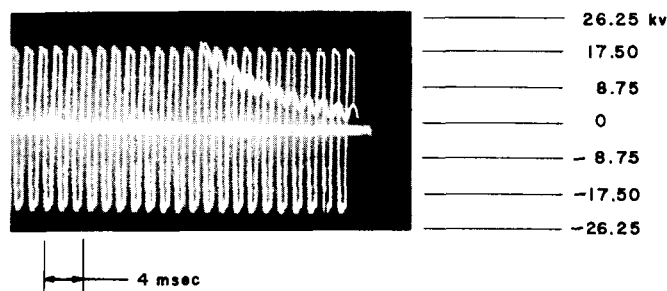


Fig. 46. Voltage across rectifier at time of crowbar

After the modifications indicated above and careful run-in of the rectifier tubes, the power supply was successfully operated at 55 kv and 10 amp dc, or an output of 550 kw. This was accomplished with six rectifier tubes. It is therefore reasonable to expect that the specified 1000 kw would not be limited by the rectifier tubes when the full complement of 12 rectifier tubes is used.

The reworked transmitter components are being reinstalled and will be operational at 100 kw on April 19 using Klystron No. 1. Klystron No. 2 is being reworked by the contractor.

5. Mod IV Planetary Radar Receiver, 2.388 Gc

a. General. The Mod IV planetary radar receiver is undergoing performance evaluation prior to being installed at the Venus site, Goldstone Tracking Station. The receiver will be used in conjunction with the high-power (100-kw) S-band transmitter for planetary exploration by radar at 2.388 Gc.

b. System configuration. A functional block diagram of the receiver is shown in Fig. 47. Five separate receiving channels are supplied from the 30-Mc IF preamplifier. These are the synchronous receiver, the AM spectrum receiver, the CW spectrum receiver, the ranging receiver, and the noise receiver. In the synchronous mode of operation, the RF carrier tracking loop is phase-locked to the received signal. This loop is comprised of a 30-Mc mixer, 455-kc IF amplifier, 455-kc phase detector, tracking filter,

VCO (voltage controlled oscillator) programmed local oscillator, frequency multipliers, first mixer, and IF pre-amplifier. In a planetary radar experiment the principal use for a synchronous receiver is for coherent doppler detection. The two-way doppler frequency shift is ordinarily beyond the electronic tuning range of the extremely stable, high Q VCO; the programmed local oscillator shifts the VCO output frequency so as to minimize the tracking loop phase error. This has the effect of extending the VCO tuning range without degrading the phase stability.

In the open-loop or nonsynchronous receiving mode, the programmed local oscillator is controlled by an ephemeris tape to generate the predicted local oscillator frequency. The three open-loop information channels are similar, except for bandwidths and third frequency conversion oscillator frequencies.

The noise channel is intended to monitor the system noise and to give a continuous indication of changes in noise temperature normally due to antenna position effects on the maser and to sky temperature changes with planet position. The second mixer is detuned 1 Mc from the received signal but within the passband of the first IF amplifier so only noise is received.

The coherent doppler detector compares the receiver local oscillator frequency, with the 31.44-Mc coherent reference. Each is multiplied 75 times and detected.

Fig. 48 is a block diagram of the coherent frequency synthesizer used to generate the receiver references. These are synthesized from 10-kc and 1-Mc signals derived from the Rubidium frequency standard by equipment in the transmitter exciter. In the bistatic radar mode (two antennas), the 10-kc and 1-Mc signals would be transmitted to the receiver by the microwave link.

References generated include 30.455 Mc for mixer injection, 31.455 Mc for the noise channel mixer, 31.44-Mc doppler reference, 30 Mc, 500 kc, and 455 kc.

A modulated 30-Mc signal for calibrating the range receiver is supplied by keying the 30-Mc reference.

The ranging clock switch loop is normally excited from the 500-kc reference (transmitter clock) but may be fed from the 500-kc receiver clock VCO which is controlled by the ranging equipment.

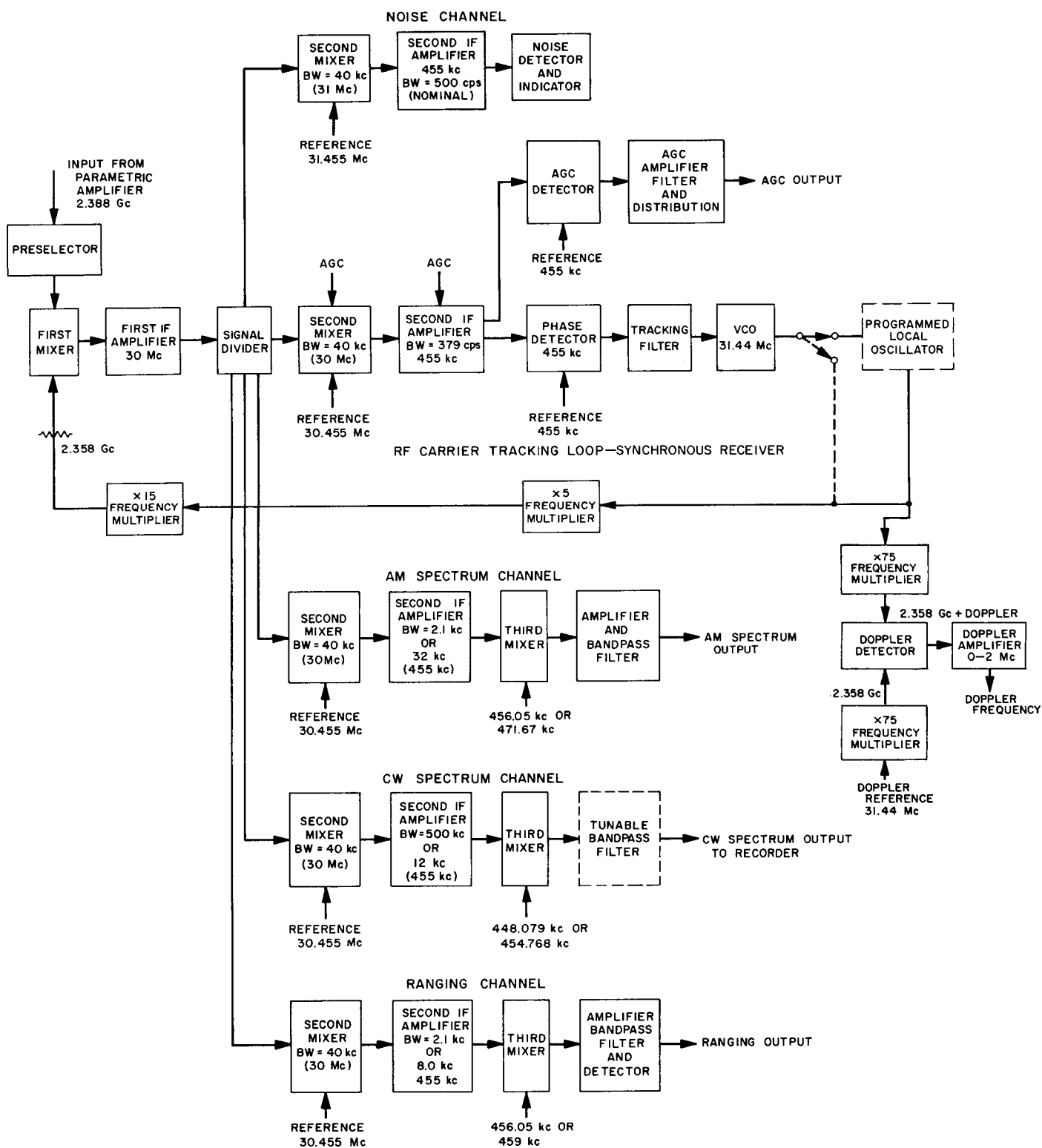


Fig. 47. Mod IV planetary radar 2.388-Gc receiver simplified block diagram

c. *Construction details.* The receiver is divided into two major parts. The microwave components and the

IF preamplifier are located in the antenna Cassegrain cone to ensure a minimum length cable run between the

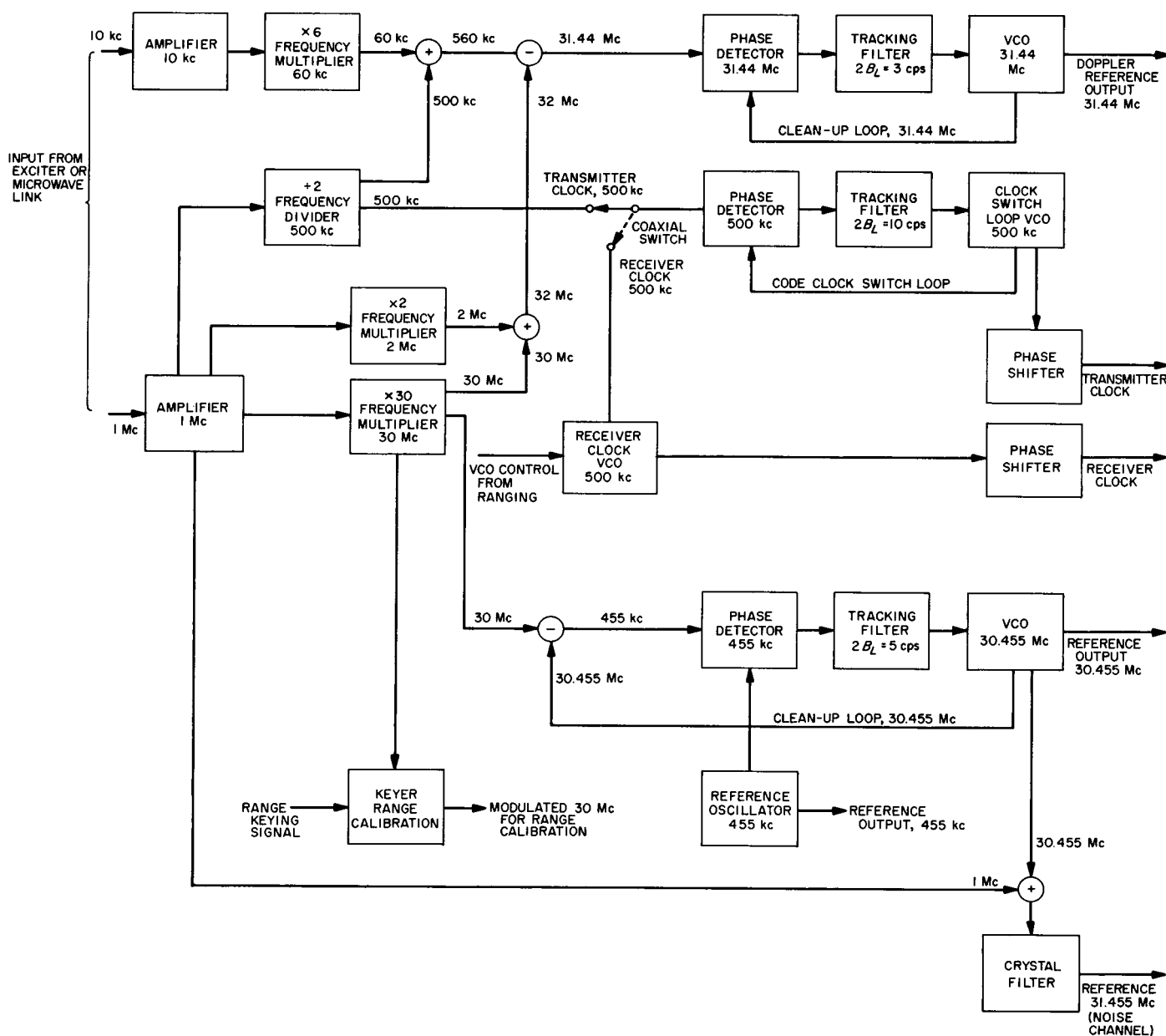


Fig. 48. Mod IV planetary radar receiver coherent reference synthesizer

parametric amplifier and receiver. These parts are assembled in a shielded, weather-tight box (Fig. 49). The power supply for these components is in a similar container.

Cables running from the antenna, through the wrap-up and in the cable-tray connect the antenna-mounted components to the remainder of the receiver in the control building. The receiver is housed in a five-cabinet assembly (Fig. 50). Controls and test equipment are mounted in the center. Each of the other four cabinets holds a heat-sink (plate) vertically mounted on slides. Modular

components are mounted on the heat-sink. Interconnecting cables are run in ducts between the modules. Fig. 51 is view of cabinet 2 with plate fully extended for servicing.

The plates can be temperature-stabilized by a circulating liquid coolant. Flexible stainless steel hoses allow free movement of the plates. In the lower part of cabinet 3, behind the circuit-breaker panel, is a liquid cooled, horizontally mounted heat-sink which supports and cools the supplies used to power the crystal oscillator ovens, relays, MGC circuits, and VCO acquisition controls.

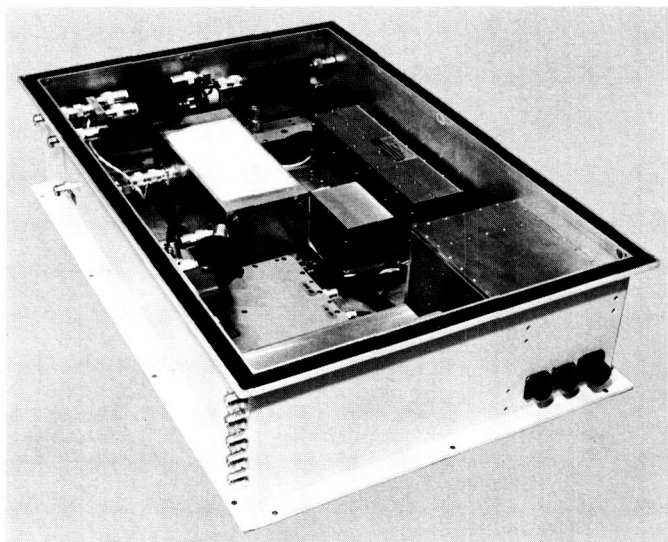


Fig. 49. Mod IV planetary radar receiver antenna mounted components

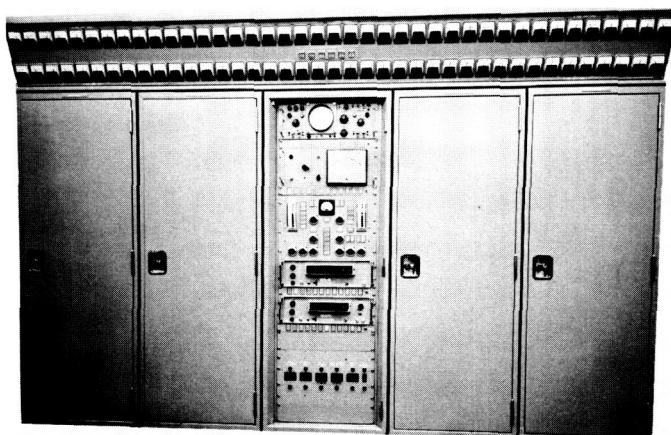


Fig. 50. Mod IV planetary radar receiver

In addition to these supplies, there are power supplies mounted on each of the four heat-sinks. These supply the modules on the plate with filament and plate voltages (6.7 and 120 v dc), and 30 and ± 15 v dc for solid-state devices.

Modular construction is used throughout the receiver. The modules are either aluminum castings or machined from solid aluminum. All surfaces are gold plated to ensure low contact resistance. Gold was used to eliminate formation of oxide films which develop on other finishes and eventually increase the RF leakage. Extensive filtering and decoupling have been provided to lower conducted RF interference. A specification of 3 μ v rms leak-

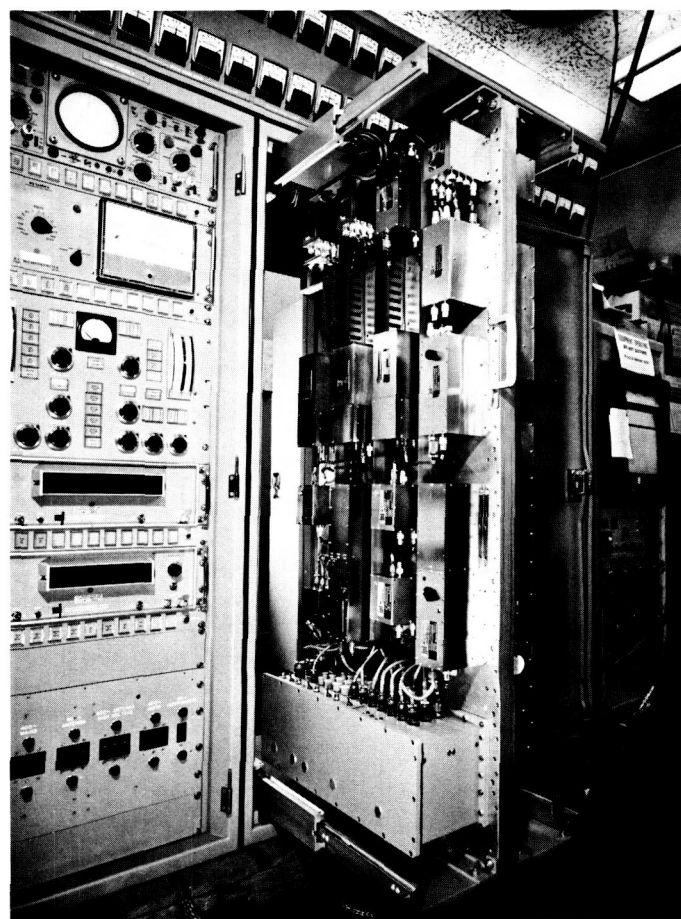


Fig. 51. Mod IV planetary radar receiver, equipment extended for servicing

age has been imposed for both conducted signals on the power lines and for radiated leakage at the joints in the cases.

d. Receiver evaluation tests. The receiver may be logically divided into several subsystems for test purposes. These are the microwave and first frequency conversion system, the RF carrier tracking loop, the synchronous AGC system, the noise receiver, the three nonsynchronous information channels, the doppler detector, and the reference generators.

Microwave and first frequency conversion subsystem. The functional block diagram of this subsystem is shown in Fig. 52. Coaxial relays are arranged to connect the noise tube or the signal generator to the receiver input. Thus, a noise figure measurement or one point signal calibration can be made from the control room. The signal generator can also be fed into the maser input with switching provided. To allow accurate system cali-

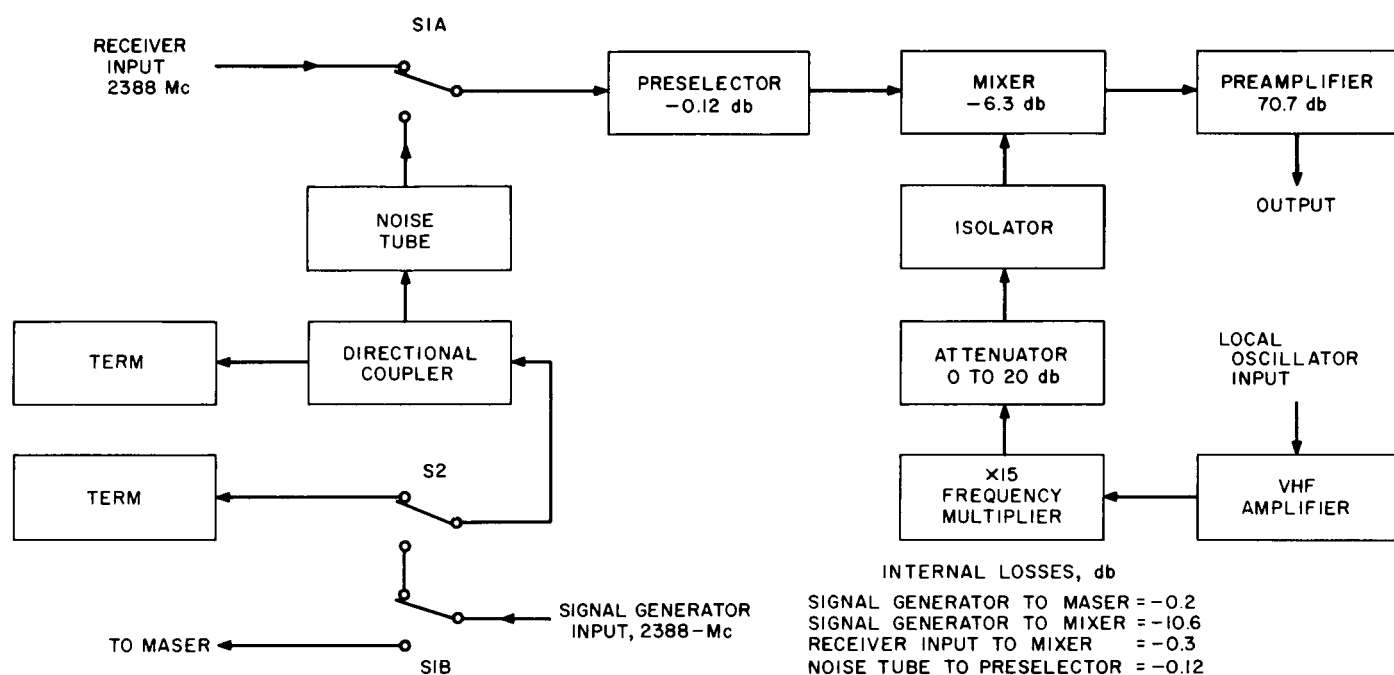


Fig. 52. Functional block diagram microwave and first frequency conversion subsystem

bration the power gains and losses through the various signal paths have been determined.

The receiver noise figure is 7.8 db (1460°K) as measured with the automatic noise figure meter and the noise

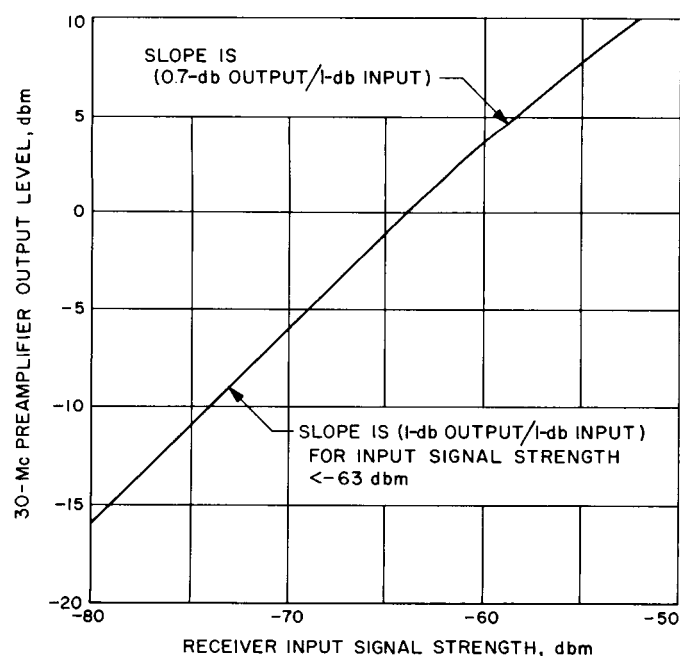


Fig. 53. Strong signal characteristics Mod IV planetary radar receiver

tube. Strong signal characteristics are shown by Fig. 53 which is a plot of 2.388-Gc signal level input versus 30-Mc output from the preamplifier. The slope of the curve is 1 db out/db in for input signal strengths less than -64 dbm. Limiting starts at -63, and at -60 dbm the slope is 0.7 db/db.

Bandwidth (3 db) of the local oscillator (LO) chain is 3 Mc, which is sufficient for planetary operations. A limiting curve of the LO chain is shown in Fig. 54.

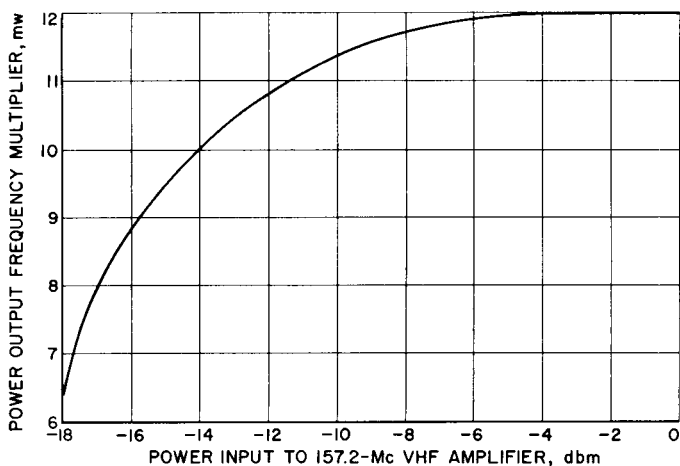


Fig. 54. Limiting characteristics, LO chain Mod IV planetary radar receiver

The crystal mixer has a conversion loss of -6.6 dbm. The mixer offers 29-db rejection to a spurious signal introduced in the LO port. The design specification was 26-db rejection. Fig. 55 shows the variation in crystal current with change in LO drive level to be a linear relation. The relationship of 30-Mc preamplifier output versus crystal current amplitude is shown in Fig. 56.

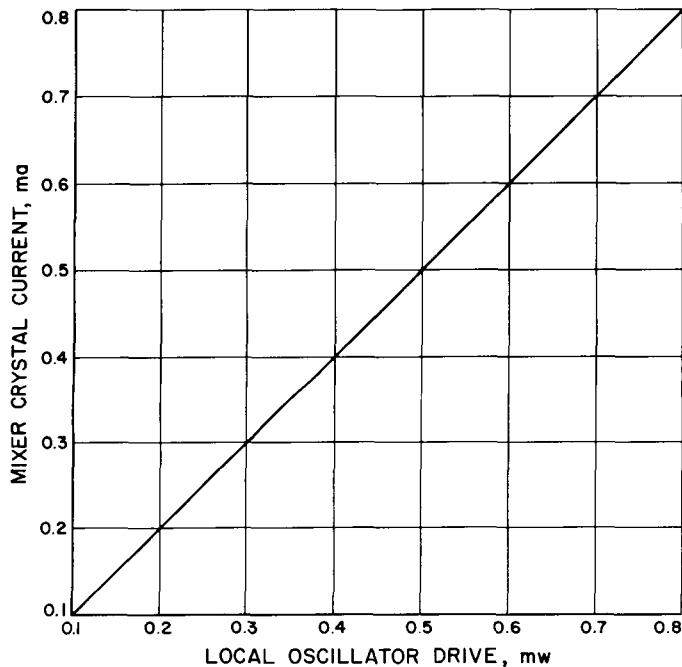


Fig. 55. Crystal mixer local oscillator drive versus crystal current

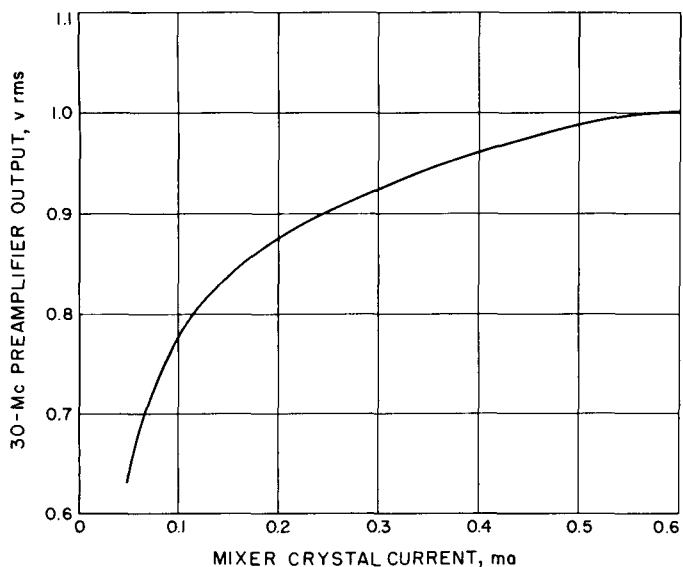


Fig. 56. Output signal level versus current output

RF carrier tracking loop. Threshold, defined as the point where the noise-to-signal ratio in the closed-loop bandwidth is equal to unity, i.e., where

$$P_s = P_n = 10 \log KT (2\beta_{L_0}) \\ = -160 \text{ dbm}$$

and

P_s = signal power, dbm

P_n = noise power, dbm

K = Boltzmann constant

$$= 1.38 \times 10^{-20} \frac{\text{MW} - \text{SEC}}{^\circ\text{K}}$$

T = system temperature, $^\circ\text{K}$

$$= 1460^\circ\text{K}$$

$2\beta_{L_0}$ = closed-loop system threshold noise bandwidth, cps

$$= 5 \text{ cps}$$

The threshold can be determined experimentally by measuring the rms phase jitter in the closed-loop bandwidth as a function of signal strength and extrapolating to 1 rad rms. The theoretical rms phase jitter is given by (SPS 37-18, Vol. III, p. 54)

$$\sigma = \left[\frac{KT}{P_s} 2\beta_L \right]^{1/2}$$

where

$$2\beta_L = \frac{2\beta_{L_0}}{3} \left(1 + 2 \frac{\alpha}{\alpha_0} \right)$$

and α/α_0 = ratio of the limiter suppression factor to its threshold value.

The test configuration is shown in Fig. 57. An external test phase detector is used to compare the instability of the receiver RF carrier VCO with the 31.44-Mc coherent reference. The measured phase noise is $1/5$ the system thermal instability. Measured and computed results are compared in Fig. 58. Oscillator noise and power line modulation contribution to the system instability are included in Fig. 58. The oscillator noise at threshold was 2.6° rms (0.046 rad rms). This measurement was made using a strong signal and an attenuator at the phase detector output to simulate the amplitude suppression and subsequent bandwidth narrowing caused by the increase of noise as the signal strength is reduced.

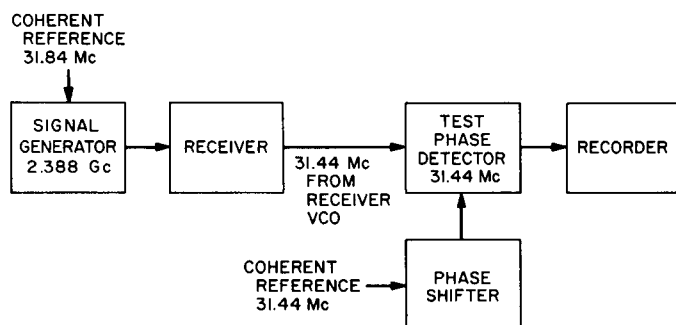


Fig. 57. Test configuration thermal noise contribution to system instability

Limiter suppression factor, α , was measured by the test configuration shown in Fig. 59. α is the ratio of the phase detector dc output with noise and signal to the output with signal only. The IF amplifier output was set to the normal operating level of 50 mv rms with signal only (no noise) and the phase detector dc output noted. Noise was then added incrementally and the attendant change in the dc level noted.

$$\text{Theoretically, } \alpha = \left(1 + \frac{4}{\pi} \frac{P_n}{P_s}\right)^{-1/2}$$

where P_n = predetection noise power and P_s = signal power. Fig. 60 is a plot of the theoretical value of α together with the measured values.

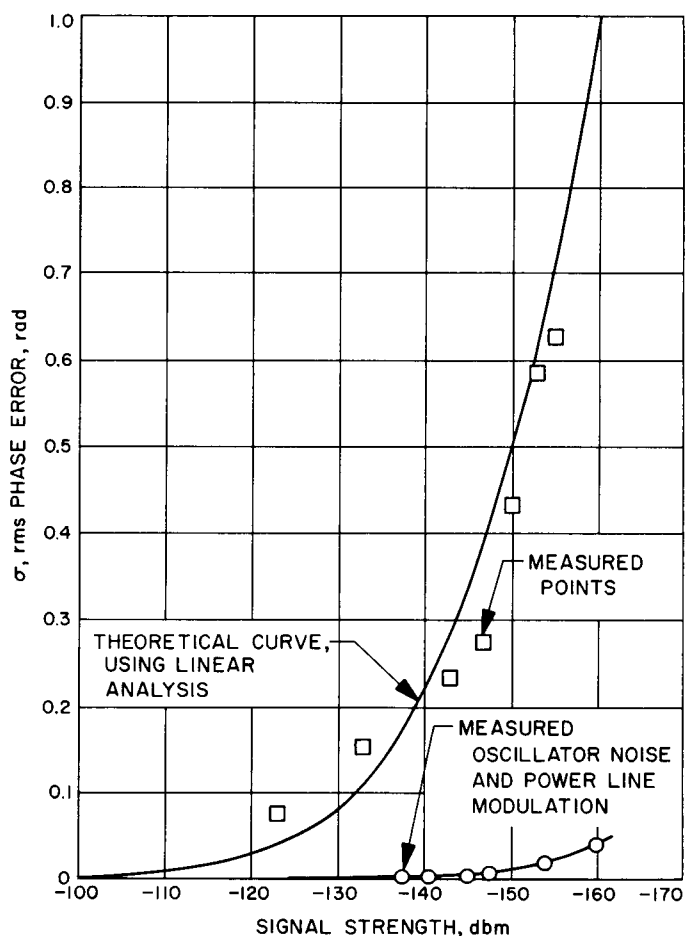


Fig. 58. Rms phase jitter in closed carrier tracking loop bandwidth

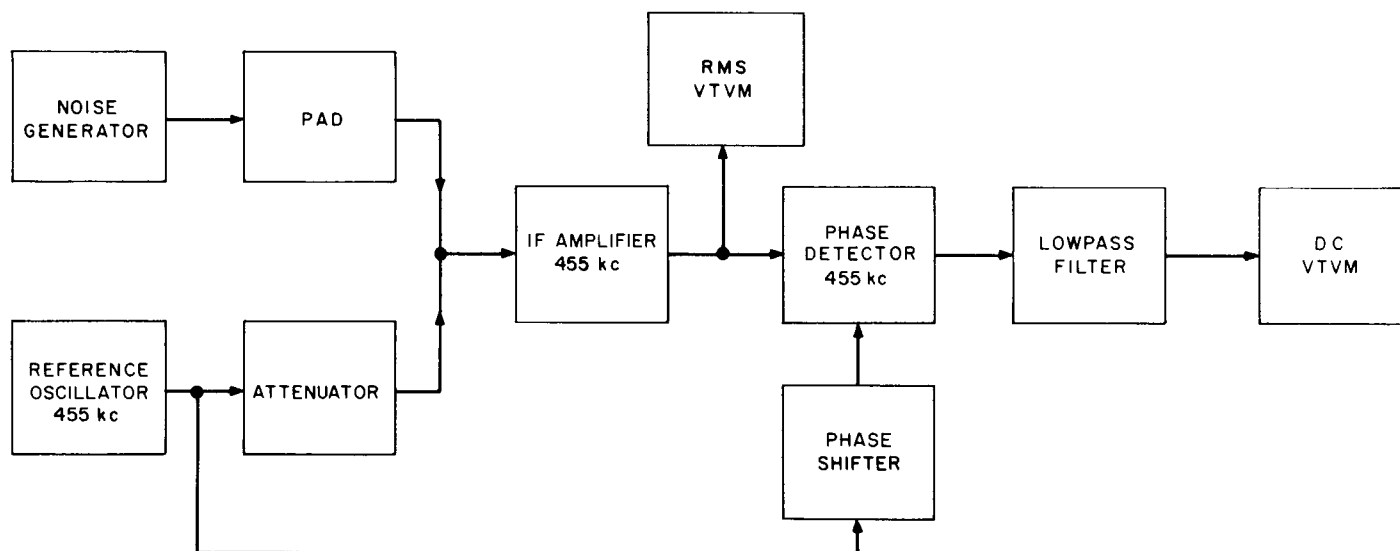


Fig. 59. Test configuration measurement of limiter suppression factor, α

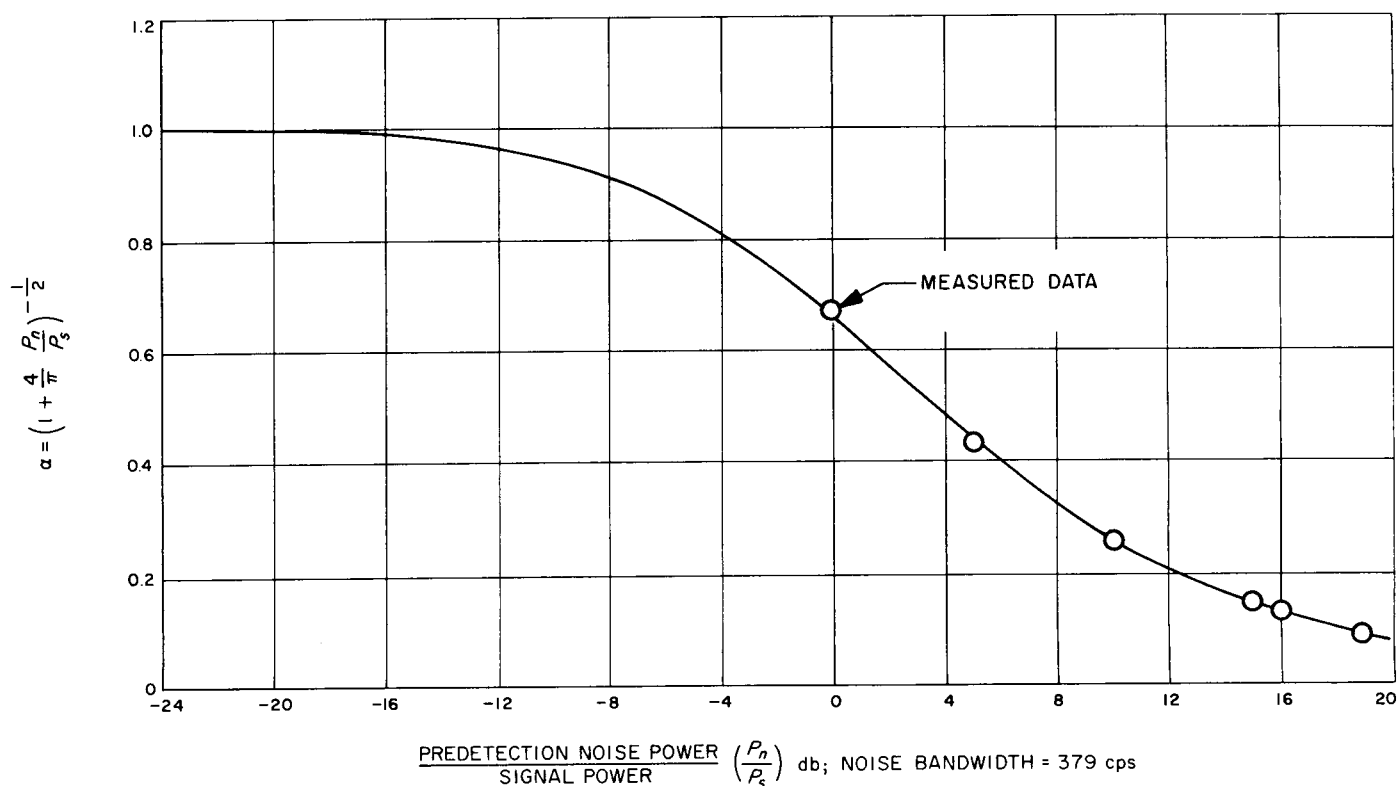


Fig. 60. Carrier tracking loop limiter suppression factor

A comparison of computed and measured values of α is tabulated:

P_n/P_s , dbm	α , computed	α , measured	Remarks
0	0.664	0.675	
5	0.446	0.437	
10	0.270	0.256	
15	0.156	0.158	
15.8	0.143	0.141	Threshold, $2\beta_{L_0} = 10$ cps
18.8	0.101	0.088	Threshold, $2\beta_{L_0} = 5$ cps

The computed variation of α with signal strength is shown in Fig. 61.

Closed-loop frequency response. The closed-loop transfer function of the receiver is (SPS 37-18, Vol. III, p. 54):

$$H(s) = \frac{G(s)}{1 + G(s)} = \frac{1 + \tau_2 s}{1 + \left(\tau_2 + \frac{1}{G\alpha} \right) s + \frac{\tau}{G\alpha} s^2}$$

where

G = open-loop gain

$$= K_v K_d \times 360 \times \alpha \times M$$

K_v = VCO constant

$$= 100 \text{ cps/v}$$

K_d = phase detector constant

$$= 0.625 \text{ v/d}$$

M = local oscillator frequency multiplication factor

$$= 75$$

τ_1, τ_2 = time constants of the compensation lag network

$$= 7.59 \times 10^4 \text{ and } 0.3, \text{ respectively}$$

α = limiter suppression factor

The closed-loop frequency response can be measured in the form $1 - H(j\omega)$ more readily than can $H(j\omega)$ which requires a 31.44-Mc reference coherent with the signal generator. Transforming to the frequency domain,

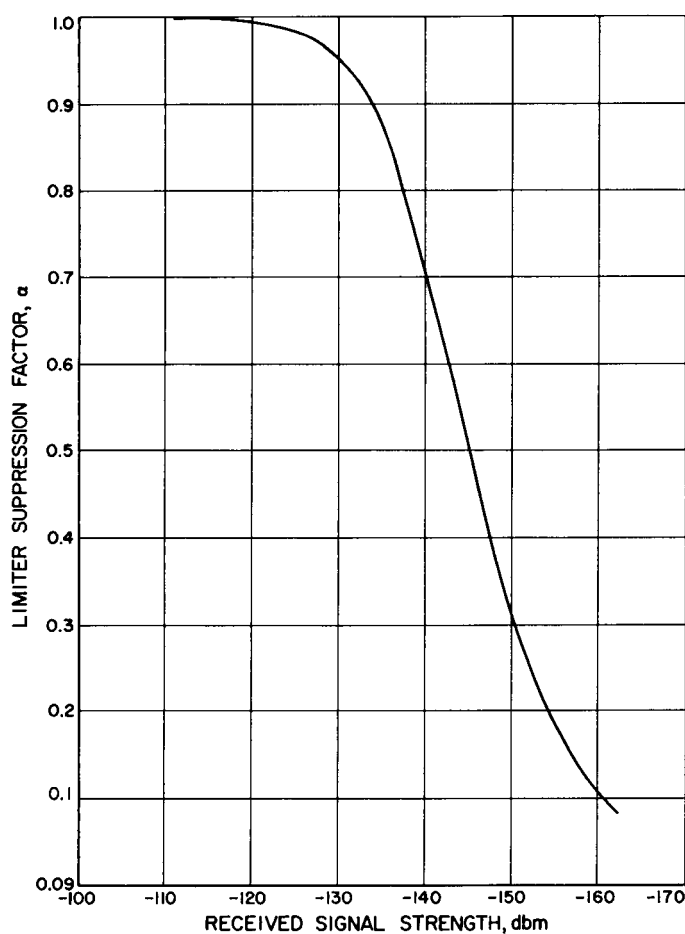


Fig. 61. Computed variation of α with received signal strength

$$1 - H(j\omega) = \frac{1 - \frac{\tau_1}{G\alpha} \omega^2}{1 - \frac{\tau_1 \omega^2}{G\alpha} + j\tau_2 \omega}$$

The test configuration is shown in Fig. 62. The loop was phase-locked to the signal generator, then phase-modulated at an audio rate. The 2.388-Gc signal level was set at a high level, and the effects of the limiter suppression factor, α , were simulated by reducing the loop gain with a potentiometer at the detector output. A family of curves of modulating frequency versus output amplitude was run for various values of α . These are shown in Fig. 63 together with a theoretical plot of the loop frequency response. The decrease in amplitude at 100 cps is due to the frequency characteristics of the bandpass filter (noise bandwidth = 379 cps) in the 455-kc IF amplifier.

Variation in the closed-loop bandwidth with signal strength. The variation in closed-loop noise bandwidth as a function of signal strength is shown in Fig. 64. The curve was computed as follows:

$$2\beta_L = \frac{2}{3} \beta_{L_0} \left(1 + 2 \frac{\alpha}{\alpha_0} \right)$$

The values of $2\beta_{L_0}$ (closed-loop threshold bandwidth), α (limiter suppression factor), and α_0 (limiter suppression factor at threshold) have been confirmed by measurement in this test.

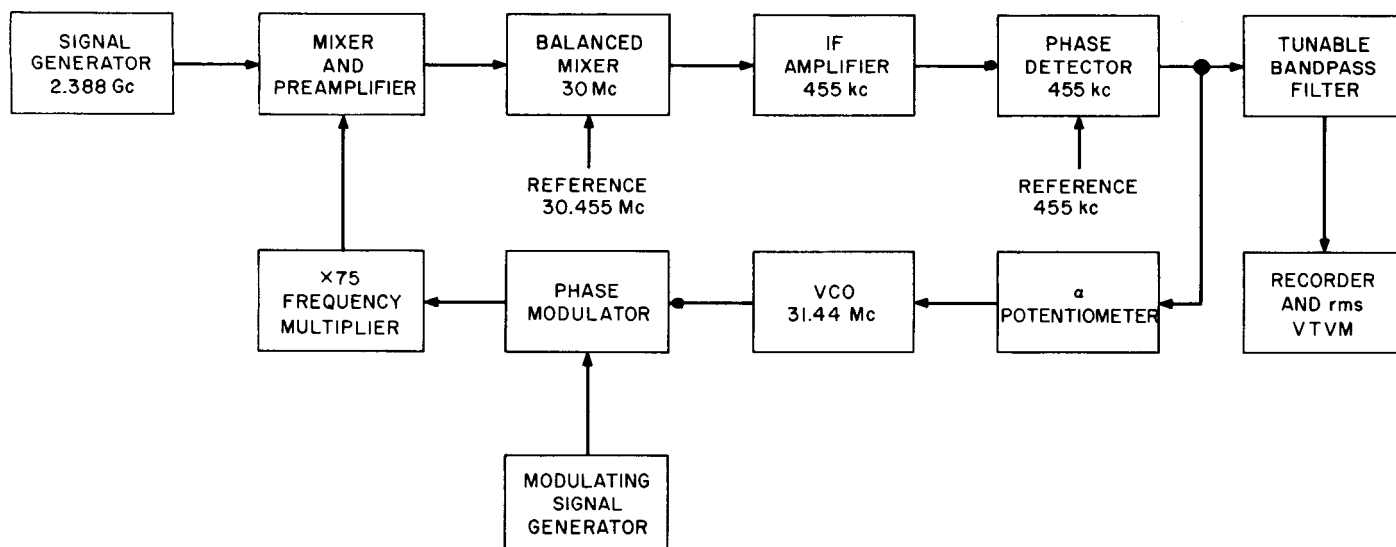


Fig. 62. Test configuration for measuring closed-loop frequency response

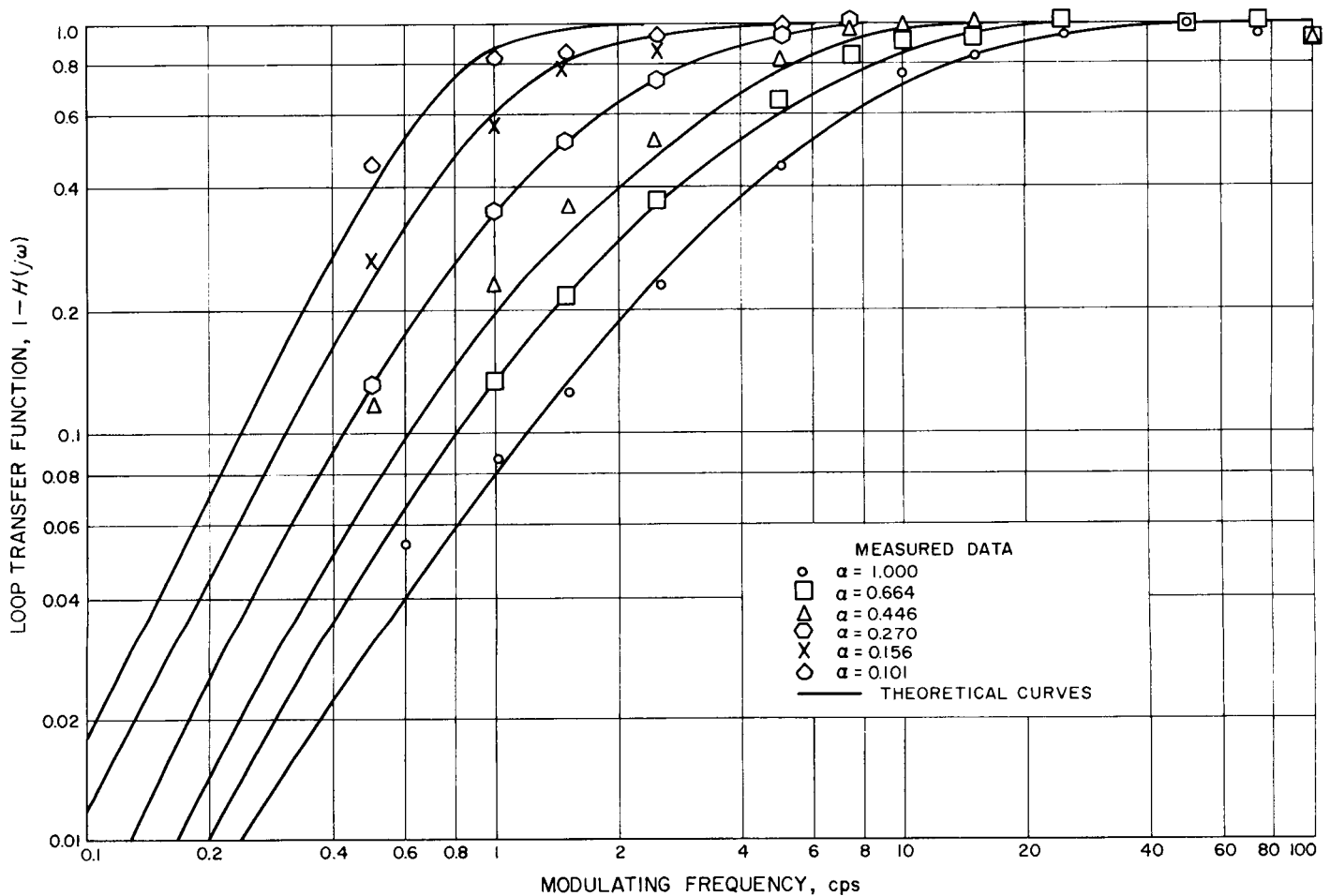


Fig. 63. Closed-loop frequency response curves for carrier tracking loop

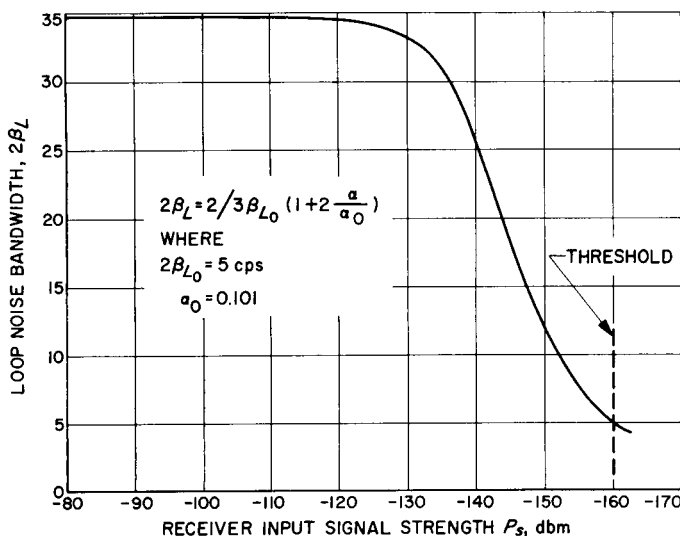


Fig. 64. Closed-loop carrier tracking loop noise bandwidth versus received signal strength

RF carrier tracking loop phase error caused by a frequency offset. The static phase error due to a step frequency offset is (SPS 37-18, Vol. III, p. 54):

$$\epsilon_s \phi = \frac{2\pi \Delta f (57.3^\circ)}{G} \text{ deg}$$

and, from SPS 37-18, Vol. III, p. 54 the static phase error offset to produce 1.0-db reduction in threshold is 6.3° . The frequency offset to produce a 6.3° static phase error is:

$$\begin{aligned} \Delta f &= \frac{6.3 G \alpha_0}{2 (57.3)} \\ &= \frac{(6.3) (1.6875 \times 10^6) (0.101)}{2 (57.3)} \\ &= 2.99 \times 10^3 \text{ cps at } 2.388 \text{ Gc} \end{aligned}$$

where

$$G = \text{loop gain} = 1.6875 \times 10^6$$

$$\alpha_0 = \text{limiter suppression factor at threshold} = 0.101$$

To measure the receiver static phase error caused by a frequency shift in the input signal to the receiver, the signal generator was offset $\pm 2.99 \times 10^3$ cps at 2.988 Gc. This precise a measurement at S-band is difficult. The corresponding frequency change at 31.84 Mc, the signal generator VCO frequency, allowing for the $\times 75$ frequency multiplier is:

$$\frac{2.99 \times 10^3}{75} = 39.9 \text{ cps,}$$

which can easily be measured on a frequency counter. To simulate the effects of noise on the loop gain at threshold and to permit measurement at a strong signal level, the loop gain was attenuated by 0.101 and the test run at -90 dbm input level. Results of the test were:

Signal generator VCO frequency	Signal generator output frequency, Gc	RF tracking loop static phase error, v
31.839960	2.3879997	+3.96
31.840039	2.388002925	-3.71

The discrepancy is due to the nonlinearity of the dc error voltage versus output frequency response of the receiver VCO.

The static phase error versus signal generator frequency offset for a strong signal condition (loop gain restored to normal) is shown in Fig. 65.

Internal coherent interference in the carrier tracking loop: The peak value of the phase detector output due to coherent leakage is required to be at least 40 db below the peak value of the phase detector output under threshold signal conditions. To perform this measurement, the spurious dc output of the phase detector was recorded as a function of the phase of the detector reference. To establish the peak value of the phase detector output due to a threshold signal and still permit shifting the reference phase, a coherent 30-Mc signal was introduced into the receiver at a level equivalent to the 30-Mc IF signal produced by a -160 -dbm, 2.388-Gc signal. The receiver "front end" (mixer and 30-Mc preamplifier) were disconnected. Fig. 66(a) shows the phase detector output as a function of the reference phase with the introduced 30-Mc coherent signal and no receiver "thermal noise." The 30-Mc preamplifier was reconnected to allow

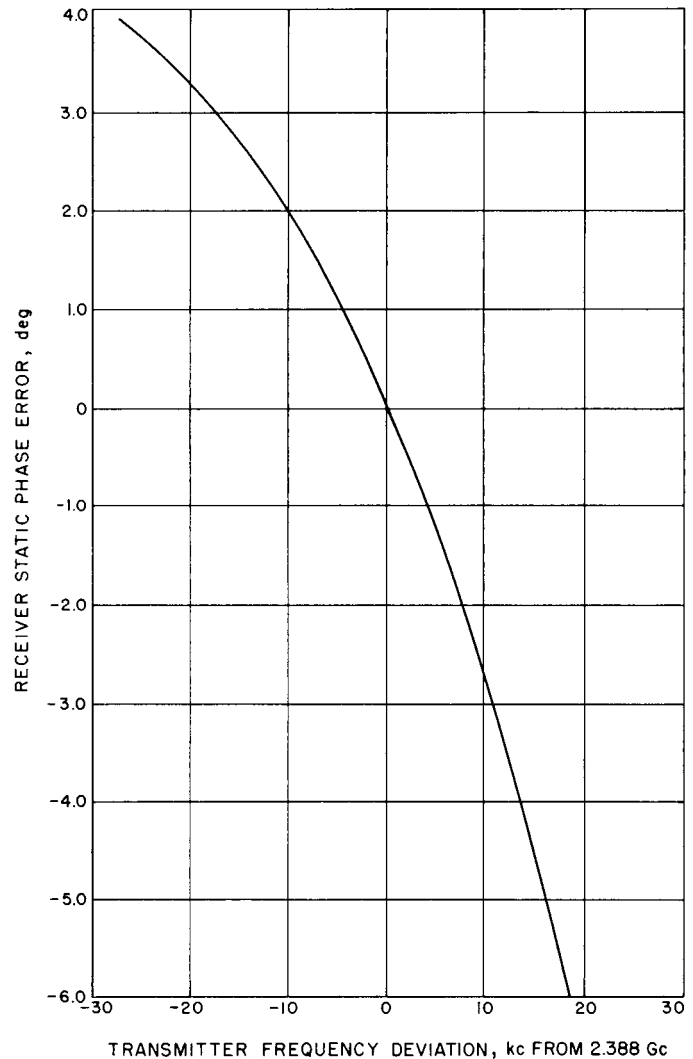
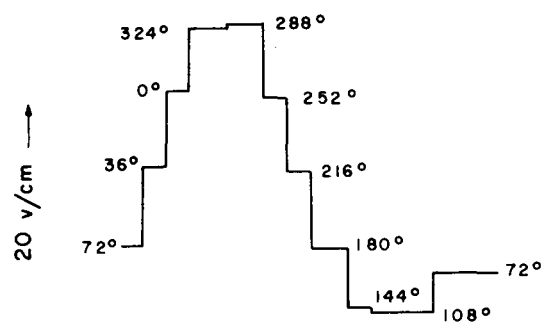


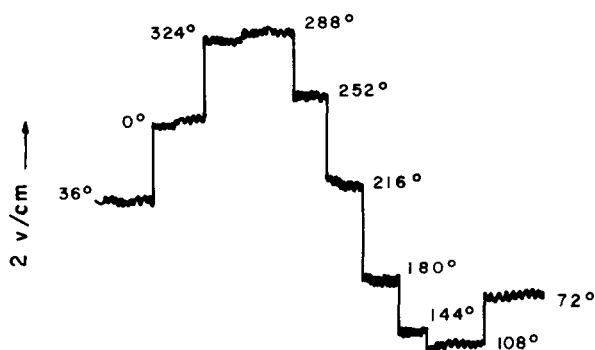
Fig. 65. Receiver static and error produced by transmitter frequency offset

the thermal noise to suppress the limiter. Fig. 66(b) shows the effects of this suppression on the signal of Fig. 66(a). This is also a graphic demonstration of α_0 , the limiter suppression factor at threshold.

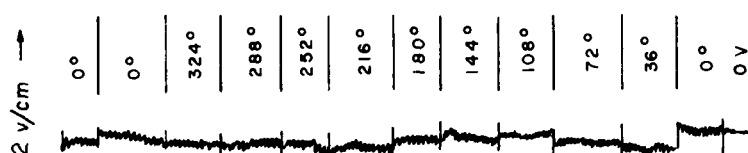
The coherent signal was removed, the receiver input was left terminated, and the phase detector output due to coherent leakage was measured as a function of the reference phase [Fig. 66(c)]. The data is *not* conclusive; recorder and system drift accounts for most of the variation. The "front end" was disconnected and the 30-Mc input to the receiver terminated. This eliminated the noise suppression of the limiter and permitted the coherent leakage in part of the receiver to be measured. The leakage produced a detector output of 0.125 v peak-to-peak.



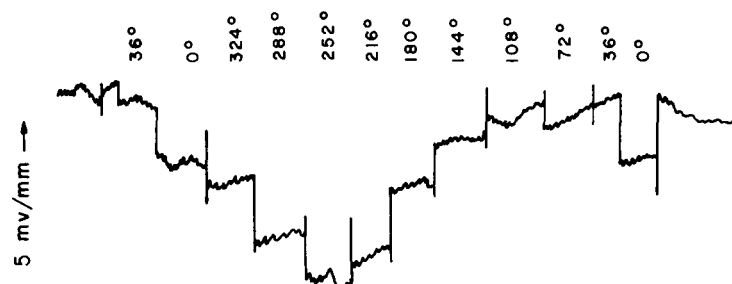
(a) THRESHOLD COHERENT SIGNAL INJECTED, NO FRONT END



(b) THRESHOLD COHERENT SIGNAL INJECTED, FRONT END NOISE ADDED



(c) COHERENT LEAKAGE, COMPLETE RECEIVER, NO INJECTED SIGNAL



(d) COHERENT LEAKAGE, RECEIVER FRONT END DISCONNECTED, NO INJECTED SIGNAL

Fig. 66. Coherent leakage RF carrier loop phase detector output versus reference phase

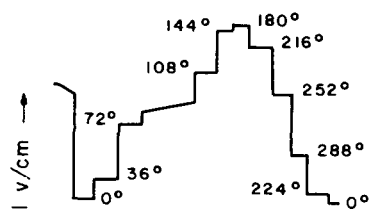
For $\alpha_0 = 0.101$, this is equivalent to $(0.125)(0.101) = 0.0126$ v peak-to-peak at threshold. From Fig. 66(b), the phase detector output at threshold was 8.2 v peak-to-peak. Thus, the ratio of the interference to the threshold signal is within specification (40 db):

$$20 \log \frac{E_1}{E_2} = 20 \log \frac{8.2}{0.0126} = 56.5 \text{ db}$$

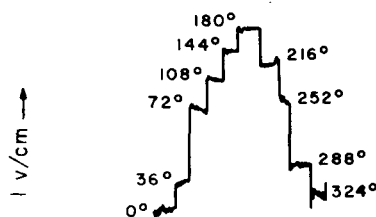
This test did not measure the coherent interference due to the "front end." Further tests are planned, with better instrumentation, to measure this. However, the

next test, coherent leakage in the AGC loop, did include the front end and the leakage was within the specified limit of -40 db.

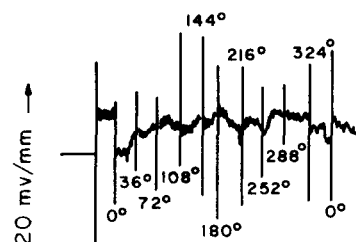
AGC loop coherent interference. Internal coherent interference in the AGC loop was measured by introducing a 30-Mc coherent signal into the receiver at a level equivalent to a threshold input signal. This established the reference for the measurement which requires that the leakage be at least 40 db below the maximum amplitude of the threshold signal.



(a) COHERENT SIGNAL INJECTED, NO FRONT END NOISE



(b) COHERENT SIGNAL INJECTED, FRONT END NOISE ADDED



(c) COHERENT LEAKAGE ONLY, NO INJECTED SIGNAL

Fig. 67. Coherent leakage AGC channel, AGC detector output versus reference phase

Fig. 67(a) is the AGC detector output versus the reference phase for the injected coherent signal with the receiver front-end disconnected and Fig. 67(b) shows the effect of the front-end noise. No limiting due to noise is evident. The injected signal was removed and the AGC detector output due to coherent leakage versus the reference phase was measured [Fig. 67(c)]. The leakage component is 46 db below the threshold signal, exceeding the specification of 40 db. This test was for the complete receiver, including the front end.

e. Additional tests. Other tests in process include coherent leakage of the RF carrier tracking loop complete receiver; AGC loop frequency response; frequency response and coherent leakage of the radiometer channels; loop bandwidth and spectral analysis of the coherent reference generator; and tests on the liquid cooling system.

6. Automatic Acquisition for Narrow Bandwidth, Phase-Locked, Reference Loops

Manual action is usually required to lock a narrow-band reference loop following equipment turn-on or

momentary loss of signal or power. This may consist of monitoring the phase-detector output with an oscilloscope and adjusting the VCO frequency until the beat-note at the detector output goes to zero. The VCO must then be readjusted for zero static phase error for best performance. In the case where $2\beta_L = 3$ cps and a high Q , temperature stabilized VCO is used, the VCO is stable enough that the loop will eventually lock unaided in 10 to 30 min. During this time any received data is invalid.

To speed the acquisition process without the requirement for manual action, the circuit of Fig. 68 was developed. In addition to providing self-acquisition to the loop, the loop status condition is monitored and displayed. Necessary conditions for a clean-up loop to be considered operable are that the reference (to which the loop must lock) and the VCO output be present in the phase detector and that they be in correct phase. A beat note will appear at the detector output if the frequencies differ, but "no beat" can mean the signals are in phase or there is no signal. To avoid this ambiguity, the signals are detected (Fig. 69) and summed in an *and* gate with a "no beat" signal. The gate controls a driver to operate a relay and lamp indicators. The gate

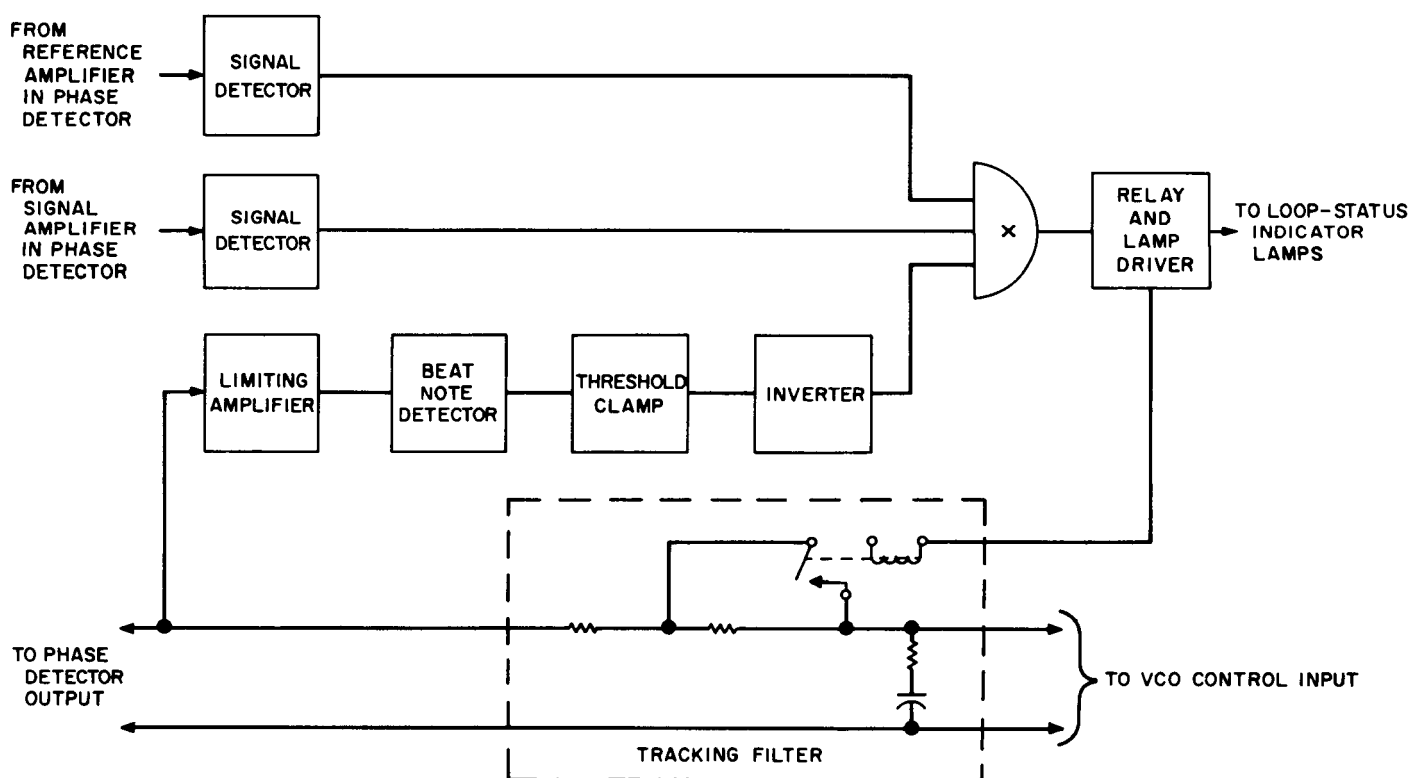


Fig. 68. Loop in-lock indicator and self-acquisition device

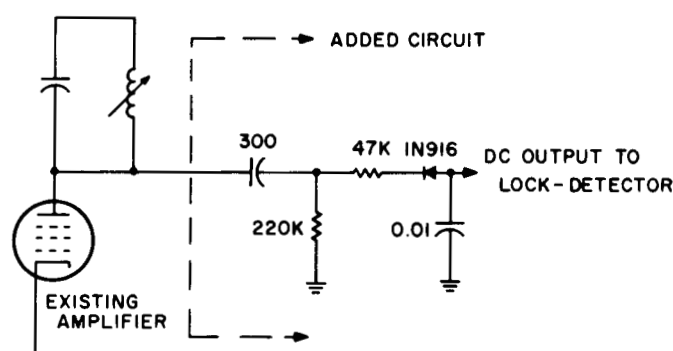


Fig. 69. Signal detector added to both amplifiers in the phase detector

is enabled by the presence of both signals and a no-beat signal, i.e.,

$$A \times B \times \bar{C} = D.$$

where

A = reference signal

B = VCO signal

C = beat note, and \bar{C} = not C

D = gate output

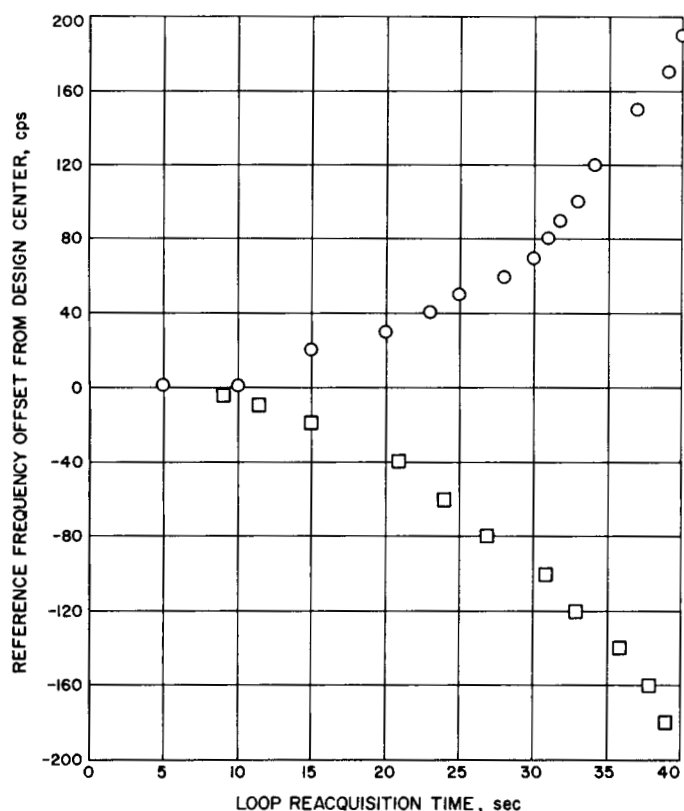


Fig. 70. Reference frequency offset versus loop reacquisition time

A relay in the tracking filter shorts one of the series resistors and increases the bandwidth. When the loop pulls into lock and the beat note disappears, the relay opens and the filter is restored to the narrow-band, operating condition.

In a further refinement, the gate outputs from several loops were summed to give a system status indication. In a test of the automatic lock-up time, the tracking filter was shorted to open the loop, the reference frequency was shifted a discrete amount, the short removed, and the time to reacquire measured. Fig. 70 is a plot of the offset frequency versus acquisition time. The tracking filter had the following characteristics:

Narrow bandwidth, $2\beta_L = 3$ cps

Wide bandwidth, $2\beta_L = 200$ cps

D. Ranging System Development

1. Mod III Ranging Equipment

a. Introduction. Although the Mod III ranging equipment (Fig. 71) is numbered in the series of interplanetary-ranging equipments, its usefulness extends far beyond any single-purpose application. Designed primarily as a medium-speed, general-purpose digital controller possessing flexible programmability and input-output diversity, the Mod III can be adapted readily to a multiplicity of control and computational applications, a few of which are listed below:

- (1) Real-time automatic range acquisition and tracking at interplanetary distances.
- (2) On-line or near on-line data handling and processing to facilitate the collection of data in suitable format for subsequent processing.
- (3) Automatic station check-out via inspection of status information of the operational systems, the analysis of this data using applicable criteria, and the generation of decisions upon which the operating personnel, or the controller itself, may act.
- (4) General sequential and simultaneous control of other equipment.

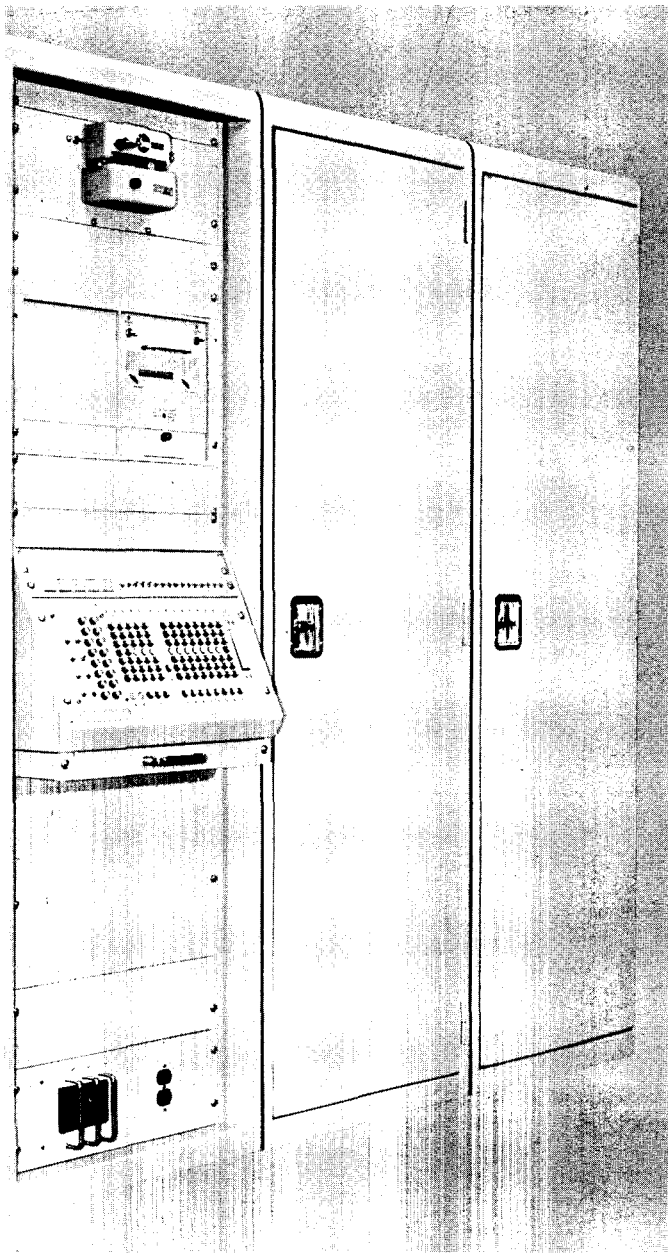


Fig. 71. Mod II ranging equipment

The potential usefulness of the Mod III has already been demonstrated successfully in recent ranging experiments by its sister machine, the Mod II ranging equipment. This work is reported in *SPS 37-18*, Vol. III, pp. 50-53 and *SPS 37-19*, Vol. III, pp. 28-29. The Mod III and Mod II ranging equipments are similar in logical design, but not in input-output capacity, peripheral devices, or physical construction. The detailed logical design forming the basis of these two equipments may be found in Reference 8.

This article is primarily concerned with the specifications of the Mod III ranging equipment and its construction. A comparison is drawn between the Mod III and Mod II ranging equipments where applicable.

b. System philosophy. In general, a ranging system must be able to:

- (1) Manipulate binary code sequences.
- (2) Make on-off selections.
- (3) Determine that on-off selections have been made.
- (4) Compute range numbers.
- (5) Make decisions based upon input information.
- (6) Follow a prescribed sequence (or program) of operations.
- (7) Quantize analog signals into digital numbers, and conversely so.

These requirements essentially describe a generalized digital controller, particularly so, if a large and diversified input-output interface and a full arithmetic capability are added. Consequently, instead of developing just a single-purpose equipment, a general-purpose digital controller was constructed, thereby removing the machine from the category of limited usefulness.

In most advanced digital control applications, computations necessarily precede control decisions. Included in this are magnitude and sign comparisons of variables with known or computed standards. In addition, different control applications require their own sequences of control operations so that it is essential that a general-purpose controller provide a convenient method of changing the sequences. Moreover, on the basis of input data, it may be necessary to provide for the automatic reprogramming of the control operations. It is, therefore, natural for the Mod III to incorporate the features of a typical stored-program, general-purpose digital computer. In such a computer, the program for solving a problem is not wired permanently into the machine. Instead, the machine is wired to execute elementary operations on data according to a sequence of instructions stored in the memory of the computer and the input information received. It is on this basis that the Mod III ranging equipment has been constructed. Because the Mod III ranging equipment can interconnect with external equipment readily and because its sequence of instructions can be easily altered, the Mod III ranging equipment can be applied to the automatic check-out, supervision, and control of large and complex ranging

and tracking systems. A functional block diagram (Fig. 72) illustrates the major sections of the machine, and Fig. 73 shows, in general form, the various inputs and outputs in the Mod III ranging equipment.

c. Functional description. Both the Mod III and the Mod II ranging equipments possess an identical central

structure, termed the stored-program controller (SPC), which is an assembly of five functional parts: an input unit, a control unit, a memory unit, an arithmetic unit, and an output unit. The input unit gathers the various data and signals from the system to be controlled. Signals comprise status information in the form of two-level static voltages, 1-Mc pulse trains, or relay-buffered con-

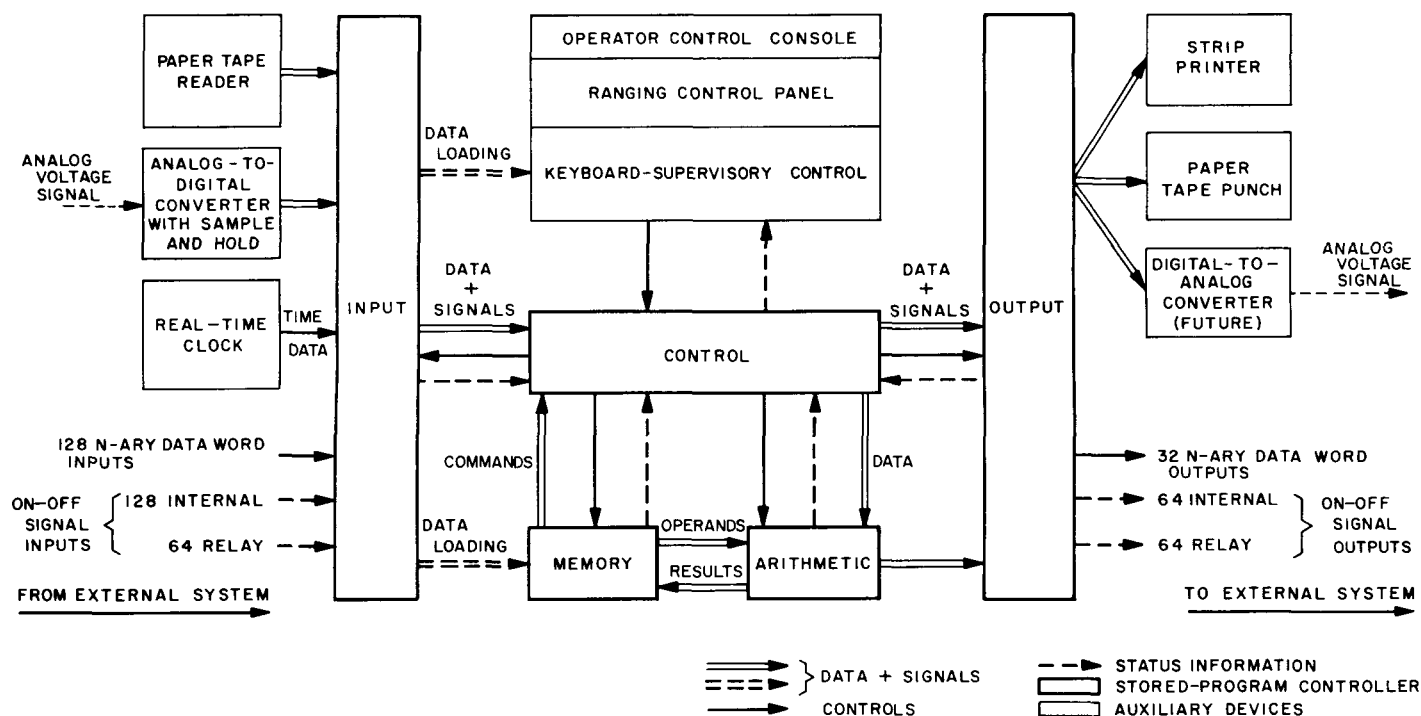


Fig. 72. Functional block diagram of Mod III ranging equipment

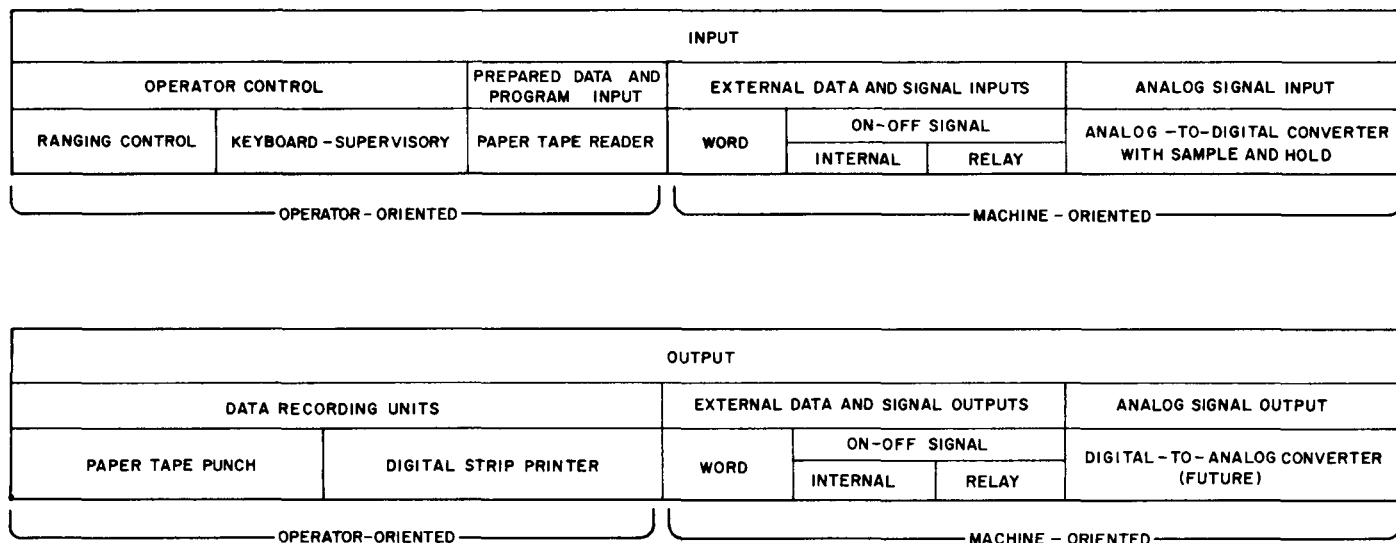


Fig. 73. Input-output classification

tact states. They can be only logically true or false. Data is in the form of 25-bit numbers or words. The information content here is usually numerical, but may also be logical. The control unit processes data and signals according to the program stored in memory and, in so doing, directs the participation of the other units as needed. The memory unit stores the operating program, data, temporary results, and such other information as may be required to carry out the program. The arithmetic unit performs the basic computational operations of add, subtract, multiply, and divide, as well as such operations as extract (logical multiply), logical exclusive OR, shift, and compare. The output unit provides a means of communicating data and signals to the system being controlled and to display and recording devices.

The input unit provides 128 input-word channels. A word is a 25-bit 1-Mc binary code sequence which can represent either an order or data. To be used in the SPC, a word must be limited to a 25-bit length, be compatible with the voltages and truth conventions of Computer Control Company Series-T digital modules (i.e., a logical 0 is denoted by a voltage more positive than -0.5 v; a logical 1 by a voltage more negative than -1.0 v), utilize the same 1-Mc clock rate and phase as used in the SPC, and be properly phased with respect to the minor-cycle period (word-time) of the SPC. The words may come from paper-tape readers, manual keyboards, frequency counters, the coordinate converter at the Goldstone Tracking Station, and the Mod II ranging equipment. Also, provided are 192 on-off signal channels of which 128 are assigned to internal signals (i.e., 1-Mc pulse trains or static dc voltage signals compatible with the SPC logic levels) and 64 to external signals (i.e., user-operated relay-buffered contact states). The on-off signal inputs may be used for any variable in a controlled system which can be characterized by two possible states. Examples of such variables are those whose states can be described by the following typical pairs: on-off; open-shut; high-low; up-down; plus-minus; etc. The external on-off signal inputs provide their own relay supply (-6 v) and common return so that it is only necessary to complete the circuit to the desired relay and this closure will be repeated internally in the SPC. Relay coil transient suppression is built-in.

The output unit structure is similar to that of the input unit. To transmit 1-Mc words to output auxiliary devices, e.g., paper-type punches, digital strip printers, digital-to-analog converters, displays and data-handling equipment, 32 channels are provided. These take the form of a common information channel in which words and their com-

plements are made available to the user and selected by 25 μ sec, 1-Mc pulse trains from the 32 selection gates. A total of 128 channels for on-off signals is provided. Of these, 64 channels are assigned to internal signals and 64 to external signals. As in the case of the input unit, the internal signals are those compatible with the SPC logic levels, and these are provided by 64 static flip-flops. The external signals are supplied by relay contacts operated by static flip-flops. These contacts are rated for maxima of 4 w, 350 v, and 125 ma for dc resistive loads, which is adequate for most control purposes.

All of the inputs and outputs are directly addressable by the SPC; i.e., they can be activated when a program order specifies an input or output by its address. Thus, data words and signals may be received by and sent from the SPC on command.

The arithmetic unit provides the ability to add, subtract, multiply, and divide numbers. Furthermore, it can perform logical operations such as extract, logical exclusive OR, shift, and compare. Because most ranging operations involve integral numbers, floating-point operations are not incorporated. Special functions, when required, are implemented by suitable subroutines. Examples of these would be square-root, trigonometric, and hyperbolic functions. In ranging at interplanetary distances, the numbers can be quite large. To handle these, the arithmetic unit is designed to perform readily double-length (50-bit) arithmetic and logical operations when so programmed.

The memory unit provides bulk storage for 1024 words in delay lines of 32 word cells each and fast-access storage for 32 words in one-word delay lines. Although this is adequate for most ranging and control tasks, the memory may be expanded readily to include a total of 8192 words of magnetic-core storage.

The control unit is an assembly of six functional sections: program counter, command register, operation decoder subsystem, address-selection subsystem, indexing subsystem, sequential control machine, and clock subsystem. The program counter specifies the address in memory of the next program instruction to be used. As each instruction is processed, the program counter contents are normally incremented by one unit so that program orders are followed in sequence. Skip commands conditionally resulting from tests of external signals or number comparisons may modify the increment to 2 or 3 units. On a transfer order the program counter contents are replaced by the address in the transfer order. The

command register holds the current instruction to be processed, thereby making available the operation code and the operand address for use by the operation-decoder and address-selection subsystems. The former subsystem decodes and stores the operation code for producing and distributing operation-control signals in the SPC. The latter subsystem controls all memory and input-output references by interpreting addresses which come from the program counter or command register.

The indexing subsystem permits address modification under program control. When so ordered, the contents of one of these index registers may be added to the address to produce a new effective address. Limit lines (one for each index register) may be loaded with limiting values. The index registers may be successively incremented as orders are executed and the contents of the index registers compared with those of the limit lines to determine the future course of the program.

Table 5. Common specifications of Mod II-III ranging equipment

Type of machine logic	Synchronous, serial dynamic
Basic clock rate	1 Mc
Bit time	1 μ sec
Word length	25 bits
Instructions:	
(1) Type	Single-address (Fig. 75)
(2) Operations	64 total with full arithmetic capability, single-or-double-precision (Fig. 74)
Memory:	
(1) Type	Recirculating magnetostrictive delay line
(2) Capacity:	
(a) Bulk memory	1024 words (in 32 32-word lines)
(b) Fast-access memory	32 words (in 32 1-word lines)
(3) Characteristics:	
(a) Bulk memory:	
Major cycle time	800 μ sec
Interlace spacing	5 word-time intervals (125 μ sec) from word cell n to $n + 1$.
Minimum access time to successive cells	125 μ sec
(b) Fast-access memory:	
Minimum access time	25 μ sec
Addresses	Refer to Table 6
Input-output	Refer to Table 6
Auxiliary devices:	
(1) Keyboard-supervisory control panel	
(2) Ranging control panel	
(3) Punched-paper tape reader and spooler (100 characters/second)	
(4) Paper-tape punch (20 characters/second)	
(5) Digital strip printer (5 lines/second)	
(6) Analog-to-digital converter with sample and hold accessory	
(7) Digital-to-analog converter (future)	
(8) Real-time clock	

The operational phases of the SPC are established by the sequential control machine. These phases in cyclic order of occurrence are: (1) command, (2) read-in, (3) wait, (4) execute 1, and (5) execute 2. In Phase (1), a search is made for a new command. In Phase (2), the new word is read into the command register. In Phase (3), the machine waits until the data is located and selected. In Phases (4) and (5) (the first and last operation cycles), the operation is executed. The machine also provides two noncyclic states: run and stop. In stop, the machine proceeds until a selection is required, at which time it halts because selections are only possible in the run state.

The clock subsystem consists of three basic clocks: the bit-time clock (i.e., the basic 1-Mc pulse rate); the word-time or minor-cycle clock (i.e., a 25- μ sec interval marking the time intervals required for words); and the major-cycle clock (i.e., an 800- μ sec interval marking the recirculation period of the 32-word storage lines in bulk memory). Included here also is a Modulo-32 counter which numbers or tags the successive words of a major cycle. These word-tags are used to interlace successively-

Table 6. Input-output specifications of Mod II-III ranging equipment

Description	Number of channels	Octal address range
Mod II^a		
Inputs:		
Compatible word channels	128	20200 to 20377
On-off signal channels:		
Internal	128	21000 to 21177
External (relay)	256	21200 to 21577
Outputs:		
Compatible word channels	32	22200 to 22237
On-off signal channels:		
Internal	64	23000 to 23077
External (relay)	128	23200 to 23377
Mod III^a		
Inputs:		
Compatible word channels	128	20200 to 20377
On-off signal channels:		
Internal	128	21000 to 21177
External (relay)	64	21200 to 21277
Outputs:		
Compatible word channels	32	22200 to 22237
On-off signal channels:		
Internal	64	23000 to 23077
External (relay)	64	23200 to 23277

^aAs currently-wired.

Note:

(1) The comparative listing of this table is based upon the currently-wired status of the two equipments. Appropriate addressing-structure exists, however, to extend the system capacity to the maximum limits listed in Table 2, p. 36 of Ref. 8.

(2) Although the Mod II incorporates an oscilloscope, no such equipment is included as an integral device in the Mod III.

numbered word cells in the 32-word lines of memory at 5-word intervals to allow successive orders to be carried out as rapidly as every 125 μ sec.

d. General specifications. Because the Mod III and Mod II ranging equipments are primarily the same, the specifications for the machines are presented on a comparative basis. Reference to the logical structure of the Mod II ranging equipment (Ref. 8) will verify this fact. The specifications in common for the two equipments are listed in Table 5.

Table 6 lists the input-output specifications for the two equipments. The essential difference between the Mod II and Mod III is one of input-output capacity.

A table of available operations is given in Fig. 74 and shows the mnemonic codes to be used for each operation as well as the associated operation code in the machine proper, i.e., the digits D and C.

e. Word structure. In the SPC, two word types are used: data words and command words (Fig. 75). All words

D	0	1	2	3	4	5	6	7
C	TRANSFER	SHIFT	TEST	STORE	ADD	SUBTRACT	MULTIPLY	DIVIDE
0	HTR	ALS	SIZ	STC	CLA	CLS	MUF	
	HALT AND TRANSFER	ACCUMULATE LEFT SHIFT	SKIP IF INPUT SIGNAL IS FALSE	STORE AC CLEAR AC (SET SIGNAL)	CLEAR AC ADD M	CLEAR AC SUB M	MULTIPLY FRACTIONAL	
	MANUAL RESTART	$\leftarrow AC \leftarrow 0$	(=0)	$AC \rightarrow M$	$0 + M$	$0 - M$	$M \times MQ$	
1	TRA	ARS	SIT	STO	ADD	SUB	MAF	
	TRANSFER	ACCUMULATE RIGHT SHIFT	SKIP IF INPUT SIGNAL IS TRUE	STORE AC (SET SIGNAL)	ADD M	SUB M	MULTIPLY AND ADD FRACTIONAL ($M \times MQ$) + AC	
		$0 \rightarrow AC \rightarrow$	(=1)		$AC + M$	$AC - M$		
2	TXI	LLS	CAS	RSE				
	INCREMENT IR AND TRANSFER	LONG LEFT SHIFT	COMPARE AC 4 M >:NEXT =:NEXT +1 <:NEXT +2	RESET SIGNAL				
		$\leftarrow AC \leftarrow MQ \leftarrow 0$						
3	TIX				LXA	LXC		
	INCREMENT IR AND TRANSFER UNLESS IR = LIM	LONG RIGHT SHIFT	ADDRESS TO INDEX TRUE	STORE INDEX IN ADDRESS	LOAD INDEX FROM ADDRESS	LOAD INDEX WITH COMPLEMENT $\neg M \rightarrow IR$		
		$0 \rightarrow AG \rightarrow MQ \rightarrow$	$CL \rightarrow IR$	$IR \rightarrow M$	$M \rightarrow IR$			
4	TZE	LGL	HIZ	ANS	ANA	NNA	MUI	
	TRANSFER IF AC = 0	LOGICAL LEFT SHIFT $\leftarrow AC \leftarrow MQ$	HALT IF INPUT SIGNAL IS FALSE (=0)	AND TO STORAGE $AC \cdot MQ \rightarrow M$	AND TO ACCUMULATOR $M \cdot MQ \rightarrow AC$	NEGATIVE AND TO ACCUMULATOR $\bar{M} \cdot MQ \rightarrow AC$	MULTIPLY INTEGER	
5	TMI	LGR	HIT	ERS	ERA	NRA	MAI	
	TRANSFER IF AC MINUS	LOGICAL RIGHT SHIFT $\rightarrow AC \rightarrow MQ$	HALT IF INPUT SIGNAL IS TRUE (=1)	EXCLUSIVE OR TO STORAGE $AC \oplus MQ \rightarrow M$	EXCLUSIVE OR TO ACCUMULATOR $M \oplus MQ \rightarrow AC$	NEGATIVE EXCLUSIVE OR TO ACCUMULATOR $\bar{M} \oplus MQ \rightarrow AC$	MULTIPLY AND ADD INTEGER	
6	TPL	RQL	ALT	PSE	LLL	LLM		
	TRANSFER IF AC PLUS	ROTATE MQ LEFT $\leftarrow MQ \leftarrow$	ADDRESS TO LIMIT TRUE $CL \rightarrow LL$	PULSE SIGNAL	LOAD LIMIT LINE $M \rightarrow LIM$	LOAD LIMIT LINE MINUS $\neg M \rightarrow LIM$		
7	TOV	RQR	TCL	STQ	LDQ	LNQ		
	TRANSFER IF OVERFLOW; RESET OVERFLOW	ROTATE MQ RIGHT $\rightarrow MQ \rightarrow$	STOP; RESTART ON NEXT TIME TICK	STORE MQ $MQ \rightarrow M$	LOAD MQ $M \rightarrow MQ$	LOAD MQ NEGATIVE $\neg M \rightarrow MQ$		
ANS, ANA, NNA, ERS, ERA AND NRA ARE LOGICAL OPERATIONS ON INDIVIDUAL BITS OF WORDS								

Fig. 74. Table of operations

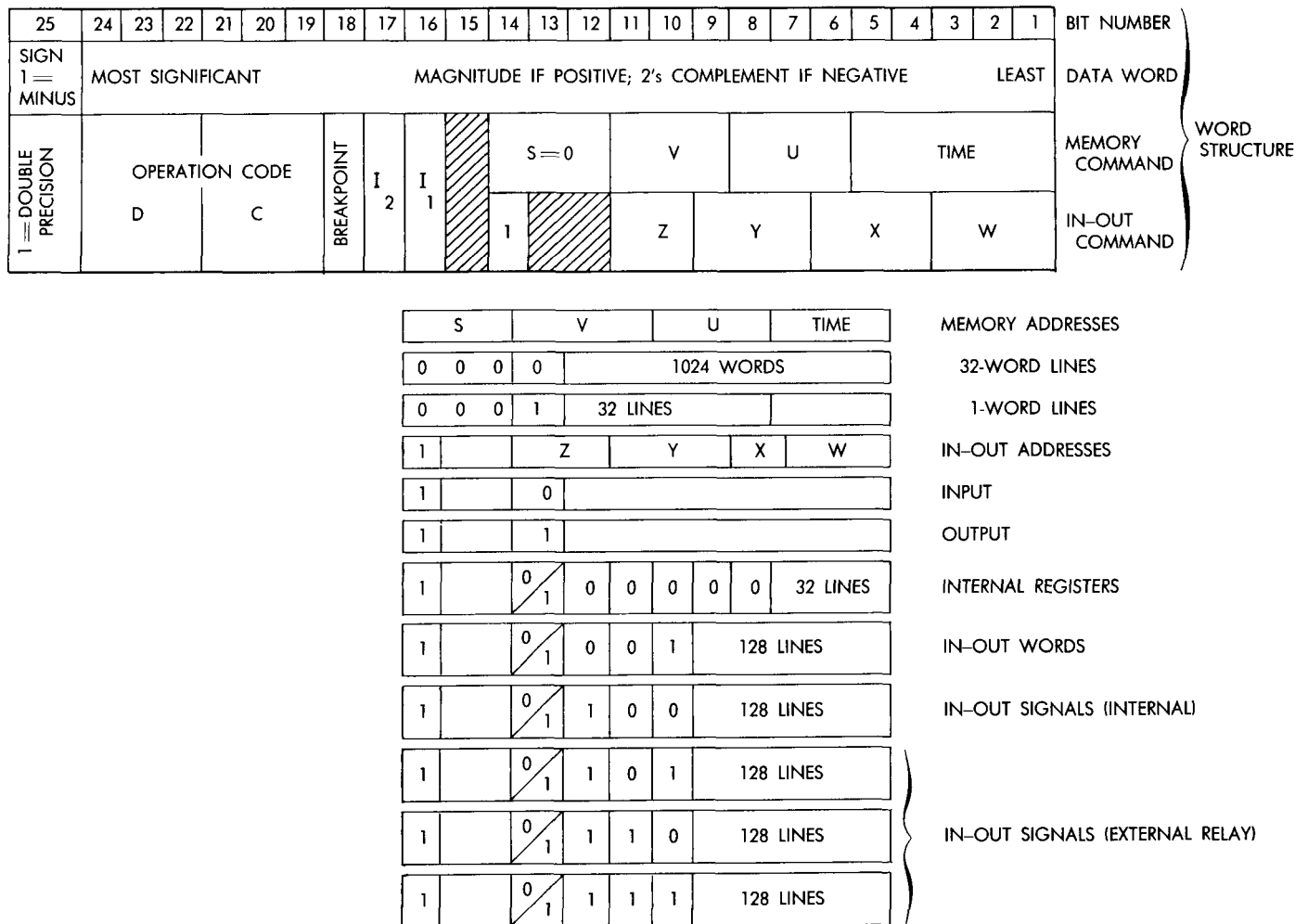


Fig. 75. Word structure

are 25 bits in length and are transmitted with the least significant bit first. In a data word, the most significant bit (bit 25) is the sign bit. The remaining bits form the magnitude if the sign bit denotes positive data; otherwise, they form the 2's complement because, in the SPC, negative numbers are so formed. Command words are further classified as memory commands and input-output commands. These are distinguished by the state of bit 14: 0 denoting memory and 1 denoting input-output selection. In a memory selection, 0 in bit 11 denotes a 32-word storage-line selection and 1 in bit 11 denotes a 1-word storage-line selection. The former requires a time selection to cause a word to enter or exit the correct word cell in a 32-word line. This is accomplished by detecting equality of the first 5 bits of the word address and the word tags from the Modulo-32 counter in the clock system. The spatial address comprises three fields: U, V, and S. The S-field (bits 12, 13, and 14) is always zero

for the memory size provided. The U- and V-fields (bits 6, 7, and 8; and bits 9, 10, and 11, respectively) locate the storage line to be used. In input-output, the address is divided into fields: W, X, Y, and Z (bits 1, 2, and 3; bits 4, 5, and 6; bits 7, 8, and 9; and bits 10 and 11, respectively). The Y- and Z-fields are treated together as the ZY-field. In general, the 3-bit field assignment is particularly convenient in that it allows octal-number coding of the words. In a command, operations are also denoted by two octal-digit fields: C and D (bits 19, 20, and 21; and bits 22, 23, and 24, respectively). When indexing operations are required, the desired index registers are specified in the command by index flags: I_1 and I_2 (bits 16 and 17, respectively).

f. Description of operations. As previously indicated, the operation code is determined by the six most significant bits in the command word, exclusive of the sign

digit (bit 25). These six bits comprise the two octal-digit fields, D and C, where D is the most significant octal digit. Each field is decoded to produce one-out-of-eight output selections. In general, octal digit D denotes a basic operation class, and C denotes a variation within the class. Combinations of D and C, therefore, permit up to 64 operations (Fig. 74). A summary of operations is given in Table 7.

Double-precision operations are denoted by a command with a minus sign digit in the bit 25 position. When this occurs, the operations are carried out on 50-bit numbers rather than 25-bit numbers. For proper results the

use of double-precision operations requires that certain rules be followed:

- (1) Store the two halves of the number in successive memory locations in one memory line, the lesser half in an even-numbered cell and the greater half in the *adjacent cell*, which, due to the interlace scheme, is numbered 13 higher, Modulo 32.
- (2) Unless intended as such, the sequence of double-precision commands must not be interrupted; otherwise, the AC-, SR- and MQ-registers will revert from their extended 50-bit length to the normal 25-bit length and half the digits will be

Table 7. Summary of operations

Numerical order code (D and C)	Mnemonic symbol code for the order	Effect
00	HTR m	Transfers Transfer control to memory address m (i.e., take next command from address m) and halt the machine. Restart the machine <i>manually</i> . Transfer control to address m unconditionally. Increment by one the contents of index register (IR) specified by index tag in the command, and transfer control to address m. Increment by one the contents of IR specified by index tag in the command and transfer m, except when contents of IR equal that of its corresponding limit line (LL), in which case, proceed to next command in normal sequence. If accumulator (AC) is zero, transfer control to address m; otherwise, take next command in sequence. If AC contains a minus sign digit, transfer control to address m; otherwise, take next command sequence. If AC contains a plus sign digit, transfer control to address m; otherwise, take next command in sequence. If AC overflows, i.e., AC capacity is exceeded, transfer control to address m, and reset overflow detector; otherwise, take next command in sequence.
01	TRA m	
02	TXI t m	
03	TIX t m	
04	TZE m	
05	TMI m	
06	TPL m	
07	TOV m	
10 through 17		Shifts These are shift commands executed on the operational registers, MQ and AC, as noted in Fig. 74. The number of bit positions to be shifted is specified in the first five low-order bits of the shift command address by the natural binary equivalent of the number of bit places to be shifted.
22	CAS m	Comparison Compare, algebraically, the contents of memory address m with that of the AC. If the contents of the AC are algebraically: (1) Larger, take next command in the program in normal sequence; (2) Equal, skip the next command in the program by incrementing the program counter (PC) by two; (3) Smaller, skip the next two commands in the program by incrementing the PC by three. In all cases, the contents of the AC remain unchanged. Note that in the execution of a command, the PC normally is incremented by one in order to select the next command in sequence. Internal and external input signal tests: conditional skips If input signal at address x is false (0), skip next command in the program, by incrementing PC by two; otherwise, take next command in sequence. If input signal at address x is true (1), skip next command in the program, by incrementing PC by two; otherwise, take next command in sequence. Internal and external input signal tests: conditional halts If input signal at address x is false (0), halt the machine. Restart manually with next command in sequence; otherwise, continue. If input signal at address x is true (1), halt the machine. Restart manually with next command in sequence; otherwise, continue.
20	SIZ x	
21	SIT x	
24	HIZ x	
25	HIT x	

Table 7. Summary of operations (cont'd)

Numerical order code (D and C)	Mnemonic symbol code for the order	Effect
27	TCL (no address)	Real-time synchronization Halt the machine, and restart on next real-time signal which is a time-tick normally available at 1-sec intervals.
23	AXT t d	Command address transmissions Copy the command address d (the five low-order octal digits) directly into the IR specified by index tag in the command.
26	ALT t d	Same as for AXT d, but copy into LL instead of IR.
30	STO m	Store operations: memory Clear AC and load storage register (SR) with contents of AC, also storing it in memory address m.
31	STO m	Load SR with contents of AC, also storing it in memory address m.
33	SXA m	Load SR with contents of IR specified by index tag in the command, storing it also in memory address m.
37	STQ m	Load SR with contents of the multiplier-quotient register (MQ), storing it also in memory address m.
30	STC x	Output signal control These are special cases of store operations: memory.
31	STO x	When the above operations are specified with an output signal address x, the load operations are carried out as stated above but the memory store operations are not. Instead, the output signal flip-flop or relay at x is set.
33	SXA x	
37	STQ x	
32	RSE x	
36	PSE x	Reset internal output signal flip-flops or relay at address x. Set internal output signal flip-flop at address x for 25 μ sec; then reset it.
44	ANA m	Bit-wise logical operations Clear AC and logically AND, bit-wise, the contents of m with that of the MQ, putting the result in the AC. This is the familiar logical multiply, mask, or extract operation.
54	NNA m	Same as ANA m, except that the 1's-complement of the contents of m is used.
45	ERA m	Clear AC and logically EXCLUSIVE-OR, bit-wise, the contents of m with that of the MQ, putting the results in the AC. This is the familiar Modulo 2 addition.
55	NRA m	Same as ERA m, EXCEPT that the 1's-complement of the contents of m is used.
34	ANS m	Logically AND, bit-wise, the contents of MQ with that of the AC, proceeding thereafter as in STO m, but leaving the contents of AC unchanged.
35	ERS m	Logically EXCLUSIVE-OR, bit-wise, the contents of MQ with that of the AC, proceeding thereafter as in STO m, but leaving the contents of AC unchanged.
43	LAX t m	Index register-limit line loading Load IR specified by the index tag in the command with the contents of m.
53	LXC t m	Load IR specified by the index tag in the command with the negative (2's-complement) of the contents of m.
46	LLL t m	Load LL specified by the index tag in the command with the contents of m.
56	LLM t m	Load LL specified by the index tag in the command with the negative (2's-complement) of the contents of m.
47	LDQ m	Multiplier-quotient register loading Clear MQ and load with the contents of m.
57	LNQ m	Clear MQ and load with the negative (2's-complement) of the contents of m.
40	CLA m	Clear AC, and add the contents of m to the AC, thus retaining the contents of m in the AC.
50	CLS m	Clear AC, and subtract contents of m from the AC, thus retaining the negative (2's-complement) of the contents of m in the AC.
41	ADD m	Add the contents of m to that of the AC, retaining the sum in the AC.
51	SUB m	Subtract the contents of m from that of the AC, retaining the difference in the AC.
60	MUF m	Multiply operations Clear the AC, and multiply the contents of m and that of the MQ, treating them as binary fractions, retaining the sign digit and high-order part of the product in the AC and the low-order part in the MQ.
61	MAF m	Same as MUF m, except that the AC is not cleared with the result that the contents of the AC are added to the low-order part of the product in the MQ. All numbers are treated as binary fractions.
64	MUI m	Same as MUF m, except that all numbers are treated as binary integers.
65	MAI m	Same as MAF m, except that all numbers are treated as binary integers.

lost. A good practice is to store the contents of the AC and MQ in a temporary location before breaking out of a double-precision sequence. Alternatively, all orders in a double-precision routine may be affixed with the negative sign. Operations in which index registers or limit lines are stored or loaded, i.e., AXT, SXA, LXA, LXC, LLL and LLM, require careful application. (See Ref. 8, pp. 19-20, for further details.)

g. Operator controls. In the Mod III stored program controller, two manual-control panels are provided: the ranging control panel and the keyboard-supervisory panel. Both of these panels are mounted so as to be available to the operator at all times.

The ranging control panel provides a basic control of the machine sufficient for its use as a ranging equipment. When main power is applied to the machine, a "status" indicator "power" window lights. Depressing a "clear and load" pushbutton switch clears the memory, resets all output flip-flops, loads the memory from punched-paper tape and connects the relay supply voltages. The flip-flops and memory are cleared within 1.6 msec, whereas the relay voltages are connected after a delay of 20 to 50 msec at which time the "status" indicator "ready" window lights. During the loading operation, a "loading" indicator is on. At the end of the loading operation, the command register and the program counter are cleared. Depressing the start switch causes the machine to proceed to the next order in sequence, the first of which begins with address 00000. When the machine is running, a "running" indicator displays red (otherwise green). Two indicating pushbutton switches, labeled A and B, are provided for control decisions requiring the operator. When decisions are needed, the machine can be connected to light the appropriate switch, thereby flagging the operator's attention. In addition, 16 break-point toggle switches, octally numbered, are provided for similar purposes. These, however, have no operator-signaling facility.

The keyboard-supervisory panel provides a facility for manually loading words into any memory cell, single-stepping the machine, and supervising the machine. The supervisory functions are grouped on a small sub-panel and provide a means of selecting words via punched tape or keyboard, a means for clearing the control unit and index registers, stopping the machine absolutely or conditionally on the existence of a 1 in bit 18 of a command word, manual transferring, stepping via external pulse source, and duplicating "start" and "clear-and-load" func-

tions of the ranging control panel. In addition, an octal display of the operation code is supplied for visual checking of the program when in a single-step mode.

h. Auxiliaries. The punched paper-tape reader is the primary input means for the Mod III. A Rheem Model RR-101-D/R tape reader and spooler is provided and reads photoelectrically at the rate of 100 characters/second. Thus, an 11-character word would be read in approximately 0.11 sec.

The tape code and format is an adaptation of the Datatron Flexowriter code as illustrated in Fig. 76. Each word consists of sign plus eight digits followed by finish code plus one of carriage return, tab or end-of-file code and is read in this order beginning with the sign digit. A delete code may appear in conjunction with any of the foregoing coded digits.

A Friden Model II paper-tape punch provides the corresponding tape output facility. This unit is mounted on a portable stand remote from the Mod III proper.

A second output recording device is provided by a Hewlett-Packard Model H24-562AR digital strip printer.

CHANNEL	1	2	3	•	4	5	6	7
SYMBOL	1	2	4	•	8	F	C	B
CHARACTERS:								
0	0	0	0	•	0	0	1	0
1	1	0	0	•	0	0	1	0
2	0	1	0	•	0	0	1	0
3	1	1	0	•	0	0	1	0
4	0	0	1	•	0	0	1	0
5	1	0	1	•	0	0	1	0
6	0	1	1	•	0	0	1	0
7	1	1	1	•	0	0	1	0
OPERATIONS:								
DELETE	φ	φ	φ	•	φ	φ	φ	1
TAB	0	0	1	•	0	0	0	0
END-OF-FILE	1	1	1	•	0	0	0	0
END-OF-WORD (SPACE)	0	0	1	•	1	1	0	0
CARRIAGE RETURN	1	0	1	•	0	0	0	0
AT START OF WORD, NUMBER								
1 = HOLE	0 DENOTES +							
0 = NO HOLE	1 DENOTES —							
φ = DON'T CARE	OTHERWISE, ASSUMES NUMERICAL VALUE							

Fig. 76. Paper-tape code, Mod III stored-program controller

Logic is provided to enable this to print out a line-at-a-time of two BCD words or one octal word with sign.

An Adage Voldicon Model VRIO-AB/SA2 bipolar, high-speed, analog-to-digital converter equipped with a sample and hold accessory is provided to accommodate analog voltage inputs to the Mod III.

A real-time clock provides 1-sec time ticks as well as real-time data words for use in real-time ranging and tracking applications.

i. Construction. The physical presentation of the Mod III ranging equipment is essentially the same as that of the Mod II in order to simplify personnel training and equipment maintenance. Figs. 71, 77, and 78 illustrate the significant features of the equipment which are as follows:

- (1) All components are housed in a three-bay, 19-in. rack-enclosure assembly, except for the paper-tape

punch which is mounted on a portable stand for remote location in an area where the punch chatter will not disturb operating personnel.

- (2) The first bay has a standard 19-in. opening for face-mounting of the reader and spooler, the digital strip printer, a breaker panel, a slide-out table, and the manual control turret. Logic power supplies, input-power ammeters and connector panel, and analog-to-digital converter are mounted at the rear.
- (3) The remaining two bays each contain two slide-out frames for the mounting of up to 11 logic blocks in each frame. Three frames are now loaded and one spare frame is available.
- (4) User connections to input-output are made through a patch panel at the rear of the center bay.
- (5) Keyboard-supervisory and ranging control panels are located on the control turret so as to be acces-

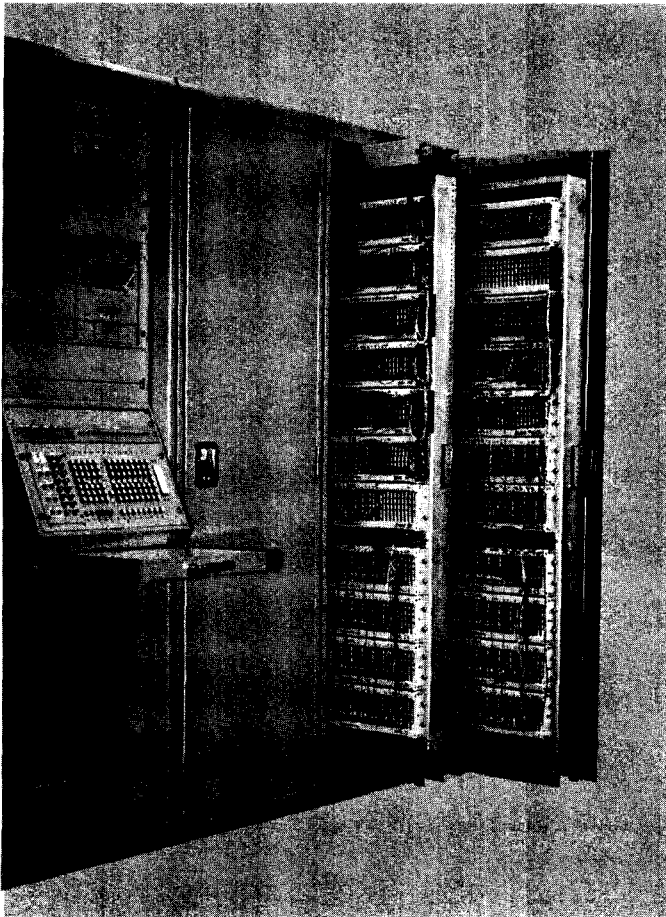


Fig. 77. Construction (front), Mod III ranging equipment

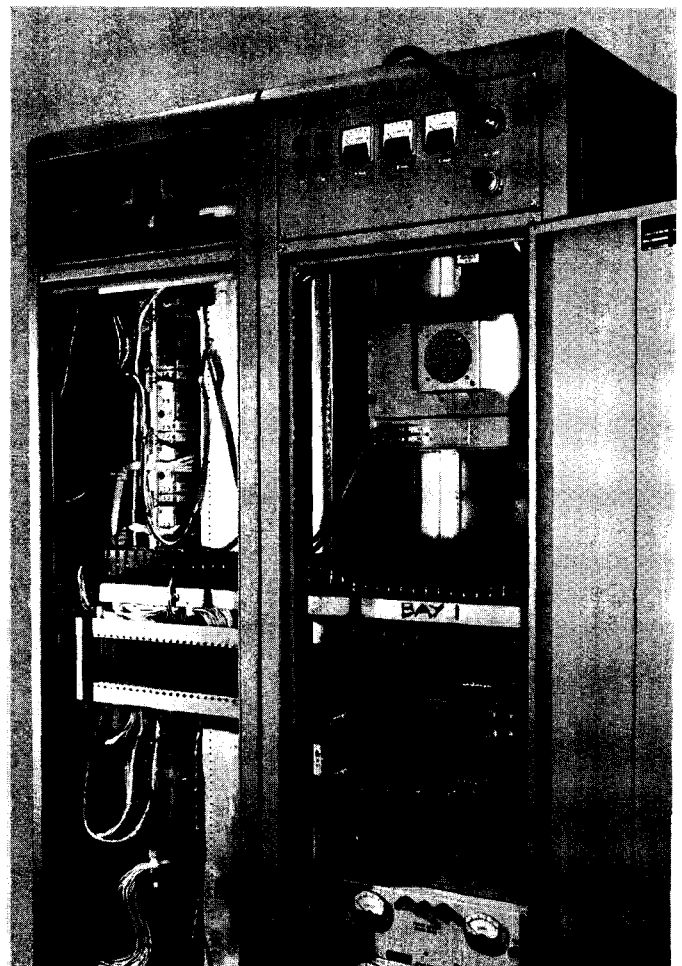


Fig. 78. Construction (rear), Mod III ranging equipment

sible to the user at all times. This is in contrast with the Mod II where the keyboard-supervisory panel is mounted in a frame inside the rack enclosure in view of its somewhat less frequent usage. The ranging control panel in the Mod II is the dominant means of manual control.

j. Project status. Construction and wiring are essentially complete. Only the divide logic and the digital-to-analog converters remain. Multiply logic has been designed and is being incorporated during the advanced check-out phase. The remaining items are planned as future modifications. Temporarily, division may be carried out by means of a subroutine. The equipment, as described, is expected to be ready for installation at Goldstone soon.

2. Programming and Documentation Support for the Stored Program Controller

a. General introduction. One of the objectives in the design of stored program controller portions of the Mod II and III ranging equipments was to make the process of writing and running programs straightforward and logical from the viewpoint of the engineer or scientist. It was intended that the experimenter would be able to gain the necessary information concerning the programming of the stored program controller (SPC) from an easily understood and quickly assimilated programming manual. This information should enable him to write and check both control and computation type programs. It should require little background in computer technology. Experience thus far with the SPC has shown that this objective is realizable.

There is, however, a need for additional documentation and programming work which includes the description of the operation codes, the use of indexing, the use of the machine language coding sheet, preparation of the program tape, loading and checking the program, the operation of the associated peripheral equipment, and specifications required for auxiliary equipment added for a particular experimenter's use. Also required are directions for the use of the relocating routines and associated subroutines.

This report describes the documentation and programming required for the proper support of the SPC. It also includes a description of the parts of this project which have already been completed.

b. Description of the support project (introductory).

As the title of the report implies, the project is broken into two parts: the documentation phase and the programming phase. The documentation part of the project concerns the writing of programming and operating handbooks. These handbooks should be at two levels: (1) *Introductory* for quick reference to the operation of the SPC, and (2) *Advanced* for a complete description of the operation of the SPC. The programming part of the project concerns the construction of the programs for the use and checking of the SPC. There are three classes of programs written for the SPC. The first is written by the experimenter with an idea for the use of the ranging equipment. The second is written for use of the experimenter by programmers and contains subroutines, programming programs, and other aids. The third is written by programmers for use in the maintenance and exercise of the machine. The first class is not properly part of this project. The second class is discussed under the *software package*; the third class is discussed under *check and diagnostic programs*.

Programming handbooks. As stated above, there is a need for two levels of operating manuals or handbooks. The *Introductory Handbook* should cover such topics as "How to Turn the SPC On," "How to Load Programs," and "How to Document Work on the SPC." The *Advanced Handbook* should cover such topics as "Forced Coding," "Exhaustive Discussion of Operation Codes," and "Description of Symbolic Processors."

Introductory Handbook. The *Introductory Handbook* is intended to provide the occasional user of the SPC with the necessary information whereby he may program the SPC to be an integral part of his experiment without requiring a programmer's time.

The Advanced Programming Handbook. The *Advanced Programming Handbook* will use as background material the *Introductory Handbook*, and assume that the reader is conversant with the field of programming. It is the purpose of this handbook to provide the programmer with the necessary information to enable him to optimally code programs, to understand the OP code fully, and to understand the construction of the symbolic processors available for the SPC.

Software package. The software package consists of the material written by a programmer for use by an experimenter and will contain the usual complement of subroutines for the evaluation of commonly used functions,

subroutines for the presentation of data (binary-to-decimal and decimal-to-binary conversion routines), and special routines of general use to the communications field. In addition, it will contain the loading programs necessary to use the above routines effectively (that is, easily by the experimenter). This latter area also covers the symbolic processors.

With any package such as this, it is necessary to provide the instructions required for the proper operation of the routines. This, then, will be included in this part of the support project.

Information about the subroutines and other routines will be placed with the SPC.

Check and diagnostic programs (detailed description). The Mod II and Mod III stored program controllers are expanded versions, with respect to input-output channels, of the stored program computer. As such, it is of great importance to determine the operating status of the machine at frequent intervals. It is also desirable to use the machine to perform part or all of this process. A suitable choice in the sequence of self-tests does allow the machine to check not only its own operation, but, to a limited degree, diagnose the fault. The check and diagnostic programs allow the determination of the operating condition and the diagnosis of faults.

There are three things to be accomplished by a program of self-checking:

- (1) It assures the operator, or programmer, that the machine is in operating condition.
- (2) Should malfunctions occur either while the machine is in use or during regularly scheduled check times, it indicates the area of the malfunction. (Because of the complexity of the interactions, this is of extreme importance.)
- (3) It provides a group of tests of the machine which can be used to evaluate the reliability of all or part of it.

These general objectives can be separated into several specific subobjectives. The subobjectives are tied directly to the design of the machine. Each section of the controller can be separated, in a functional sense, from other sections to enable a complete testing of that section. The areas of the controller that can be tested separately are:

- (1) Operation codes.

- (2) Indexing operations.
- (3) Memory (storage).
- (4) Input channels.
- (5) Output channels.
- (6) Auxiliary equipment.

It should be noted that the sequence of the tests has an effect on the separability of the sections. Therefore, the sections are listed in this sequential order.

Up to this point only the complete check and diagnostic program has been discussed. There is a need for a set of "spot checking" programs to aid in the correction of malfunctions once detected. Some of these subprograms can be drawn from the larger diagnostic program.

If these subprograms are provided with self-scoring abilities, they can be used to evaluate the reliability of the controller. An example of the latter type of testing is given by the "Random Memory Test." This program loads the memory with randomly generated numbers. The contents of the memory are then checked against what was loaded. If a discrepancy occurs, the location of the fault is printed and the error is tallied. Each successful cycle through memory is also tallied. A résumé of the results of the test can be printed on demand.

This program is used to test the margins of the memory, with respect to voltage, as well as the general reliability of the memory section.

Project status and direction. A part of the information that is to be included in the *Introductory Handbook* has been published (Ref. 8). This report describes the operation codes and some of the auxiliary equipment. It will be necessary to add to this information about the use of the console, operation of the remaining auxiliary equipment, the loading programs, the subroutines, and the proper program documentation.

The *Advanced Handbook* is still in the planning stage. There is considerable work to be done with the machine to determine the total effect of some combinations of operating codes. Work on this task is hindered by the additions and modifications to the SPC. These additions and modifications are expected to continue for several months. Further, it will be necessary to complete the programming part of the support project in order that the information concerning the construction of the processing programs can be included.

Programming. Considerable work has been done in the area of programming the SPC. Much of this programming has been of an experimental nature, that is, for specific experiments using the ranging equipment. However, several useful subroutines have been produced in the course of the construction of the experimental programs. Some of these subroutines were written to aid the programmer in the check-out of the program that he had written. Some were written to present the data in a manner easily used by the experimenter. Others were written to free the machine of the waiting period required by the output devices. A list of these subroutines is given in the following:

- (1) Memory dump.
- (2) Breakpoint set and reset.
- (3) Tape read.
- (4) Multiply.
- (5) Divide.
- (6) Sine-cosine.
- (7) Binary-to-decimal conversion (positive integer).
- (8) Binary-to-decimal conversion (positive fraction).
- (9) Square root (integer).
- (10) Random number generation.
- (11) Punch and print buffer.
- (12) Tape input change routine.

Most of the subroutines are self explanatory; however, two require a word of explanation.

The breakpoint set and reset routine is used during the check-out of a program to place a bit in the order specified to enable the programmer to execute a block of orders and stop at the one specified to check the results of the program. It also inserts bits to change the orders from single to double precision and vice versa.

The punch and print buffer routines were written to free the machine for computation when the output devices are overloaded. When these devices are required to operate at a rate faster than they are able, the buffer routine stores the information and returns the machine to the computation problem. When the output device is free to accept new information, the buffer routine is again entered and the information stripped from it.

Two forms of loading routines are available for use with most of the above subroutines. The first, General

Loader I, merely performs the work necessary to relocate a subroutine. It does not determine the linkages. The second, General Loader III, relocates the subroutine, establishes linkages from and to the main program, and assigns common working storage and intercommunications cells for the over-all program.

A symbolic loading or assembly routine has been written. The Drop Program will accept symbolic machine language programs and produce numerically coded programs which the machine accepts directly. This is primarily a clerical routine which frees the programmer from the labor of translating symbolics to numerics. It does not free the programmer from machine language coding. A description of the DROP Program appears at the end of this article.

Throughout the construction of the SPC, it has been necessary to test or exercise parts of the machine. Programs were written for this purpose. While these programs do not fulfill the needs of an over-all Check and Diagnostic Program, they provide a basis upon which to build the superstructure of the Diagnostic Program. Some of the test programs already written are:

- (1) Input-output
 - (a) Reader test
 - (b) Punch test
 - (c) Printer test
- (2) Operation code
 - (a) Add-subtract
 - (b) Shift tests
- (3) Memory
 - (a) Memory only
 - (b) Memory in the presence of input-output operations

A set of programs is being written which will test the machine using a minimum of auxiliary equipment. The philosophy of this program assumes that none of the functions work or are reliable. By successive tests based upon this philosophy using the self-contained abilities of the controller to communicate with the outside, the reliability of the equipment can be established. It is the aim of this step-by-step process to check each area as thoroughly and as rigorously as possible.

Use of the DROP Program. The DROP Program is really two programs used together to enable the programmer to write his program in symbolic terms and have the machine translate it into the machine coding. Both object and source programs are in machine language.

To illustrate the use of the DROP Program we will assume that a program has been written and it is now desired to assemble it in numeric coding. The first step is to type and punch the program on the Flexowriter. It is important that no errors be made. If errors are made and corrected on the tape by deletion it will be necessary to repunch the tape to eliminate the deleted codes. The origin of the program and the extent of the memory are written as two 8 octal digit numbers with signs followed by a space and tab or carrier return and precedes the program.

After the tape has been written and purged of errors, it is inspected by the label preparation routine of the DROP Program. This routine is loaded into the SPC and the source tape read in under its control. This routine produces a tape of the labels used by the symbolic program and their location in the memory.

With the source tape, the label tape prepared by the first half of the DROP Program, and the second half of the program, the final assembling of the Source program can proceed. First, the second half of the program is loaded into the Mod II. The breakpoint switches are all off. The label tape is read under the control of the DROP Program. (The label tape must have a stop code as the last character. The label preparation tape does not punch one.) BP0 is turned on and the symbolic tape loaded. The processing is automatic from this point on.

BP1 is used to reset the program to accept the label tape for the next source program to be processed. With BP0 off and BP1 on, the machine is started. It will stop automatically when ready for the next label tape. BP1 is turned off and the next label tape loaded. The assembly process can be repeated in this manner as often as required.

If there is an error in the source program, that is, if it contains a symbol or group of symbols which are not permitted, the printer will print out a code number. The following list explains these codes:

-
- 24. Too many labels to be processed by this program
 - 120. An undefined label appeared as an address
 - 153. The source program has too many instructions for the size of the memory
 - 157. A nonpermissible symbol was used (\$,!)
 - 173. A nonpermissible symbol was used (=, -, ", !)
 - 225. A nonpermissible symbol was used in a data word or in the absolute portion of an instruction (any symbol not a number or a period)
-

DROP format. Programs written to be assembled by the DROP Program must be written in the following way:

- (1) All comments must be enclosed in parentheses. The closing parenthesis signals the end of the comment.
- (2) A label is followed by a semicolon if it is the label of an instruction, and by a colon if it is the label of a data word.
- (3) Commas separate all groups within an instruction.
- (4) A period ends a statement or instruction.
- (5) The plus or minus sign precedes all groups of symbols to be taken as an octal word when used in an instruction. The octal word must be followed by a period or an error will result.
- (6) All data words must be signed.
- (7) The asterisk is used to denote the present location when coding.

The following is a typical listing of a program. The program is intended for illustration only and does not do anything.

STRT; CLA,	TRG. (TRG is listed in the acceptable mnemonics)
STO,2.	(second comma not necessary)
ALS,A,	+5
TIX,2,	BRA.
TRA,	*-3 (transfers to the STO,2. Instruction)
BRA; ADD,	DEC. (; label of instruction)

DEC: +0237764.	(: label of data)

3. A Phase-Locked Loop with Sideband Rejecting Properties

A monostatic interrupted CW radar system necessitates the alternate keying of the transmitter and receiver as shown in Fig. 79. While eliminating the need for a

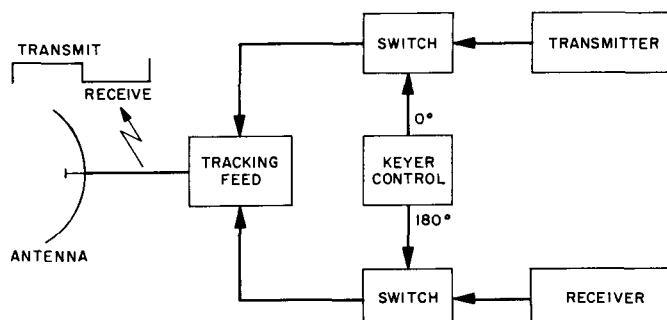


Fig. 79. Keyed radar system

second antenna, the use of this technique introduces other problems, (SPS 37-19, Vol. III, pp. 29-32). One of these problems results from the sidebands generated by the keying frequency. Thus, significant power is present not only at the fundamental carrier frequency but also at the sideband frequencies. Difficulty arises in achieving the initial RF lock of the receiver. If the power contained in the sidebands is sufficient, the result may be a sideband lock rather than the desired carrier lock.

Since the keying waveform is square (i.e., a 50% duty cycle), only the odd numbered sidebands will be present and need be considered. A technique for detecting and rejecting these sidebands is shown in Fig. 80. The method results in the generation of a cancelling signal which prohibits locking to a sideband. The system (Fig. 80) consists of a conventional phase-locked loop, an anti-sideband loop, a sideband lock detector, and an "any lock" (i.e., carrier or sideband) detector. The two lock detectors are necessary to provide sufficient evidence of a carrier-locked condition.

To understand the system's operation, consider first the phase-locked loop consisting of the phase detector,

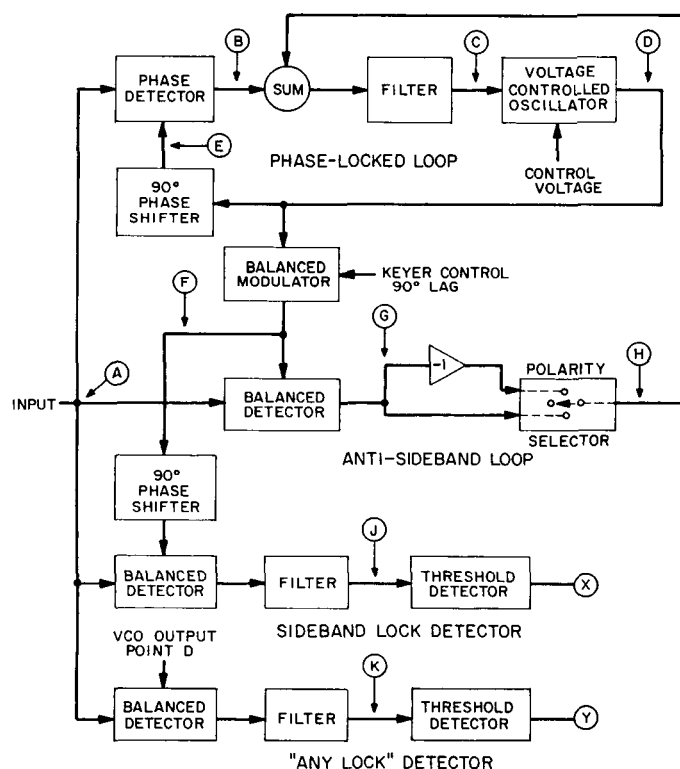


Fig. 80. Phase-locked loop with sideband rejection

filter, voltage controlled oscillator, and phase shifter. If the input to the phase detector (Point A) is

$$\begin{aligned} v_A &= a \cos \omega_c t & (0 \leq t < T/2) \\ &= 0 & (T/2 \leq t < T) \end{aligned} \quad (1)$$

where T = period of the keying waveform, then the output from the VCO (Point D) will have the following form

$$v_D = \cos [(\omega_c + N\omega_k)t + \theta(N)] \quad (2)$$

where

$$\begin{aligned} N &= \text{number of sideband} \\ &(\text{i.e., } 0, \pm 1, \pm 3, \dots, \pm(2N-1)) \end{aligned}$$

$$\omega_c = \text{angular frequency of the carrier}$$

$$\omega_k = \text{angular frequency of the keying signal}$$

$$\theta(N) = \text{the phase angle between the VCO output and the input taken as a reference}$$

In general, $\theta(N)$

- (1) Approximates 0° for carrier lock.
- (2) Approximates -90° for upper sidebands.
- (3) Approximates $+90^\circ$ for lower sidebands.

The phase shifter provides an additional 90° phase shift, with the result that the second input to the phase detector (Point E) is

$$v_E = \cos [(\omega_c + N\omega_k)t + \theta(N) + 90^\circ] \quad (3)$$

A multiplicative operation takes place in the phase detector such that its output (Point B) becomes

$$v_B = \frac{a}{2} \cos [N\omega_k t + \theta(N) + 90^\circ] \quad (4)$$

Eq. (4) represents a general expression for the time varying signal to be found at the output of the detector for any condition of lock. Filtering within the detectors removes the double frequency term resulting from the multiplicative operation. The average value can be found by integrating the above expression; thus

$$V_B = \frac{a}{4N\pi} \{ \cos [N\pi + \theta(N)] - \cos \theta(N) \} \quad (5)$$

represents the effective error voltage in the phase-locked loop. The values of V_B for the carrier and first two sidebands have been computed and are found in Table 8.

Table 8. Signals occurring for various conditions of lock

Lock condition	Phase angle relationships					
	Phase detector output (Point B)	Anti-sideband loop output (Point G)	Polarity selector output (Point H)	Summing junction output (Point C)	Sideband lock detector (Point J)	"Any lock" detector (Point K)
Third upper	$-a/6\pi \cos \theta (N)$	$-a/6\pi \cos \theta (N)$	$a/6\pi \cos \theta (N)$	0	$a/6\pi \sin \theta (N)$	$-a/6\pi \sin \theta (N)$
First upper	$-a/2\pi \cos \theta (N)$	$a/2\pi \cos \theta (N)$	$a/2\pi \cos \theta (N)$	0	$-a/2\pi \sin \theta (N)$	$-a/2\pi \sin \theta (N)$
Carrier	$-a/4 \sin \theta (N)$	0	0	$-a/4 \sin \theta (N)$	0	$a/4 \cos \theta (N)$
First lower	$a/2\pi \cos \theta (N)$	$a/2\pi \cos \theta (N)$	$-a/2\pi \cos \theta (N)$	0	$-a/2\pi \sin \theta (N)$	$a/2\pi \sin \theta (N)$
Third lower	$a/6\pi \cos \theta (N)$	$-a/6\pi \cos \theta (N)$	$-a/6\pi \cos \theta (N)$	0	$a/6\pi \sin \theta (N)$	$a/6\pi \sin \theta (N)$

Next, consider the operation of the anti-sideband loop composed of the balanced modulator, balanced detector, polarity selector, and summing junction. The operation of this loop is contingent upon the availability of a keyer signal which has been shifted by 90° . In practice, this can be accomplished by delaying the output of the keyer control by $\frac{1}{4}$ cycle as shown in Fig. 81. This delayed keying signal and the VCO output, represented by Eq. (2) form the inputs to the balanced modulator. The modulator is designed such that its output (Point F) is

$$v_F = \cos [(\omega_c + N\omega_k)t + \theta(N)] \quad (0 < t < T/4) \quad (6)$$

$$= -\cos [(\omega_c + N\omega_k)t + \theta(N)] \quad (T/4 < t < T/2) \quad (7)$$

for the two intervals of interest.

Phase detection of the above with the input reference signal results in the following

$$v_G = \frac{a}{2} \cos [N\omega_k t + \theta(N)] \quad (0 < t < T/4) \quad (8)$$

and

$$v_G = -\frac{a}{2} \cos [N\omega_k t + \theta(N)] \quad (T/4 < t < T/2) \quad (9)$$

Integrating to find the average value over the period results in the generalized expression

$$V_G = \frac{a}{2N\pi} \left[\sin \left(\frac{N\pi}{2} + \theta(N) \right) \right] \quad (10)$$

The computed values for V_G for the carrier and first two sidebands are found in Table 8. A comparison of these values with those previously calculated for the phase-locked loop (Point B) yields some interesting observations. The functions and their magnitudes are

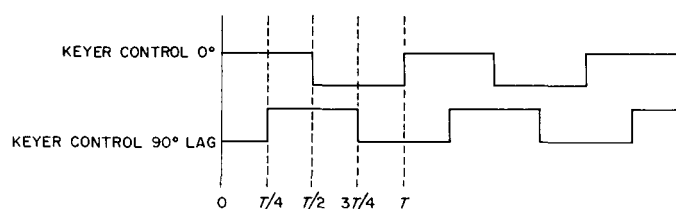


Fig. 81. Keyer control output

identical for all sidebands except for a sign reversal that exists in the first upper and third lower sidebands. For the phase-locked loop (Point B) all upper sidebands produce a negative sign, while the lower sidebands are characterized by a positive sign. The anti-sideband loop (Point G) exhibits a sign reversal for successive sidebands (i.e., first positive, third negative, fifth positive, seventh negative, etc.). Therefore, by reversing the appropriate signs and summing V_B and V_G , the system can be made to reject all sideband lock conditions. Furthermore, since the anti-sideband loop output is zero for a carrier lock, no cancellation will occur in this condition. The sign reversal can be accomplished by inserting an amplifier, with a phase inversion and unity gain, at the appropriate times. A switching device, preferably with a high open-to-closed impedance ratio, can be used to select the appropriate polarity. Thus, the output from the polarity selector (Point H) is equal in magnitude, but opposite in sign, to that generated in the phase-locked loop. A simple summation of the two signals results in a device which rejects all but the carrier-locked condition.

The canceling voltage from the anti-sideband loop contains noise as well as the desired signal which causes degradation of the system's performance. The resulting increase in threshold is 3 db. For very small echoes this increase might be intolerable; therefore, the polarity switches should be left open until the first sideband lock has been detected. With the switches open, the system operates as a conventional phase-locked loop, and no

threshold degradation occurs. Since the first sideband is nearly 4 db below the carrier, the switches may be left closed following a sideband detection without masking the fundamental.

To make the device operative a method must be devised for selecting the proper polarity for sideband rejection. The sideband lock detector, composed of the phase shifter, balanced detector, filter, and threshold detector, is used to make this selection. Its operation is similar to that of the anti-sideband loop except that an additional 90° phase shift has been inserted. Thus, the output from the sideband lock detector (Point J) can be characterized by the following expression:

$$V_J = \frac{a}{4N\pi} \left\{ 2 \cos \left[\frac{N\pi}{2} + \theta(N) \right] - \cos [N\pi + \theta(N)] - \cos \theta(N) \right\} \quad (11)$$

Values of V_J for the carrier and first two sidebands have been computed and are found in Table 8. The need for such a detector becomes apparent when one recalls the approximations for $\theta(N)$. Inserting these approximations for $\theta(N)$, a negative voltage appears at the detector output whenever a phase inversion is required. Therefore, a simple polarity sensor can be used to close the appropriate switch in the anti-sideband loop.

Since the output from the sideband lock detector is zero in the carrier locked state, a second lock detector is required to provide definite evidence of this condition. The "any lock" detector consists of a balanced detector, filter, and threshold detector. Its operation is similar to that of the other detector and the generalized expression governing its output is

$$V_K = \frac{a}{4N\pi} \{ \sin [N\pi + \theta(N)] - \sin \theta(N) \} \quad (12)$$

Values of V_K for the carrier and first two sidebands are found in Table 8. Substitution of the approximations for $\theta(N)$ yields positive voltages for all values of N .

A simple logical combination of the two lock detectors can be used to determine which condition exists. The possible combinations are shown in Table 9, together with the conditions which they represent. Note that $U_i + L_j$ describes all sidebands for which a phase inversion of the anti-sideband loop is necessary. This illustrates the earlier statement that X alone is sufficient to make the polarity selection.

Table 9. Lock detector truth table

Sideband lock detector (X)	"Any lock" detector (Y)	Indicated lock condition	Polarity reversal required?
0	0	None	—
0	+1	Carrier	No
+1	+1	$U_i + L_i$	No
-1	+1	$U_i + L_j$	Yes
U represents upper sidebands L represents lower sidebands $i = 4k - 1$ $j = 4k - 3$ for $k = 1, 2, 3, \dots, n$			

The monostatic radar system will include a stored program controller (SPC) (Ref. 8) to perform the ranging operations. The SPC resembles a general purpose computer in that commands defining sequential operations can be stored in the machine's memory. The machine is capable of performing arithmetic operations as well as making logical decisions. Its ability to make logical decisions renders the SPC suited to control the anti-sideband locking system. If the conditions defined by the truth table (Table 9) are stored in the controller's memory, a corrective action can be effected whenever an undesirable lock condition exists.

Consider a typical ranging operation. First, both polarity selection switches in the anti-sideband loop are opened to prevent degradation of the receiver threshold. Next, the VCO frequency is offset from the fundamental carrier frequency by a fixed amount. The determination of this offset involves an estimate of the maximum expected doppler shift. For example, suppose that the frequency of the VCO has been decreased beyond the ninth lower sideband. The frequency is then gradually returned by a slowly changing control voltage toward the fundamental until an RF lock occurs. If the power in one of the lower order sidebands exceeds the threshold of the receiver, a phase lock will result. The relationship of the power contained in the carrier to that contained in several of the sidebands is shown in Table 10 and

Table 10. Relative signal power

Lock condition, N	Below carrier, db	Δ , db
0	0	0
1	-3.9	-3.9
3	-13.5	-9.6
5	-17.9	-4.4
7	-20.8	-2.9
9	-23.0	-2.2

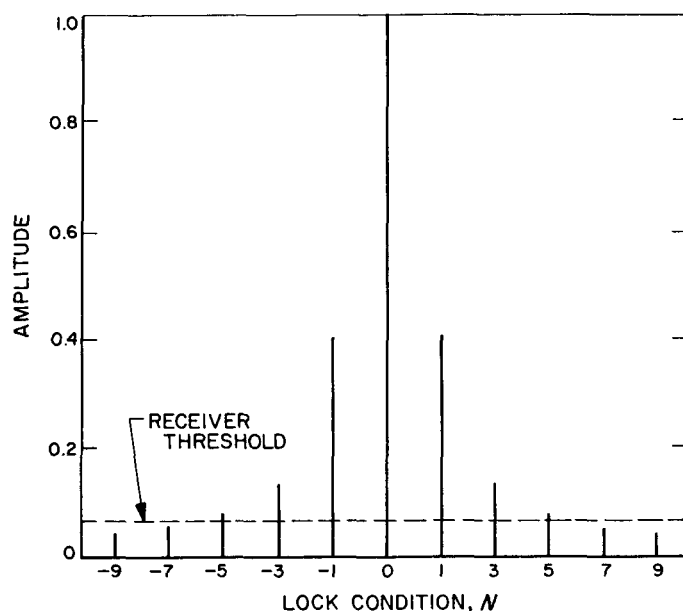


Fig. 82. Spectral distribution

Fig. 82. Referring to Fig. 82, assume that the fifth order sideband is the first to exceed the receiver threshold. Thus, as the VCO frequency is increased, an RF lock will not occur on either the ninth or the seventh lower order sidebands, but will take place when the fifth is reached. From Table 9 it is found that a fifth lower order sideband is indicated by

sideband lock detector, $X = -1$;

thus, a phase inversion of the anti-sideband loop is required. The stored program controller closes the correct switch to provide the canceling signal and the lock is broken. Closing the switch results in an increase in threshold of approximately 3 db, and this alone may be sufficient to break the first lock. Since the filters used in the system have long time constants, it is advisable to discharge them following closure of the appropriate switch. This discharge can be effected by momentarily shorting the output terminals. Once lock has been broken the control voltage causes the VCO to begin moving toward the fundamental once more. When the third lower sideband is reached, RF lock will recur. Referring to Table 10 it will be found that this condition is indicated by

sideband lock detector, $X = 1$.

Therefore, inversion of the anti-sideband loop is not required. Having the wrong switch closed effectively increases the signal strength of the sideband. The SPC

recognizes the error, reverses the polarity of the anti-sideband loop, and discharges the filters. The VCO then moves on to a first-order lock where the procedure is repeated. Once carrier lock is achieved, the canceling signal from the anti-sideband loop vanishes and the lock will not be broken.

The existence of a carrier lock must be verified by an examination of the "any lock" detector. If the time constant of the "any lock" detector is several times that of the sideband lock detector, the "any lock" detector will produce an output only for the carrier-locked condition. The "any lock" detector can be used to inhibit the VCO control voltage and to disconnect the anti-sideband loop. Thus, the phase-locked loop is returned to conventional operation.

Laboratory tests are now being conducted to verify the theoretical performance of the system. Prospective tests include a determination of the noise contributed by the anti-sideband loop, the optimum method for summing the cancellation signal, and the system's performance with very weak signals.

4. Sideband Lock Investigation

The problem of spurious lock to modulation sidebands may arise in any closed-loop system in which a modulation component exists whose frequency differs from the carrier by more than the loop bandwidth but less than the tuning range of the receiver. In general, these modulation components include PCM/PM and FM/PM telemetry subcarriers and AM sidebands resulting from high-frequency (hundreds of cycles per second) keying of the carrier in satellite radar applications. Not included are information sidebands on telemetry subcarriers, low-frequency (fractional cycles per minute) keying in planetary radars, nor clock sidebands typical of precision ranging systems.

A means of immunizing the receiver to this problem would ideally perform under the following conditions:

- (1) No degradation of receiver sensitivity at carrier lock.
- (2) No change in received spectrum.
- (3) Immunity to sideband lock extending to receiver threshold.
- (4) Capability of functioning at acquisition sweep rates approaching those dictated by other parameters.

Approaches studied to date which meet (1) and (2) have, in general, utilized the second intermediate frequency output of the receiver in a subsystem which detects either synchronously or nonsynchronously some characteristic of the spectrum of the modulated carrier. Simplest of these is the quadrature synchronous detector which develops the automatic gain control voltage. This is a very effective lock indicator, but without an *a priori* estimate of the received signal strength, it yields an ambiguous indication of lock, including that of a sideband. A means of resolving this ambiguity or, better yet, avoiding the sideband lock altogether is the subject of this investigation.

The ability to approach condition (3) or (4) tends to bring about a sacrifice in the other. In short, the alternative appears to be whether or not synchronous detection in the subsystem can be accomplished. Both of these choices have been analyzed for applicability in the general problem areas discussed above, and preparations are underway to evaluate each in the laboratory.

a. Synchronous sideband detector. The underlying concept of the amplitude keyed monostatic radar depends upon the availability of a keying waveform whose period corresponds to the round-trip propagation time (SPS 37-15, Vol. III, p. 40). Since this waveform tracks the received phase of the modulation sideband, it is suitable as a reference waveform in the synchronous detection of the spurious sideband condition. The block diagram of such a subsystem is shown in Fig. 83. Inherent in the dynamic phase error during false lock is a principal component whose frequency is equal to Nf_m , where f_m is the modulation fundamental frequency (keying rate) and N is the order of the Fourier term (sideband) to which the receiver is locked. The frequency and phase (with respect to the local reference) together uniquely define the extent and direction of mistuning. While this information could be used to program a proper retuning and resulting carrier lock, a straightforward approach of simply detecting the presence of the false lock may be used with an acquisition system in which the tuning is programmed at a given constant rate through the total

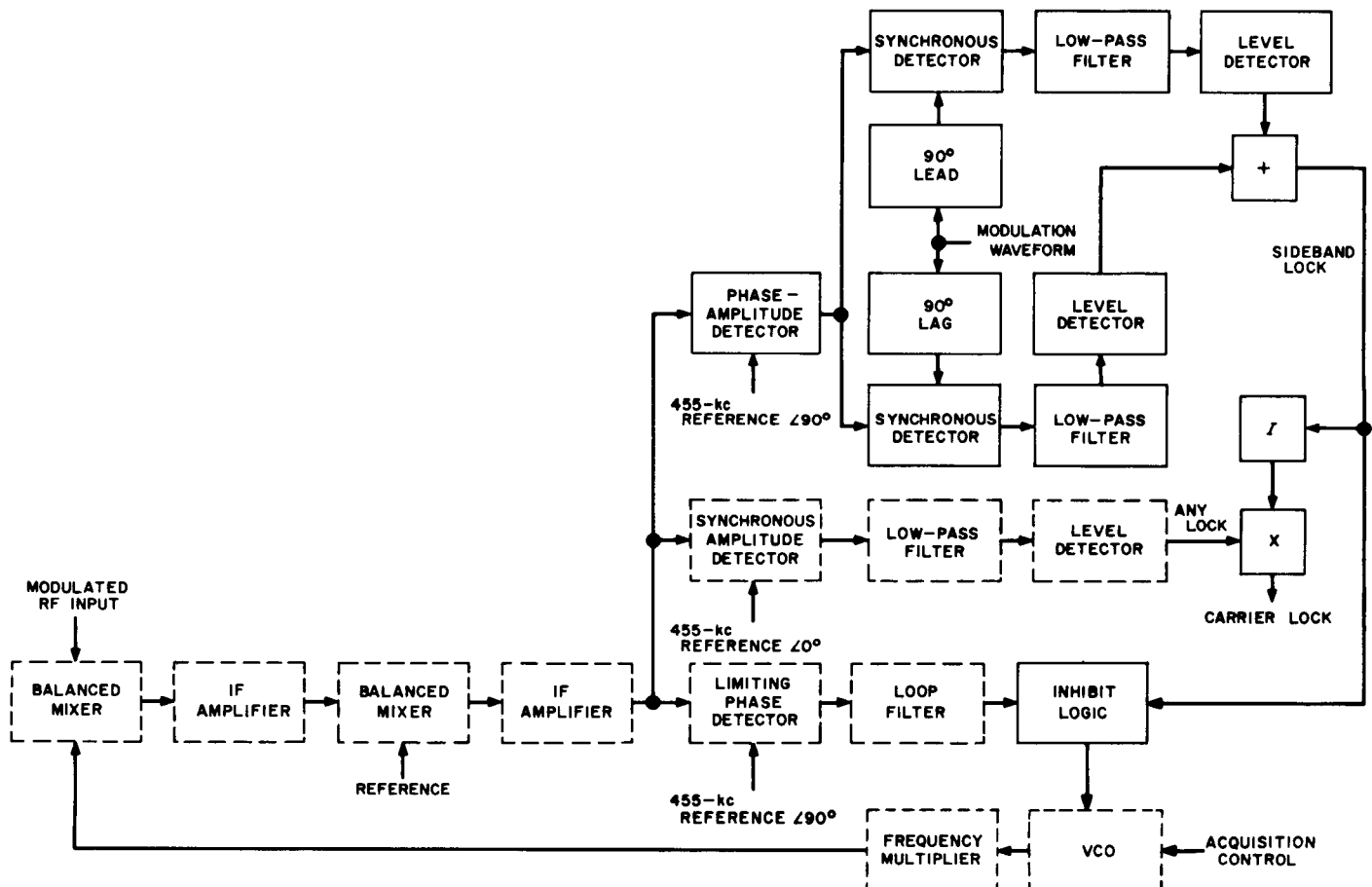


Fig. 83. Synchronous sideband detector

spectrum of interest. No loss of time to proper acquisition will result provided that the false lock can be rejected in a period less than the time required for the tuning to change through the interval $\Delta f = f_m$.

In order to evaluate the trade-off of (3) and (4), an attempt will be made to establish a relationship among the pertinent variables.

The time constant of the two post-detection filters in the "sideband lock" channel must be such that the noise bandwidth of the latter approximates that of the main loop. For a low-pass filter,

$$\beta = \frac{\pi \omega_0}{2 \cdot 2\pi} = \frac{1}{4\tau} \text{ cps}$$

where β = noise bandwidth and $\tau = RC$. Therefore, since $\beta \leq \beta_{L_0}$, where β_{L_0} = loop noise bandwidth at threshold,

$$\frac{1}{4\tau} \leq \beta_{L_0} \text{ or } \tau \geq \frac{1}{4\beta_{L_0}} \text{ sec}$$

for condition (3).

The maximum sweep rate for a second-order feedback system is limited by the transient phase error. Assuming $\frac{1}{2}$ rad as the maximum tolerable error, the limiting sweep rate is given by:

$$\frac{df}{dt} = \frac{1}{2\pi} \frac{1}{2} \frac{32}{9} \beta_{L_0}^2 = \frac{8}{9\pi} \beta_{L_0}^2 \text{ cps/sec}$$

Then the time available for false lock detection and rejection to meet condition (4) is:

$$\Delta t = \frac{\Delta f}{\frac{df}{dt}} = \frac{9\pi f_m}{8\beta_{L_0}^2} \text{ sec}$$

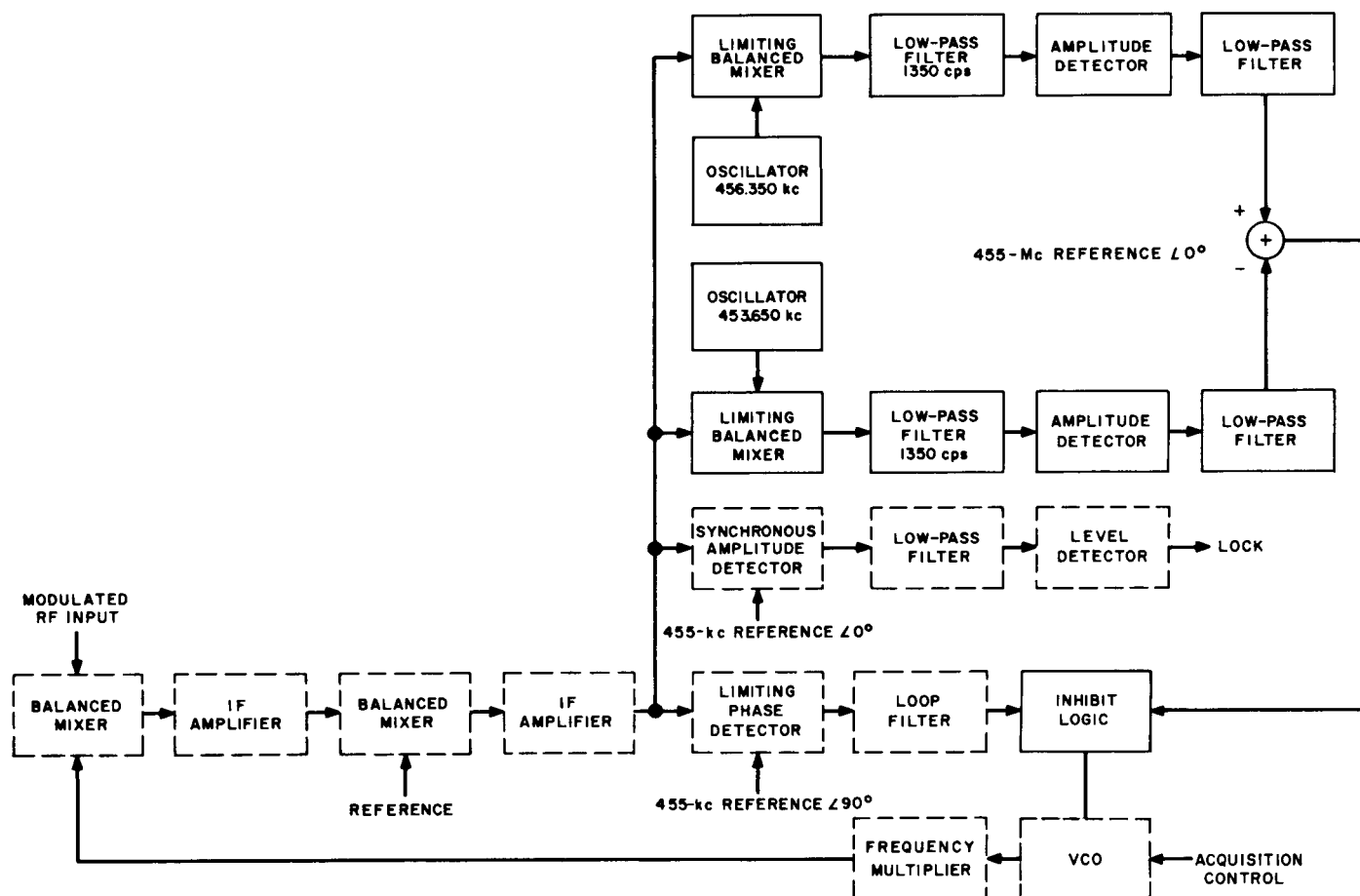


Fig. 84. Strong signal sideband discriminator

Assuming a false lock detection time equal to one time constant, τ , of the detector,

$$\Delta t = \tau$$

Combining conditions (3) and (4) yields:

$$\frac{9\pi f_m}{8\beta_{L_0}^2} \geq \frac{1}{4\beta_{L_0}} \text{ or } f_m \geq \frac{2\beta_{L_0}}{9\pi} \text{ cps}$$

Since the initial hypothesis sets a lower limit on the modulation frequency of β_{L_0} , this restriction is easily satisfied.

Due to the fact that the monostatic satellite radar must acquire the carrier in a minimum period of time and at a time when the signal level is the weakest for which the system is designed, that is, conditions (3) and (4), this approach will be pursued for this application.

b. Strong signal sideband discriminator. In the DSIF application, the presence of telemetry modulation appearing in the dynamic phase error even at carrier lock would complicate, if not render useless, the synchronous system described above, even though a hypothetical local reference were available.

However, since the problem of spurious sideband lock is most severe during initial acquisition of the spacecraft transponder signal, the typically strong signal (in excess of 30 db above threshold) allows square law sideband detection with a predetection bandwidth of $1000\beta_L$. Predetection bandwidths (one-sided) in the main loop are typically $100\beta_L$ and those of telemetry channels the order of $500\beta_L$. A subsystem acting upon spectrum symmetry could provide a continuous inhibit except in the region of the carrier. This function is exactly that of the common frequency discriminator plus inhibit logic. Such a subsystem is depicted in Fig. 84.

The requirements on the discriminator of (1) crystal stability at 455 kc and (2) a wide frequency range (approximately that of the associated predetection bandwidth) have resulted in a mechanization involving third conversion to frequencies at which conventional circuit elements will provide the required characteristics.

For use with systems in which telemetry subcarrier fundamental frequencies lie outside the predetection bandwidth of the main loop (shown dotted in Fig. 84), this same approach could be used by driving the discriminator from the telemetry channel and by appropriate scaling of the third conversion oscillators and filter time constants.

E. Tiefort Mountain Antenna Range

An experimental long-range collimation tower station for measurement of large ground antennas has been completed. It is in operation at X-band.

The Goldstone Tiefort Mountain Experimental Station described in SPS 37-20, Vol. III, pp. 52-54, has been completed.

The operating building (Fig. 85) contains space for three 7-ft equipment racks, two bunks, water cooler, and an oil heater. The station has a private radio link operating on the GTS communication network frequency.

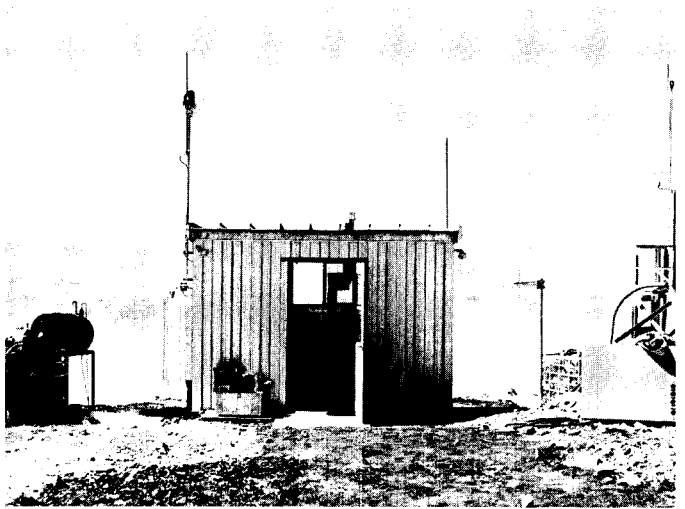


Fig. 85. Tiefort instrument building

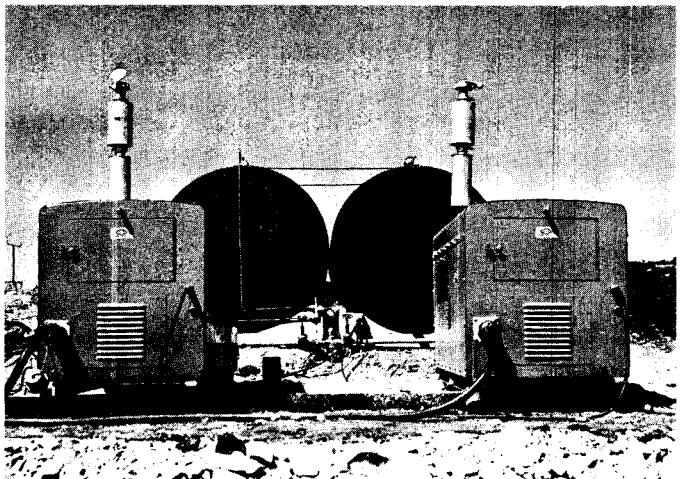


Fig. 86. Tiefort 10-kw diesel generators

The prime power for the station is supplied by two 10-kw air cooled diesel generators (Fig. 86). They are designed to allow continuous unattended operation for 4 days. The normal station operation allows one generator to run with the second unit in stand-by. The fuel tanks hold a full month's fuel supply.

The two antenna towers (Fig. 87) have been equipped with a jib crane, a polarization rotator to remotely position the antennas, and a large equipment box to allow transmitter equipment to be mounted directly behind the antenna feeds.

The heliport has been equipped to allow emergency night landings. All structures have aircraft clearance lights. A low-power flashing beacon with a solar cell switch operates at night to mark the station when unattended.

The station is presently operating at X-band to support the 30-ft antenna surface tolerance versus RF performance program measurements. The station will have equipment installed shortly to support S-band measurements at the Venus and Echo sites.

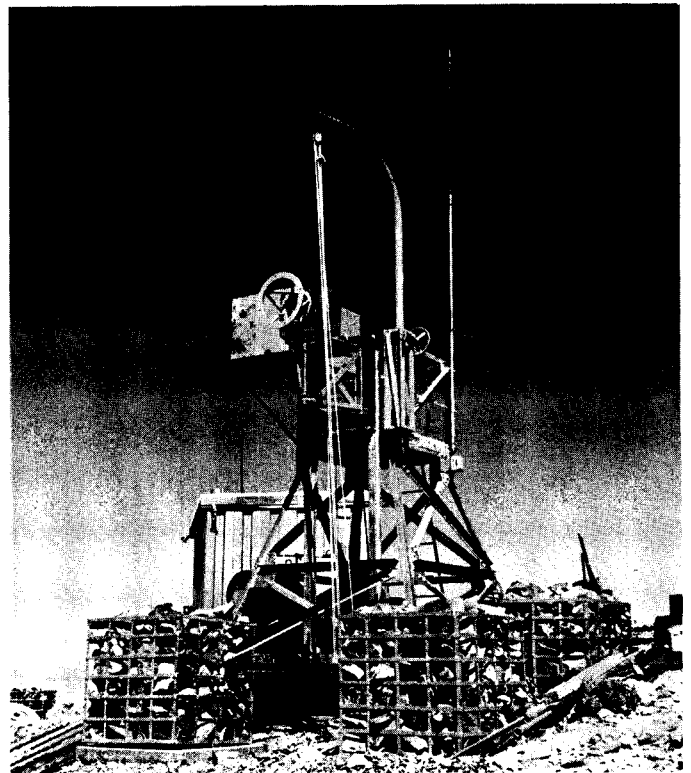


Fig. 87. Tiefort illuminator tower

References

1. Siegman, A. E., "Thermal Noise in Microwave Systems," *The Microwave Journal*, pp. 66-73, April 1961.
2. Drake, F. D., and Ewen, H. I., *Proceedings of the IRE*, Vol. 46, p. 53, January 1958.
3. Schildknecht, R. O., *Transactions on Radio Frequency Interference*, Vol. 4, No. 3, pp. 63-66, October 1962.
4. Pressey, B. G., and Ashwell, G. E., "Radiation from Car Ignition Systems," *Wireless Engineer*, Vol. 26, No. 304, pp. 31-36, January 1949.
5. Silver, S., "Microwave Antenna Theory and Design," *MIT Radiation Laboratory Series*, Vol. 12, p. 173, McGraw-Hill Book Company, New York, 1949.
6. Hogg, D. C., "Effective Antenna Temperature Due to Oxygen and Water Vapor in the Atmosphere," *Journal of Applied Physics*, Vol. 30, No. 9, pp. 1417-1419, September 1959.
7. Victor, W. K., Stevens, R., and Golomb, S. W., "Radar Exploration of Venus; Goldstone Observatory Report for March through May 1961," pp. 62-69, Technical Report No. 32-132, Jet Propulsion Laboratory, Pasadena, California, August 1, 1961.
8. Baugh, H. W., *Mod II Ranging Equipment*, Technical Report No. 32-337, Jet Propulsion Laboratory, Pasadena, California, September 15, 1962.

IV. Advanced Antenna System

A. Synopsis

In January 1963, NASA announced that JPL would proceed to negotiate a contract with the Rohr Corporation, Chula Vista, California, for the final design, fabrication, and erection of the first Advanced Antenna System (AAS) to be erected at the Goldstone Tracking Station. The negotiations are nearly complete.

Supporting studies at JPL are also continuing. Further refinements are being made in the computer programs which are to be used in the design of the reflector structure. This extension is described in detail in Section IV-B.

B. Supporting Studies

1. Computer Studies, Statics

The STAIR Computer Program calculates the weight of every bar in the space frame and assigns one-half of the bar weight to the bar joints for use in the gravity

loading condition. This is done with input data consisting only of joint coordinates in cartesian coordinates and the bar areas. The bar is described by noting the joint numbers at the ends of the bars.

A byproduct of this load calculating portion of the program has been the calculation of the total weight of the space frame structure as well as the center of gravity of the structure.

A modification was made by JPL to code the program to calculate the weight moment inertias of the whole structure about the three axes of the coordinate system used to describe the joint positions. Since the position of the center of gravity is calculated, it is then possible to calculate the weight moment of inertia about any other axis parallel to the original coordinate system by the parallel-axis theorem, i.e.,

$$I = \bar{I} + Md^2$$

\bar{I} = moment of inertia of the body with respect to an axis through the mass center

M = weight

I = moment of inertia with respect to a parallel axis which is at distance d from the axis through the mass-center

The \bar{I} of the structure can be calculated using d equal to the center-of-gravity position with respect to the coordinate system.

The mathematical formulation used for coding the program was as follows:

The weight of each bar was calculated using the actual span times the density and the cross-sectional area

$$\text{span} = (\Delta X^2 + \Delta Y^2 + \Delta Z^2)^{1/2}$$

The moment of inertia with respect to each coordinate axis was calculated using the following theorem:

The sum of the moment of inertia of a body with respect to two perpendicular planes is equal to the moment of inertia of the body with respect to the line of intersection of the two planes.

For example:

$$I_x = I_{xy} + I_{xz}$$

I_{xy} = moment of inertia with respect to the xy plane

I_{xz} = moment of inertia with respect to the xz plane

I_x = moment of inertia with respect to the line of intersection of the xy and xz planes

$I_{xy} = \frac{1}{12}$ weight of the bar $\cdot (\Delta Z)^2$ + weight of the bar

$$\left(\frac{Z_1 + Z_2}{2} \right)^2$$

$I_{xz} = \frac{1}{12}$ weight of the bar $\cdot (\Delta Y)^2$ + weight of the bar

$$\left(\frac{Y_1 + Y_2}{2} \right)^2$$

As a sample problem, the space frame (Fig. 1) consisting of two spoked wheels separated by 20-ft long posts or

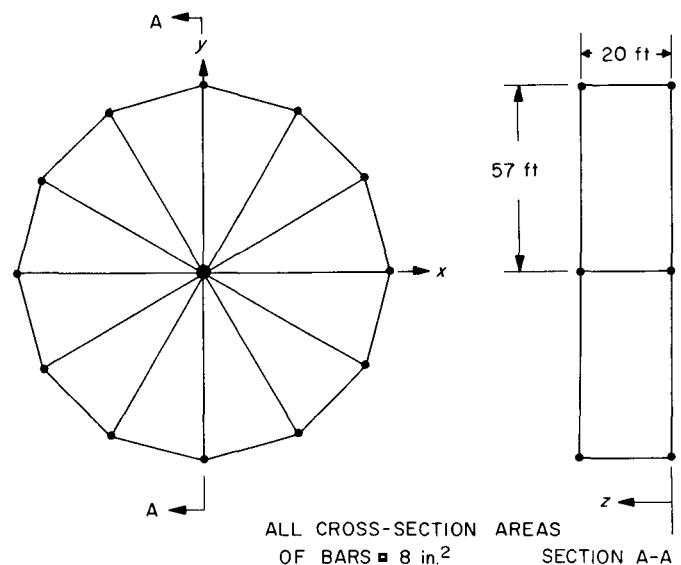


Fig. 1. Space frame for sample calculation of I

bars was input to the STAIR Computer Program. The answers from the program were:

Total weight using a density of 490 lb/ft³
= 63.594 thousand pounds

Weight center was

$$X = 0$$

$$Y = 0$$

$$Z = 10 \text{ ft}$$

Weight moment of inertia

$$I_x = 72,941 \text{ Kip ft}^2$$

$$I_y = 72,941 \text{ Kip ft}^2$$

$$I_z = 121,390 \text{ Kip ft}^2$$

Using d distances as determined by a graphical diagram and the parallel-axis theorem, the computer results were checked within 0.5% by slide rule calculations.